

Lehrstuhl für Zellbiologie der Technischen Universität München  
Wissenschaftszentrum Weihenstephan

# **Inhibition studies of soluble epoxide hydrolase**

Development of two novel fluorescence-based inhibitor assay systems  
and cellular inhibition by RNAi

Nicola M. Wolf

Vollständiger Abdruck der von der Fakultät Wissenschaftszentrum Weihenstephan für Ernährung,  
Landnutzung und Umwelt der Technischen Universität München zur Erlangung des akademischen  
Grades eines

Doktors der Naturwissenschaften (Dr. rer. nat.)

genehmigten Dissertation.

Vorsitzender: Univ.-Prof. Dr. Dieter Langosch  
Prüfer der Dissertation: 1. Univ.-Prof. Dr. Bertold Hock  
2. Univ.-Prof. Dr. Siegfried Scherer  
3. Prof. Bruce D. Hammock, Ph.D.  
University of California, Davis/USA  
(schriftliche Beurteilung)

Die Dissertation wurde am 29.06.2006 bei der Technischen Universität München eingereicht und durch die Fakultät Wissenschaftszentrum Weihenstephan für Ernährung, Landnutzung und Umwelt am 29.08.2006 angenommen.

*Für meine Eltern*

## CONTENTS

CATALOGUE OF FIGURES .....	vi
CATALOGUE OF TABLES .....	ix
ABBREVIATIONS .....	xi
PREFACE .....	xv
ACKNOWLEDGEMENTS .....	xvi
ABSTRACT .....	xviii
ZUSAMMENFASSUNG .....	xx
<b>INTRODUCTION .....</b>	<b>1</b>
<b>THEORETICAL BACKGROUND .....</b>	<b>2</b>
1 Soluble epoxide hydrolase .....	2
1.1 General properties of epoxide hydrolases .....	2
1.2 Subcellular and tissue distribution of sEH .....	4
1.3 Induction of sEH .....	5
1.4 Molecular biology and protein structure .....	5
1.5 Catalytic mechanism of sEH .....	7
1.6 Substrates and inhibitors .....	9
1.7 Biological role .....	11
1.8 Soluble epoxide hydrolase as potential therapeutic target .....	13
2 RNA interference .....	14
2.1 Molecular mechanism of RNAi .....	14
2.1.1 Dicer .....	15
2.1.2 RISC .....	17
2.1.3 RISC assembly .....	19
2.1.4 mRNA degradation .....	19
2.2 RNAi in mammalian cells .....	20
2.3 Original role of RNAi and closely related mechanisms .....	23
2.4 Current role of RNAi in research .....	27
2.5 Potential of RNAi for therapeutic approaches .....	29

---

<b>EXPERIMENTAL PART</b> .....	<b>33</b>
1 Development of two novel fluorescence-based assay systems for sEH inhibitors .....	33
1.1 Introduction and objective .....	33
1.2 Reaction mechanism and synthetic properties of fluorescent sEH substrates ...	35
1.3 Materials and methods .....	36
1.3.1 Chemicals and reagents .....	36
1.3.2 Enzymes .....	37
1.3.3 Buffer .....	37
1.3.4 Standardization curves .....	37
1.3.5 Determination of aqueous solubility .....	38
1.3.6 Determination of aqueous stability .....	39
1.3.7 Determination of specific activity .....	40
1.3.8 Determination of $K_m$ , $V_{max}$ and $k_{cat}$ .....	40
1.3.9 Optimization of detection of 6-methoxy-2-naphthaldehyde .....	42
1.3.10 Assay optimization .....	42
1.3.11 Assay validation .....	43
1.3.12 Evaluation of candidate stop solutions .....	45
1.4 Results .....	46
1.4.1 Aqueous solubility .....	46
1.4.2 Aqueous stability .....	47
1.4.3 Specific activities .....	49
1.4.4 Michaelis-Menten parameters .....	50
1.4.5 Excitation and emission maximum of 6-methoxy- 2-naphthaldehyde .....	54
1.4.6 Assay optimization .....	54
1.4.7 Inhibitor assays and assay validation .....	57
1.4.8 Evaluation of stop solutions .....	59
1.5 Discussion .....	62
1.5.1 Aqueous solubility and stability .....	62
1.5.2 Specific activities and Michaelis-Menten parameters .....	64
1.5.3 Assay development .....	67
1.5.3.1 Substrate selection .....	67
1.5.3.2 Assay optimization .....	69
1.5.3.3 Confirmation of epoxide hydrolysis as rate-limiting step .....	71
1.5.3.4 Inhibitor potency tests and assay validation .....	73
1.5.3.1 Stop solution .....	75
1.5.4 Further applications for the novel fluorescent sEH substrates .....	76
1.6 Conclusion .....	76

---

2 Cellular inhibition of sEH by RNA interference and potential role in therapy .....	78
2.1 Introduction and objective .....	78
2.2 Materials and methods .....	80
2.2.1 Chemicals and reagents .....	80
2.2.2 Cell lines .....	80
2.2.3 Determination of specific sEH activity of different cell lines .....	80
2.2.4 Cell culture .....	81
2.2.5 Optimization of electroporation .....	82
2.2.6 siRNAs and RNAi experiments .....	82
2.2.7 sEH activity determination of siRNA-treated cells .....	84
2.2.8 RNA extraction and RT-PCR .....	84
2.2.9 Quantitative PCR .....	84
2.3 Results .....	86
2.3.1 Expression of sEH in human cell lines .....	86
2.3.2 Optimization of electroporation conditions for 22RV1 .....	87
2.3.3 RNAi experiments .....	88
2.4 Discussion .....	92
2.4.1 Selection of a suitable cell model system .....	92
2.4.2 RNAi experiments .....	93
2.4.3 RNAi as potential therapy approach to down-regulate human sEH activity .....	94
2.5 Conclusion .....	96
<b>REFERENCES .....</b>	<b>97</b>
<b>PUBLICATIONS .....</b>	<b>126</b>
<b>CURRICULUM VITAE .....</b>	<b>127</b>

## CATALOGUE OF FIGURES

Figure 1	Conversion of epoxides by sEH. (R = rest) .....	2
Figure 2	Protein structure of human soluble epoxide hydrolase. Picture was generated by means of the software Cn3D 4.1. ....	6
Figure 3	Catalytic mechanism of sEH illustrated by presenting the involved amino acid residues of human sEH. After Morisseau and Hammock (2005). ....	8
Figure 4	Substrates of soluble epoxide hydrolase for assay purposes. <b>A</b> <i>trans</i> -stilbene oxide (TSO) <b>B</b> <i>t</i> DPPO ( <i>trans</i> -1,3-diphenylpropene oxide) <b>C</b> 4-nitrophenyl (2 <i>S</i> ,3 <i>S</i> )-2,3-epoxy-3-phenyl-propylcarbonat (NEPC) <b>D</b> 9,10-phosphonoxy-hydroxy-octadecanoic acid (serves as substrate for the N-terminal domain of sEH). ....	9
Figure 5	Endogenous metabolic pathways with sEH participation. <b>A</b> Conversion of the arachidonic acid-derived epoxide 11,12-EET to 11,12-DHET <b>B</b> Illustration of leukotoxin diol production from linoleic acid. ....	11
Figure 6	Schematic illustration of the RNAi mechanism. ....	15
Figure 7	Model for Dicer activity essentially following Zhang and coworkers (2004a). ....	16
Figure 8	Model for Slicer activity of Argonaute in RISC. While the 5' phosphate of the siRNA guide strand is bound by the PIWI domain, the 3' end is attached to the PAZ domain. The mRNA is cleaved by the RNase H fold of the PIWI domain in the middle of the siRNA guide strand. ....	17
Figure 9	Schematic overview of mammalian responses to dsRNA in the cytosol besides RNAi. This illustration summarizes information and results from various sources (Sarkar et al., 2004; Wang and Carmichael, 2004; Hornung et al., 2005; Robbins and Rossi, 2005; Takeda and Akira, 2005). dsRNA longer than 70 bp can bind to <b>2'-5' oligo adenylate synthase</b> . This again activates RNase L leading to RNA degradation in the cytosol. Binding of 30-80 bp long dsRNA to <b>protein kinase R (PKR)</b> initiates phosphorylation of several cytosolic factors such as eIF2 $\alpha$ (eukaryotic transcription initiation factor 2 $\alpha$ ) and I $\kappa$ B. This process triggers the inhibition of further mRNA translation and thus protein production as well as transcription initiation of inflammatory cytokines and interferon-I (IFN-I) proteins via translocation of the transcription factor NF- $\kappa$ B to the nucleus. Furthermore, long viral dsRNA is recognized by <b>toll-like receptor 3 (TLR-3)</b> causing the nuclear translocation of IRF followed by the induction of the IFN-I system. Finally, binding of certain siRNA sequences to <b>TLR-7</b> leads to a potent IFN-I response. Moreover, the activation of this receptor is also known to induce the production of inflammatory cytokines. All of the here described signaling pathways consist of a multitude of intermediate steps and mediating compounds (mostly not displayed in this scheme), which are still not completely revealed and understood. (ER = endoplasmatic reticulum; IFN-I = interferon-I; IL = interleukin; IRF = interferon regulatory factor(s); seq.-dep. = sequence-dependent; TNF = tumor necrosis factor). ....	21
Figure 10	Scheme of miRNA biogenesis and function. See text for detailed explanation. ....	25

Figure 11	Novel fluorescent substrates for sEH. All compounds have the chemical motive <b>1</b> in common while various ester or carbonate groups holding an epoxide each complete the structures ( <b>2</b> through <b>9</b> ). These variable molecule parts are positioned at the 'R' moiety of the basic structure. (R = rest) .....	35
Figure 12	Reaction mechanism of novel fluorescent substrates for sEH - ester <b>3</b> serves as example. ....	36
Figure 13	Determination of aqueous solubility for compound <b>2</b> . The presented absorbance data correspond to mean values $\pm$ standard deviation (n=3). ....	46
Figure 14	Aqueous stabilities of compound <b>5</b> at different pH values. Data are shown as mean values $\pm$ standard deviation (n=3). ....	47
Figure 15	Self-hydrolysis rates of fluorescent substrates. Data correspond to means $\pm$ standard deviation (n $\geq$ 30). ....	48
Figure 16	Aqueous stability of NEPC and substrate <b>7</b> at two concentrations each. Values represent means $\pm$ standard deviation (n $\geq$ 3). ....	48
Figure 17	Enzyme kinetics of compound <b>7</b> in combination with various recombinant sEHs. Data are shown as average velocities $\pm$ standard deviation (n=4 for human and mouse sEH; n=3 for cress, rat and potato sEH). ....	51
Figure 18	Enzyme kinetics of compound <b>4</b> in combination with various recombinant sEHs. Data represent average velocities $\pm$ standard deviation (n=4 for human and mouse sEH; n=3 for cress, rat and potato sEH). ....	51
Figure 19	Appearance of 6-methoxy-2-naphthaldehyde over time in reactions with various concentrations of human sEH and substrate <b>7</b> at 10 $\mu$ M. This chart illustrates the observed lag times of reactions employing low enzyme concentrations. ....	54
Figure 20	Time course of normalized 6-methoxy-2-naphthaldehyde appearance for optimized endpoint assay conditions ( $[E]_{\text{final}} = 3 \text{ nM}$ ; $[S]_{\text{final}} = 50 \text{ } \mu\text{M}$ ; 200 $\mu$ l assay volume) in comparison to self-hydrolysis of compound <b>3</b> . The dashed line exemplifies the linear regression analysis result after 90 min of enzymatic reaction ( $r^2=0.994$ ). ....	56
Figure 21	Increase of initial velocity $v$ caused by increasing human sEH amounts per well at a compound <b>3</b> concentration of 50 $\mu$ M. ....	56
Figure 22	Influence of $\text{ZnSO}_4$ and $\text{Zn}(\text{NO}_3)_2$ at 0.2 M on the fluorescent signal of 6-methoxy-2-naphthaldehyde. ....	62
Figure 23	Schematic plot of initial velocity $v$ versus substrate concentration $[S]$ following the theory of Michaelis-Menten. ( $V_{\text{max}}$ = maximal velocity; $K_m$ = Michaelis-Menten constant) .....	68
Figure 24	Specific activities of selected human cell lines. Displayed data represent means $\pm$ standard deviation from determinations in triplicate. ....	86

Figure 25	GFP expression of 22RV1 cells, which were electroporated employing the Nucleofector program T-27 to introduce a GFP-encoding mammalian expression vector. The picture was taken 24 h after electroporation by means of an inverted light / fluorescent microscope and an attached digital camera at 100x magnification. The right part of the figure displays the sight under light-microscopic conditions, whereas the left one shows the same cells when viewed utilizing the fluorescent mode of the microscope equipped with the dichroic mirror unit IMT2-DMB. ....	87
Figure 26	Effect of lipofection-mediated introduction of 4 different siRNAs as well as a mixture of them on human sEH activity in 22RV1 cells. Enzyme activities at 48 h past lipofection are displayed relative to treatment with a non-targeting siRNA. Data represent results of 3 independent experiments and are shown as means $\pm$ standard deviation (refer to method part for calculation details). ....	88
Figure 27	Representative photomicrographs of 22RV1 cells treated with fluorescently labeled siRNAs. All pictures were taken at 48 h after treatment by means of an inverted light / fluorescent microscope (Olympus IMT-2, Olympus Corp., Melville, NY, USA) and an attached digital camera (Olympus MicroFire, Olympus Corp., Melville, NY, USA) at 400x magnification. The right part of each picture documents the sight under light-microscopic conditions, whereas the left one displays the same cells when viewed by means of the fluorescent mode of the microscope equipped with the dichroic mirror unit IMT2-DMG. siRNA introduction was performed via lipofection ( <b>A</b> ) and electroporation ( <b>B</b> ). ....	89
Figure 28	RNAi effect of several siRNAs on human sEH activity in 22RV1 cells following electroporation. Results of three individual experiments, represented by the different bar types, are displayed relative to treatments with a non-targeting siRNA. Data are shown as means $\pm$ standard deviation of determination (see text for detailed information on calculation). ....	89
Figure 29	Time-response of 22RV1 cells to electroporation introducing a mixture of 4 human sEH-targeting siRNAs. Each datum point was set relative to simultaneously performed cell treatment with non-targeting siRNAs. <b>A</b> RNAi effect on enzyme activity. Data represent results from 3 independent experiments and are shown as means $\pm$ standard deviation (refer to method part for calculation details). However, datum points at 36 h and 96 h only represent findings from 2 independent experiments. <b>B</b> Direct comparison of enzyme activity level and mRNA level during a single time-response experiment. Data are displayed as relative means of calculated values $\pm$ standard deviation (for calculation of these values see methods part). ....	90
Figure 30	Dose-response of 22RV1 cells to electroporation with siHsEH 3 as well as a mixture of all 4 siRNAs. Human sEH activities indicating the RNAi effect are displayed relative to the respective variants, which were treated with the same amount of non-targeting siRNAs. Data represent results of 3 independent experiments and are shown as means $\pm$ standard deviation. ....	91



## CATALOGUE OF TABLES

Table 1	Final enzyme concentrations employed in the determination of the Michaelis-Menten parameters $K_m$ and $V_{max}$ . $[E]_{final}$ in nM. ....	41
Table 2	Determined concentration range for the apparent LS of fluorescent substrates <b>2</b> through <b>9</b> . ....	47
Table 3	Specific activities of recombinant soluble epoxide hydrolases and porcine liver esterase for compounds <b>2</b> through <b>9</b> in $\text{nmol min}^{-1} \text{mg}^{-1}$ . Specific activities are given as slopes $\pm$ standard error determined by linear regression analysis. ....	49
Table 4	$K_m/V_{max}$ values of combinations between several sEHs and fluorescent substrates <b>2</b> through <b>9</b> . Results were obtained by linear regression analyses of Lineweaver-Burk plots. Numbers are given as means $\pm$ standard deviation ( $n=4$ for human and mouse sEH; $n=3$ for cress, rat and potato sEH) in $\text{min } \mu\text{M nmol}^{-1}$ . ....	52
Table 5	$k_{cat}/K_m$ values of substrates <b>2</b> through <b>9</b> in combination with various soluble epoxide hydrolases. Numbers are given as means $\pm$ standard deviation ( $n=4$ for human and mouse sEH; $n=3$ for cress, rat and potato sEH) in $\text{s}^{-1} \mu\text{M}^{-1}$ . ....	53
Table 6	Results of the checkerboard assay for the optimization of human sEH and compound <b>3</b> concentrations. The three numbers given for each combination of concentrations represent – from top to bottom – (a) the squared linear correlation coefficient $r^2$ analyzing reporter molecule appearance for 60 min reaction time, (b) the ratio of fluorescent signal to background after 60 min and (c) the percentage of compound <b>3</b> turned over after 60 min. ....	55
Table 7	Assay conditions and $IC_{50}$ values of sEH inhibitors determined with the new assay systems that employ substrates <b>7</b> and <b>3</b> . Numbers are given as average of at least three replicates in $\text{nM } \pm$ standard deviation. ....	57
Table 8	Precision and accuracy data as well as $Z'$ values acquired from the fluorescent endpoint system validation. Mean accuracy was determined by calculating the ratio of the determined inhibition percentage, divided by the nominal value, and multiplying it with 100%. Precision or CV (coefficient of variation) values represent standard deviations of fluorescent signal, divided by the mean fluorescent signal of maximum enzyme activity, and multiplied by 100%. $Z'$ was calculated as previously described (Zhang et al., 1999). ....	59
Table 9	Qualitative influence of stop solutions on enzymatic hydrolysis rate and fluorescence level under endpoint assay conditions. After 60 min of incubation at room temperature in the dark, 50 $\mu\text{l}$ of stop solution were added to the enzymatic reaction (200 $\mu\text{l}$ ), and the fluorescent signal was monitored for 10 min. Variations were classified with the terms <i>constant</i> (difference to the reference value $\pm$ 10%), <i>slightly elevated / reduced</i> (10 to 20% variation relative to the reference), <i>elevated / reduced</i> (20-50% above / below the reference value), or <i>significantly elevated / reduced</i> ( $>$ 50% difference to the reference value). ....	60

---

Table 10	Influence of different concentrations of ZnSO <sub>4</sub> and Zn(NO <sub>3</sub> ) <sub>2</sub> on hydrolysis rate and fluorescence level of ongoing reactions between human sEH and compound <b>3</b> . Zinc salts were employed as aqueous stop solutions after 1 h of enzymatic reaction and results were set relative to the reference value obtained by buffer addition. Values are displayed as means ± standard deviation (n=3). .....	61
Table 11	$k_{cat}/K_m$ values for various recombinant sEH enzymes with <i>t</i> DPPO and NEPC obtained from earlier studies. Quotients are given in s <sup>-1</sup> μM <sup>-1</sup> . .....	66
Table 12	Previously (see text) determined IC <sub>50</sub> values for selected sEH inhibitors and employed assay conditions. Data are shown as means ± standard deviation in nM. ....	73
Table 13	siRNA sequences of the present study directed against human sEH. Sequences were provided by Dharmacon, Inc. (Chicago, IL, USA) and are given in 5'-3' direction. ....	83

## ABBREVIATIONS

μg	microgram(s)
μl	microliter(s)
μM	micromolar
Å	ångström
A <sub>800</sub>	absorbance at 800 nm
Ago	Argonaute
ALS	amyotrophic lateral sclerosis
AMD	age-related macular degeneration
ARDS	acute respiratory distress syndrome
Asp	aspartic acid
ATP	adenosine triphosphate
AUDA	12-(3-adamantane-1-yl-ureido)-dodecanoic acid
BCA	bicinchoninic acid
bp	base pair(s)
BisTris	2-[bis(2-hydroxyethyl)amino]-2(hydroxy-methyl)-1,3-propanediol (BisTris)
BSA	bovine serum albumin
c.	circa
cDNA	copy DNA
CDU	1-cyclohexyl-3-dodecyl-urea
CEU	1-cyclohexyl-3-ethyl urea
cf.	compare (from latin “confer”)
CHU	1-cyclohexyl-3-hexyl urea
CIU	N-cyclohexyl-N’—(4-iodophenyl)urea
cM	centimorgan
COPD	chronic obstructive pulmonary disease
CV	coefficient of variation
DNA	deoxyribonucleic acid
DCU	dicyclohexylurea
dFXR	Drosophila homolog of the fragile X protein
DHET	dihydroxyeicosatrienoic acid
DMF	dimethyl formamide
DMSO	dimethyl sulfoxide
dsRBD	double-stranded RNA binding domain
dsRNA	double-stranded RNA

DTT	dithiothreitol
[E] or [E] <sub>final</sub>	final enzyme concentration
EDTA	ethylenediaminetetraacetic acid
EET	epoxyeicosatrienoic acid
EH	epoxide hydrolase
eIF2C2	eukaryotic translation initiation factor 2C2
ER	endoplasmatic reticulum
et al.	and coworkers
FBS	fetal bovine serum
Fig.	Figure
FMRP	fragile X mental retardation protein
GAPD	glyceraldehyde-3-phosphate dehydrogenase
GFP	green fluorescent protein
GST	glutathione <i>S</i> -transferase
H <sub>2</sub> O <sub>2</sub>	hydrogen peroxide
HCl	hydrochloric acid
His	histidine
HLC	human liver cytosol
HP	heterochromatin protein
[I]	final inhibitor concentration
IC <sub>50</sub>	inhibitor concentration, by which 50% of the enzyme activity of interest is blocked
IFN	interferon
IL	interleukin
IRF	interferon regulatory factor(s)
kbp	kilo base pair(s)
<i>k</i> <sub>cat</sub>	catalytic constant
kDa	kilodalton(s)
<i>K</i> <sub>i</sub>	inhibitor constant
<i>K</i> <sub>m</sub>	Michaelis-Menten constant
LS	limit of solubility
LSC	liquid scintillation count(ing)
M	molar
mEH	microsomal epoxide hydrolase
Met	methionine
mg	milligram(s)
miRNA	microRNA
miRNP	microRNA-containing ribonucleoprotein complex

min	minute
ml	milliliter(s)
mm	millimeter(s)
mM	millimolar
mRNA	messenger RNA
n	number or replicates
nd	not determined
NEB	4-nitrophenyl <i>trans</i> -3,4-epoxy-4-phenylbutanoate
NEH	4-nitrophenyl <i>trans</i> -3,4-epoxyhexanoate
NEPC	4-nitrophenyl- <i>trans</i> -2,3-epoxy-3-phenylpropyl carbonate
ng	nanogram(s)
nm	nanometer(s)
nM	nanomolar
nmol	nanomole(s)
NSD	nonstop decay
nt	nucleotide(s)
OD	optical density
P450	cytochrome P450
PAZ	protein consisting of PIWI, ARGONAUTE and ZWILLE domains
PCR	polymerase chain reaction
PEG	polyethylene glycol
PEI	polyethylenimine
pH	logarithmic measure of hydrogen ion concentration
PKR	protein kinase R
pmol	picomole(s)
PMSF	phenylmethylsulphonylfluoride
PPAR $\alpha$	peroxisome proliferator-activated receptor $\alpha$
PTGS	post-transcriptional gene silencing
QSAR	structure activity relationship
R	rest
$r^2$	squared correlation coefficient
RDR	RNA-dependent RNA polymerase
RDRP	RNA-dependent RNA polymerase
RFU	relative fluorescence unit(s)
RIG	retinoic acid-inducible gene
RISC	RNA-induced silencing complex
RNA	ribonucleic acid

RNase	ribonuclease
RNAi	RNA interference
s	second(s)
[S] or [S] <sub>final</sub>	final substrate concentration
SDS	sodium dodecyl sulphate
SDS-PAGE	sodium dodecyl sulphate polyacryl amid gel electrophoresis
sEH	soluble epoxide hydrolase
SHR	spontaneously hypertensive rat
shRNA	short hairpin RNA
siRNA	short interfering RNA
<i>t</i> DPPO	<i>trans</i> -1,3-diphenylpropene oxide
THF	tetrahydrofurane
TLR	toll-like receptor
TNF	tumor necrosis factor
TRBP	HIV-1 TAR RNA binding protein
TSO	<i>trans</i> -stilbene oxide
Tyr	tyrosine
<i>v</i>	initial velocity
v	volume
Val	valine
<i>V</i> <sub>max</sub>	maximal velocity
w	weight

## PREFACE

*“Satisfaction of one's curiosity is one of the greatest sources of happiness in life.”*

Linus Pauling (1901-1994)

According to this statement of the great American chemist, physicist and Nobel Prize winner Linus Pauling, the ideal profession has to be – probably besides working as a journalist – in science. I have always felt that way, even though I had my fair share of frustrations and failures doing research. But to my experience, all annoyance and disappointment about weeks of wasted lab work (and in my case there has been plenty of that) simply vanish with a single successful experiment or interesting experimental results.

Overall, the past three years have been full of happiness for me – partially because my curiosity was well satisfied (never enough though!), but also because the time was filled with exciting events and experiences in two distinct parts of the world: California and Bavaria. In both places I enjoyed scientific, philosophical as well as interpersonal discussions, wonderful hikes in stunning nature, multicultural exchanges and culinary events, enlightening and valuable collaborations, water-balloon fights, plenty of board games and great people to share these things with. I had the wonderful opportunity to get to know the sunshine state California a little and am sure to be longing not only for the climate there for at least a couple more years. Naturally and as already mentioned, I also went through setbacks. But despite (or because of?) those I think I was able to learn a lot – scientifically as well as generally about human nature and my own person.

Concluding, I would like to quote a sentence from one of my favorite books, which became a valuable maxim for me during the last few years and which probably most graduate students get to learn during their studies:

*“... anything's possible if you've got enough nerve.”*

J.K. Rowling, Harry Potter and the Order of the Phoenix

## ACKNOWLEDGEMENTS

Before starting off my actual thesis I would like to take the opportunity and thank all the people and institutions, who made my graduate studies at UC Davis and the Center of Life Sciences in Weihenstephan either possible, much more enjoyable or both.

The Bavarian research foundation (“**Bayerische Forschungsstiftung**”) granted me with a fellowship and thus made the extraordinary experience to do research in two different parts of the world possible. Hereby, a special “thank you” goes to **Prof. Dr. Friedrich R. Kreißl**, who was extremely helpful and obliging.

**Prof. Dr. Bertold Hock** and **Prof. Dr. Bruce D. Hammock** kindly took me on as their PhD student, provided me with exciting projects, lab space, freedom in research and a great deal more confidence in my work than I sometimes had. I cannot thank both of them enough for this opportunity and recommend to any other graduate student to have two considerate ‘doctorate fathers’ just as I did.

In this context, I would also like to express my gratitude to **Prof. Dr. Siegfried Scherer** as well as to **Prof. Dr. Dieter Langosch** for agreeing to serve on my examination committee.

**Dr. Christophe Morisseau** was my mentor for enzymatic and philosophical problems during the last three years. He always had an open ear for me, answered all my more or less fatuous questions with patience and wit and determined the  $IC_{50}$ s with the continuous fluorescent assay (I am still waiting for the bill!). During the concluding writing process he was extremely helpful with constructive critics and valuable suggestions. I am particularly thankful for all he did.

I am also indebted to **Dr. Paul Jones**. He not only provided me with the fluorescent substrates for one of my dissertation projects, but too was very patient in explaining chemistry and all sorts of other things worth knowing.

A series of people kindly provided me with cell lines that made the second project of my dissertation possible. **Prof. Dr. Michael ‘Ernie’ Arand** (Department of Medicine, University of Zurich) started me off with sEH-expressing and nicely growing cells. **Ruth Vinall** and **Prof. Dr. Ralph De Vere White** from the UC Davis Cancer Center as well as **Prof. Dr. Robert Rice** (Department of Nutrition, UC Davis), **Alan Epstein** (MD, PhD; USC, Keck School of Medicine, Los Angeles, CA,



USA) and **Gerald DeNardo** (MD; UC Health Center, Sacramento, CA) generously made a number of cell lines available for sEH activity testing. A big thank belongs to all of them.

The **group of Dr. Charles Stephensen** (Department of Nutrition, UC Davis) and here in particular **Alina Wettstein** was extremely helpful and allowed me to use their LightCycler® instrument, which I am still very grateful for. The same statement is valid for the group of **Prof. Dr. Dr. Johann Bauer** and **Angelika Notzon** in Weihenstephan, who introduced me to the fascinating world of quantitative PCR.

Furthermore, I would like to thank **Dr. Hiromasa Tanaka, Dr. Katja Dettmer, Dr. Jeanette Stok, Dr. Marja Koivunen, Dr. George Kamita** and **Zung Do** for being my Davis lab family throughout this period. Their friendship and expertise helped me through hard times and let me enjoy the good times even more. I am sure that their encouragement and trust in me and my work contributed to the completion of my studies.

I had the great pleasure to meet and work with a lot of extraordinary people in the **Hammock lab** as well as the **Hock lab**, but it would lead way too far to name them all. Nevertheless I am thankful to all of them, each one for different reasons.

I owe a lot to my Davis housemates **Lassie, Bruce, Bruce and Frances** who made my life in Davis a lot more fun with discussions, evening walks, hikes and settler games. I had a wonderful time living with them and the cats and am grateful to have got to know all of them.

Last but not least I would like to thank **my parents** for their never ending love and faith in me. I owe them all I was, am and will be and am very thankful for everything they did and still do to support me.

**ABSTRACT**

Soluble epoxide hydrolase (sEH) represents a promising new drug target in the treatment of hypertension and vascular inflammation. Its chemical inhibition was previously shown *in vivo* to lower blood pressure, protect the kidney from hypertension-caused damage as well as trigger anti-inflammatory effects. This dissertation is based on two projects connected to the elimination of sEH activity: the development of novel fluorescent assay systems testing potential sEH inhibitors and the post-transcriptional down-regulation of this enzyme on the cellular level by RNA interference (RNAi).

In the first part, a series of novel  $\alpha$ -cyanoester and  $\alpha$ -cyanocarbonate epoxides were evaluated as potential sEH substrates for the development of two test systems: a rapid kinetic assay with improved sensitivity compared to the existing spectrophotometric test system as well as an endpoint assay with long incubation times that could be used for high-throughput screening of large compound libraries. Cyano(6-methoxy-naphthalen-2-yl)methyl *trans*-((3-phenyloxiran-2-yl)methyl) carbonate displayed a comparatively high specific activity with human sEH and was therefore selected for the rapid test system, while (3-phenyl-oxiranyl)-acetic acid cyano-(6-methoxy-naphthalen-2-yl)-methyl ester was chosen for the endpoint assay due to its high aqueous solubility and stability. Enzyme and substrate concentrations were optimized for both systems to achieve the desired assay sensitivity, reliability and reproducibility. The subsequent assay validation, which employed these optimized concentrations to test previously characterized inhibitors, confirmed the usefulness and applicability of both systems regarding sensitivity, accuracy and precision. The two novel fluorescence-based assay systems will be valuable tools in the development of improved sEH inhibitors and will thus help to enhance the treatment of vascular inflammation and hypertension.

The second part deals with the endogenous silencing mechanism RNAi to post-transcriptionally down-regulate sEH and thus to provide an alternative to its chemical inhibition, which is still lacking a compound of therapeutic value. This objective first required the search for an appropriate human cell model system expressing sEH in easily detectable amounts. Out of the examined cell lines, the prostate carcinoma cell line 22RV1 was selected due to its comparatively high specific sEH activity. Subsequent experiments introducing synthetic siRNAs (short interfering RNAs) into the cells by electroporation

were able to repeatedly show a 50% down-regulation of the target gene expression up to at least 96 h. This result is based on analyses of enzyme activity levels as well as mRNA levels of siRNA-treated cells. Although a higher impact on sEH mRNA and enzyme activity level was expected by RNAi, this study might represent a first step toward an alternative therapeutic approach for the cure of glaucoma, COPD (chronic obstructive pulmonary disease) and maybe even hypertension.

## ZUSAMMENFASSUNG

Die chemische Hemmung des Enzyms Lösliche Epoxidhydrolase (sEH) bietet einen neuen Ansatz zur Therapie von Bluthochdruck und vaskulären Entzündungskrankheiten. In *in vivo* Experimenten konnte bereits belegt werden, dass durch diese Behandlung sowohl die Senkung von Bluthochdruck, der Schutz von Nieren vor bluthochdruckbedingter Schädigung als auch ein weiterer antiinflammatorischer Effekt möglich ist. Die hier vorliegende Dissertation basiert auf zwei unterschiedlichen Projekten, die beide mit der Ausschaltung der sEH-Aktivität in Zusammenhang stehen: der Entwicklung neuer, fluoreszenzbasierter Testsysteme, die chemische Verbindungen auf ihr sEH-Inhibitionspotential überprüfen, und der posttranskriptionellen Ausschaltung dieses Enzyms auf zellulärer Ebene durch RNA Interferenz (RNAi).

Im ersten Teil wurde eine Reihe neuartiger  $\alpha$ -Cyanoester- und  $\alpha$ -Cyanokarbonatepoxide als sEH-Substrate im Zusammenhang mit der Entwicklung sowohl eines schnell durchführbaren kinetischen Tests als auch eines Endpunktassays charakterisiert und erprobt. Die hohe spezifische Aktivität von Cyano(6-methoxy-naphthalen-2-yl)methyl-*trans*-((3-phenyloxiran-2-yl)methyl)-carbonat in Kombination mit humaner löslicher Epoxidhydrolase gab den Ausschlag für die Wahl dieses Substrates für den kinetischen Test. Dieser sollte im Vergleich zum bestehenden spektrophotometrischen System eine deutlich erhöhte Sensitivität aufweisen, um so bisher in ihrer Inhibitionskraft schwer unterscheidbare sEH-Inhibitoren differenzieren zu können. (3-Phenyl-oxiranyl)-essigsäure-cyano-(6-methoxy-naphthalen-2-yl)-methylester wurde dagegen aufgrund seiner hohen Löslichkeit und Stabilität in wässriger Umgebung als Substrat für einen Endpunkttest mit langer Reaktionszeit gewählt. Die Entwicklung eines solchen Assays sollte es ermöglichen, große Bibliotheken chemischer Verbindungen in einem Verfahren mit hohen Durchsatzraten auf sEH-inhibierende Stoffe zu sichten. Enzym- und Substratkonzentrationen wurden für beide Systeme optimiert, um die angestrebten Testempfindlichkeiten und -reproduzierbarkeiten zu gewährleisten. Die darauf folgende Validierung der entwickelten Assays mit bereits charakterisierten sEH-Inhibitoren bestätigte und bekräftigte deren Nutzen und praktische Durchführbarkeit. Die beiden beschriebenen Testsysteme werden sich bei der Weiterentwicklung bestehender und Entdeckung neuer sEH-Inhibitoren mit

Sicherheit als äußerst wertvoll erweisen und damit höchstwahrscheinlich die Behandlung von Bluthochdruck und vaskulären Entzündungen verbessern.

Im zweiten Teil wurde die Möglichkeit untersucht, sEH durch den endogenen Mechanismus RNAi, der posttranskriptionell und spezifisch der Expression von Zielgenen entgegenwirkt, herunterzuregulieren und somit eine Alternative zur chemischen Hemmung des Enzyms zu schaffen. Voraussetzung für dieses Projekt war allerdings, ein zelluläres Modellsystem zu finden, das sEH in detektierbaren Mengen exprimiert. Nach der Untersuchung mehrerer humaner Zelllinien wurde die Prostatakrebszelllinie 22RV1 aufgrund ihrer vergleichsweise hohen spezifischen sEH-Aktivität ausgewählt, als Modell für die weiteren Experimente dieser Studie zu fungieren. Hierbei konnte – ausgelöst durch Elektroporation mit synthetischen siRNAs (short interfering RNAs) – reproduzierbar eine 50%ige sEH-Reduktion ausgelöst werden, die sowohl auf Enzymaktivitätsebene als auch auf mRNA-Ebene feststellbar war und bis mindestens 96 h nach der Elektroporation anhielt. Obgleich die Wirkung der siRNA-Behandlung auf die zelluläre sEH-Expression geringer war als erwartet, kann diese Studie doch einen ersten Schritt in Richtung eines alternativen therapeutischen Ansatzes zur Behandlung von grünem Star, chronischem unspezifischem respiratorischem Syndrom (COPD) und vielleicht sogar Bluthochdruck darstellen.

**INTRODUCTION**

For the present dissertation two distinct major projects were carried out, which are both connected to the enzyme soluble epoxide hydrolase (sEH) and the elimination of its activity. In recent years, this protein has been drawing more and more attention due to its potential as novel drug target: In various experiments, chemical sEH inhibition triggered successful treatment of hypertension (Yu et al., 2000; Imig et al., 2002), protection against renal damage caused by hypertension (Zhao et al., 2004) and inflammatory diseases (Schmelzer et al., 2005; Smith et al., 2005) in rodent models.

The first part of this dissertation illustrates the development of two novel enzymatic *in vitro* inhibitor assays, which are based on the release of a fluorescent reporter molecule after substrate turnover by sEH. These became mandatory due to the extensive quest for highly potent chemical sEH inhibitors as well as their progressing refinement.

The cellular knockdown of sEH by RNAi (RNA interference), representing the second part, was intended to ultimately offer an alternative to chemical inhibition of the enzyme. This approach employed the relatively recently discovered endogenous mechanism RNAi, which post-transcriptionally and specifically silences target proteins by means of short double-stranded RNA (dsRNA).

For the better understanding of these two distinct projects, a literature overview on sEH as well as RNAi is given, which precedes the experimental part of the present work.

## THEORETICAL BACKGROUND

The following section introduces properties and biological role of the soluble epoxide hydrolase as well as gives an overview of the RNAi mechanism, its original role and applicability.

### 1 Soluble epoxide hydrolase

The properties of the enzyme soluble epoxide hydrolase (sEH), the protein of interest in this dissertation, will be described first. Emphasis will be laid upon mammalian sEHs and hereby in particular upon murine and human sEH since these two proteins have been characterized best so far.

#### 1.1 General properties of epoxide hydrolases

Soluble epoxide hydrolase (sEH) belongs to the general group of epoxide hydrolases (EH; EC 3.3.2.3), which is defined via its ability to catalyze the conversion of epoxides to their corresponding diols. This involves, as indicated in Figure 1, the addition of a water molecule (Oesch, 1973; Arand et al., 1994).

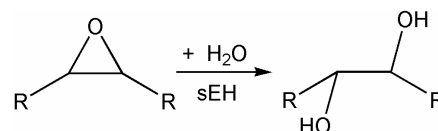


**Fig. 1** Conversion of epoxides by sEH. (R = rest)

Epoxides or oxiranes are three-membered organic ring systems containing one oxygen each. They originate from endogenous as well as xenobiotic compounds via chemical and enzymatic oxidation processes including the cytochrome P450 monooxygenase system. Some members of this compound group are typically unstable in an aqueous environment and chemically reactive, while at the other extreme, some epoxides are environmentally persistent. For xenobiotics and certain endogenous substances, epoxide intermediates have been shown to be highly potent mutagens, carcinogens and toxins (Guengerich, 1982; Sayer et al., 1985; Adams et al., 1995). The hydration of epoxides, possibly catalyzed by EH, generally leads to more stable and less reactive intermediates. However, exceptions do exist (Fretland and Omiecinski, 2000).

Overall, the main functions of EHs are regarded as detoxification, catabolism and regulation of signaling molecules. In microorganisms, they seem to play a significant role in the catabolism of specific carbon sources from natural supplies (Allen and Jacoby, 1969; van der Werf et al., 1999) as well as environmental contaminants (Jacobs et al., 1991). However, microbial EHs are mainly studied due to their chiral selectivity and thus potential uses in chemistry (Archelas and Furstoss, 2001; de Vries and Janssen, 2003). Several plant EHs have been described, which possibly have similar roles attributed to mammalian EHs in addition to being involved in the production of cutin and phytoalexins (Blee and Schuber, 1992; Kiyosue et al., 1994; Stapleton et al., 1994). In insects an EH with activity against octane oxide has been purified (Mullin and Wilkinson, 1980) and seems to be distinct from other insect EHs involved in the degradation of certain cyclodiene insecticides and insect juvenile hormone. The insect EHs that degrade the juvenile hormone may be important regulators of insect development and reproduction (Hammock et al., 1985; Halarnkar and Schooley, 1990).

Five different forms of mammalian EHs are reported in the literature: cholesterol epoxide hydrolase (or cholesterol 5, 6-oxide hydrolase), hepoxilin A<sub>3</sub> hydrolase, leukotriene A<sub>4</sub> hydrolase, microsomal epoxide hydrolase and soluble epoxide hydrolase. **Cholesterol epoxide hydrolase** hydrates compounds related to the 5,6-epoxide of cholesterol (Nashed et al., 1985; Finley and Hammock, 1988) and is widely distributed in all tissues with its greatest enzymatic activity in liver microsomes (Astrom et al., 1986). Just as it is the case for hepoxilin A<sub>3</sub> hydrolase, its gene or cDNA has not been cloned and characterized yet. **Hepoxilin A<sub>3</sub> hydrolase** is described as a cytosolic enzyme that metabolizes hepoxilin A<sub>3</sub>, a hydroxyl-epoxide derivative of arachidonic acid (Pace-Asciak and Lee, 1989). **Leukotriene A<sub>4</sub> hydrolase** is a cytosolic, bi-functional Zn<sup>2+</sup> containing enzyme that exhibits both hydrolase activity as well as aminopeptidase activity (Haeggstrom et al., 1994). The human gene for this ubiquitously expressed enzyme (McGee and Fitzpatrick, 1985; Fu et al., 1989; Rybina et al., 1997) that produces hormone derivatives of arachidonic acid (Samuelsson, 1983) has been cloned and characterized (Mancini and Evans, 1995). Based on sequence alignment studies, leukotriene A<sub>4</sub> hydrolase is unlikely to be related to other EHs, in particular microsomal and soluble epoxide hydrolase and does not share their enzymatic mechanism (Beetham et al., 1995). **Microsomal epoxide hydrolase** (mEH) as well as sEH belong to the  $\alpha/\beta$ -hydrolasefold family of proteins, which also includes esterases,



some proteases, dehalogenases and lipases (Beetham et al., 1995; Hammock et al., 1997). Microsomal epoxide hydrolase is mainly located in the smooth endoplasmic reticulum (Lu and Miwa, 1980) with highest tissue activity in liver followed by testis, lung and heart (Morisseau and Hammock, 2002). However, it dissociates from the microsomes and may be found in serum under some pathological conditions. In this case it is referred to as the preneoplastic antigen (Hammock et al., 1997). The principal function of mEH is the detoxification of xenobiotics (Oesch, 1973) and it is especially active towards epoxides on cyclic and polycyclic systems and hydrates both monosubstituted and *cis*-disubstituted epoxides (Wixtrom and Hammock, 1985). Its subcellular localization, substrate preferences and pH optima (Hammock et al., 1997) distinguish mEH from **soluble epoxide hydrolase** (sEH).

### *1.2 Subcellular and tissue distribution of sEH*

Recent studies point toward the cell-specific subcellular localization of sEH. In hepatocytes and renal tubules, sEH was found in the cytosol as well as in peroxisomes (Mullen et al., 1999; Enayetallah et al., 2006). However, in a variety of other sEH expressing tissues, such as intestinal epithelium, adrenal gland or blood vessels, sEH was detected exclusively in the cytosol of the cells. On the other hand, no cell types could be found, in which sEH localized solely to the peroxisomal organelles (Enayetallah et al., 2006).

Regarding tissue distribution, sEH displays ubiquitous expression in mammals with highest levels in liver, kidney, breast tissue and heart. In intestine and vascular tissue high sEH levels were observed as well, whereas lung, testis, brain and spleen comparably express sEH in trace amounts. Additionally, sEH is expressed in various components of the human blood, predominantly though in lymphocytes and macrophages. It should be noted, that it is possible for the sEH protein level to be very high in certain cell types within a tissue whereas total tissue levels seem low (Wixtrom and Hammock, 1985; Pacifici et al., 1988; VanRollins et al., 1993; Fang et al., 1995; Johansson et al., 1995; Yu et al., 2000; Morisseau and Hammock, 2002). Moreover, levels of mammalian sEH, its activity respectively, were observed to be highly dependent on sex, age and species: they were found to be higher in male

than in female mice, higher in adult than fetal human tissue as well as 100-fold higher in mouse liver than in rat liver (Hammock et al., 1997; Morisseau and Hammock, 2002).

Interestingly, constitutive expression in many cancer cell lines has not been observed (Morisseau and Hammock, 2002). After a few days *in vitro*, primary cells drop dramatically in sEH expression, which complicates its *in vitro* investigation.

### *1.3 Induction of sEH*

Induction of sEH in rodent models has been observed during treatment with compounds causing peroxisome proliferation such as the anticholesteremic drug clofibrate – a phenomenon, which is thought to be connected to the PPAR $\alpha$  pathway (Moody et al., 1992; Grant et al., 1994; Fretland and Omiecinski, 2000). Besides this effect, administration of these particular chemicals results in the formation of hepatocellular carcinomas in rodents (Rao and Reddy, 1991).

Moreover, steroids display effects on changing the activities of the enzyme in mice (Hammock et al., 1997). For example, when supplemental testosterone was administered to castrated male mice, it was able to induce renal sEH expression and activity levels (Pinot et al., 1995b).

### *1.4 Molecular biology and protein structure*

Mammalian sEH genes have been cloned from several species: rat, pig, mouse and human (Beetham et al., 1993; Grant et al., 1993; Knehr et al., 1993; Newman et al., 2004). The latter two proteins are characterized best, and thus they will be emphasized regarding their molecular biology and protein structure.

The murine soluble epoxide hydrolase gene is located on chromosome 14 at  $14,0 \pm 3,7$  cM distal to Np-1 and  $19,2 \pm 4,3$  cM proximal to D14Mit7 (Grant et al., 1994) with a 1659 bp long open reading frame coding for a 553-residue protein of 62,5 kDa (Grant et al., 1993). The human sEH gene is found in chromosomal region 8p21-p12 (Larsson et al., 1995), stretches over approximately 45 kbp and consists of 19 exons of 27 to 265 bp (Sandberg and Meijer, 1996). The gene codes for 555, 554 respectively, amino acid residues (Beetham et al., 1993; Sandberg and Meijer, 1996) resulting in a monomeric protein of around the same molecular weight as its murine counterpart. The human and the

murine sEH gene are supposed to have developed from common ancestors due to a sequence identity of 73% and similar biochemical characteristics on protein level (Beetham et al., 1995). Genetic polymorphisms of the human gene were reported and investigated (Sandberg et al., 2000; Przybyla-Zawislak et al., 2003; Fornage et al., 2004; Sato et al., 2004; Srivastava et al., 2004; Fornage et al., 2005; Enayetallah and Grant, 2006; Lee et al., 2006a) suggesting possible biological roles in human metabolism and diseases.

Earlier sequence homology comparisons indicated a mammalian sEH protein organization of mainly two parts: a C-terminal domain homologous to bacterial haloalkane dehalogenase, mEH and plant sEH, and an N-terminal domain homologous to haloacid dehalogenase of *Pseudomonas* spec. (Beetham et al., 1995). Crystallographic analyses of murine and human sEH confirm this hypothesis and show the sEH protein to be a domain-swapped homodimer (Argiriadi et al., 1999; Gomez et al., 2004), that consists of two globular domains per subunit joined by a proline-rich linker (Thr-219 – Asp-234 for murine and Ile-219 – Asp-234 for human sEH; Gomez et al., 2004; Figure 2). However, it was also shown, that in solution both the monomeric as well as the dimeric protein are active (Gill, 1983; Dietze et al., 1990). The overall tertiary and quaternary structures of the murine and the human enzyme are highly similar, although some differences in the loop segments of the proteins as well as a shift of the two subunits away from each other by  $\sim 4$  Å were found (Gomez et al., 2004). Interestingly, plant sEHs lack the N-terminal domain of the protein (Beetham et al., 1995).

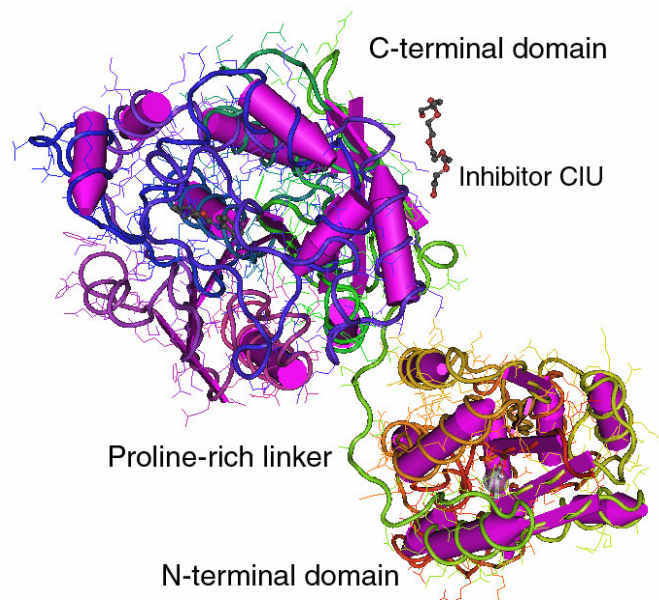


**Fig. 2** Protein structure of human soluble epoxide hydrolase. Picture was generated by means of the software Cn3D 4.1.

The **C-terminal domain** of sEH belongs to the  $\alpha/\beta$ -hydrolase fold family and displays epoxide hydrolase activity. Its catalytic site is located in a 25 Å long, “L”-shaped hydrophobic tunnel, with catalytic residues located at the bend. This holds true for both, the murine and the human enzyme (Argiriadi et al., 1999; Gomez et al., 2004).

The **N-terminal domain** of sEH has recently been demonstrated to possess  $Mg^{2+}$ -dependent phosphatase activity (Cronin et al., 2003; Newman et al., 2003). It adopts an  $\alpha/\beta$ -fold homologous to that of bacterial haloacid dehalogenase, the likely ancestor. The active site cleft in this domain displays the form of a hand with the  $Mg^{2+}$  binding site at the bottom of a 15 Å deep, negatively charged pocket. Additionally, a conserved hydrophobic tunnel of ~14 Å length was found, that would be sufficiently long enough to bind an aliphatic substrate (Gomez et al., 2004). Asp-9 is proposed to act as catalytic nucleophile (Cronin et al., 2003) in this case.

It should be noted, that both domains act independently. Cronin et al. (2003) demonstrated that the N-terminal domain of human sEH by itself exhibits  $Mg^{2+}$ -dependent phosphatase activity similar to the one measured for the complete enzyme. The biological function of the N-terminal domain is still unclear. However, at the very least it plays an important role in the stabilization of the domain-swapped quaternary structure of the homodimeric protein (Argiriadi et al., 1999).

### *1.5 Catalytic mechanism of sEH*

The current understanding of the epoxide hydrolase catalytic mechanism (Figure 3) is mainly supported by being part of the  $\alpha/\beta$ -hydrolase fold family of proteins with a nucleophile-histidine-acid catalytic triad as well as its relation to bacterial enzymes (Ollis et al., 1992; Verschueren et al., 1993; Arand et al., 1994; Holmquist, 2000) and several site-directed mutations of the active site of sEH (Pinot et al., 1995a; Yamada et al., 2000). Furthermore the isolation of a hydroxyacyl enzyme intermediate (Hammock et al., 1994) and crystal structure analyses of human and mouse sEH contributed to its comprehension (Argiriadi et al., 1999; Argiriadi et al., 2000; Gomez et al., 2004; Gomez et al., 2006).

The actual catalysis starts with a quick binding of the epoxide to the active site of the enzyme in its L-shaped hydrophobic tunnel. The active site consists in the human (murine) protein of Asp<sup>334</sup> (Asp<sup>333</sup>) as nucleophilic acid, His<sup>523</sup> (His<sup>523</sup>) as basic histidine, Asp<sup>495</sup> (Asp<sup>495</sup>) as orienting acid and

Tyr<sup>382</sup> as well as Tyr<sup>465</sup> (Tyr<sup>381</sup> and Tyr<sup>465</sup>) as polarizing tyrosines (Morisseau and Hammock, 2005; Gomez et al., 2006). The epoxide group is polarized by the mentioned tyrosine residues which form hydrogen bonds with the epoxide oxygen and thus act as general acid catalysts. Simultaneously, Asp<sup>334</sup> attacks the epoxide backside at the most reactive and usually least sterically hindered carbon, leading to the ring opening of the epoxide and an ester bond between the enzyme carboxylic acid and one alcohol functionality of the diol. This transiently existing compound is called the hydroxyl alkyl-enzyme intermediate. His<sup>523</sup>, Asp<sup>495</sup> and possibly other amino acids in the catalytic site of human sEH activate and orient the nucleophilic acid Asp<sup>334</sup>.

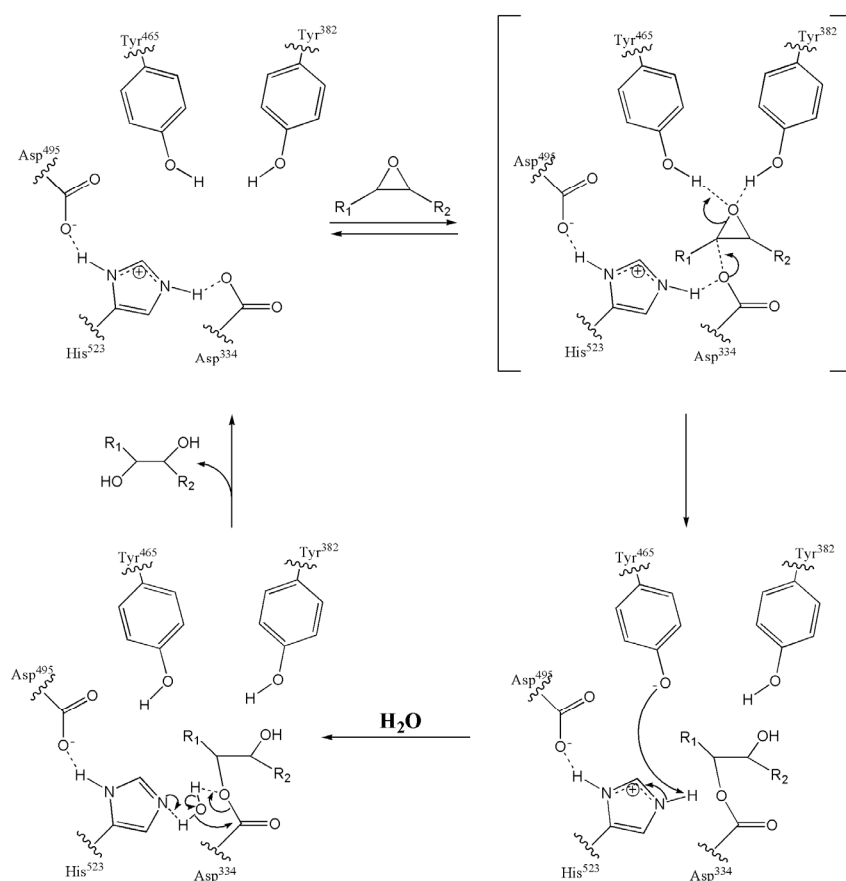


**Fig. 3** Catalytic mechanism of sEH illustrated by presenting the involved amino acid residues of human sEH. After Morisseau and Hammock (2005).

Once the intermediate between enzyme and substrate is formed, the histidine moves away from the ester making it possible for a water molecule to be activated by the ester-histidine pair. The activation of the water can only happen, if the histidine is not protonated (Schjøtt and Bruice, 2002).

The very basic water is now able to attack the carbonyl of the ester releasing the diol product and the original enzyme.

### 1.6 Substrates and inhibitors

The knowledge of specific substrates and inhibitors is crucial when characterizing an enzyme and exploring its biological role. Thus, an overview of these compounds will be given in the following passage.

In general, the C-terminal domain of sEH catalyzes the conversion of a broad spectrum of lipophilic substrates, but seems to prefer mono- (except styrene oxide), *cis*-di- and *trans*-di-substituted epoxides (Wixtrom and Hammock, 1985; Hammock et al., 1997). On the other hand, it shows very low activity on 1,1-disubstituted epoxides and epoxides on cyclic systems (Magdalou and Hammock, 1988). Endogenous substrates are epoxides formed during P450-mediated oxidation of polyunsaturated fatty

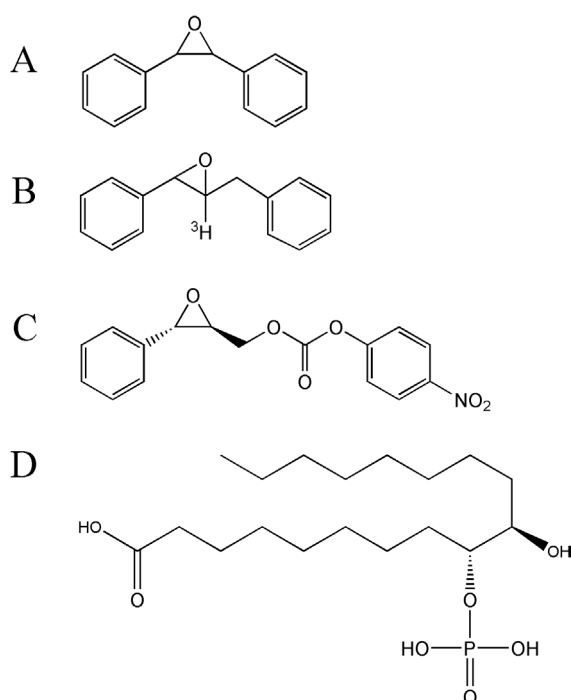


**Fig. 4** Substrates of soluble epoxide hydrolase for assay purposes. **A** *trans*-stilbene oxide (TSO) **B** *t*DPPO (*trans*-1,3-diphenylpropene oxide) **C** 4-nitrophenyl (2*S*,3*S*)-2,3-epoxy-3-phenylpropylcarbonat (NEPC) **D** 9,10-phosphonoxy-hydroxy-octadecanoic acid (serves as substrate for the N-terminal domain of sEH).

acids (Chacos et al., 1983; Halarnkar et al., 1989; Zeldin et al., 1993; Zeldin et al., 1995) creating or degrading oxylipins with a potential biological role. *trans*-Stilbene oxide (TSO; Figure 4 A) and *trans*-1,3-diphenylpropene oxide (*t*DPPO; Figure 4 B) represent first-rate surrogate substrates that are employed in radiometric *in vitro* partitioning assays. These are based on the separation of the epoxide into an organic and the formed diol into an aqueous phase (Wixtrom and Hammock, 1985; Borhan et al., 1995). 4-Nitrophenyl (2*S*,3*S*)-2,3-epoxy-3-phenylpropylcarbonat (NEPC; Figure 4 C) serves as photometric substrate for recombinant sEH (Dietze et al., 1994). Dihydroxy lipid

phosphates such as 9,10-phosphonoxy-hydroxy-octadecanoic acid (9,10-PHO; Figure 4 D) were suggested as possible endogenous substrates of the N-terminal domain of sEH (Newman et al., 2003).

The first identified inhibitors for sEH were epoxide containing compounds that acted as substrates with a relatively low turnover rate. This results in a transient *in vitro* inhibition with no relevance for cell culture and *in vivo* experiments (Magdalou and Hammock, 1988; Hammock et al., 1997; Morisseau et al., 1998). 1,3-disubstituted ureas, carbamates and amides were reported to represent more potent and stable inhibitors of sEH, that act stoichiometrically with purified recombinant sEH (Morisseau et al., 1999; Morisseau et al., 2002). These competitive tight-binding inhibitors with  $K_I$  values in the nanomolar range (Morisseau et al., 1999) were further improved using classical quantitative structure activity relationship (QSAR), 3D-QSAR and medicinal chemistry approaches (Nakagawa et al., 2000; Morisseau et al., 2002; McElroy et al., 2003; Kim et al., 2004c; Kim et al., 2005b). Crystallographic analyses show that the urea inhibitors form hydrogen bonds and salt bridges between the urea group of the inhibitor and the catalytic site of sEH, mimicking the intermediate during the catalyzed epoxide ring opening (Argiriadi et al., 1999; Argiriadi et al., 2000; Gomez et al., 2004). Surprisingly, there are major differences in the inhibitor binding between the human and the mouse enzyme: For example, N-cyclohexyl-N'-(4-iodophenyl)urea (CIU) displays opposite orientations in murine and human sEH when bound to the active site (Argiriadi et al., 2000; Gomez et al., 2004). This is due to the presence of a methionine residue (Met<sup>337</sup>) in the human enzyme – in contrast to Val<sup>337</sup> of the murine sEH – pointing into the catalytic cavity and thus constricting one side of the active site tunnel (Gomez et al., 2004; Gomez et al., 2006).

Additionally, sEH can be inhibited by  $Hg^{2+}$ ,  $Cu^{2+}$ ,  $Cd^{2+}$  and  $Zn^{2+}$  (Draper and Hammock, 1999). The latter cation acts noncompetitively on human sEH with a  $K_I$  around 20  $\mu M$ . It has also been found to inhibit the phosphatase activity of sEH (Newman et al., 2003) implying that the binding of  $Zn^{2+}$  at the  $Mg^{2+}$  site of the N-terminal domain results in some yet unknown allosteric effect leading to a loss of both catalytic activities of sEH (Morisseau and Hammock, 2005).

## 1.7 Biological role

For a long time, sEH – like mEH – was assumed to participate in xenobiotic metabolism, but there is no evidence supporting this hypothesis in mammals *in vivo* (Hammock et al., 1997; Arand et al., 2003). Nevertheless and as indicated before, sEH clearly participates in the conversion of endogenous mammalian arachidonic epoxides (epoxyeicosatrienoic acids or EETs; compare to Figure 5 A) and linoleic acid epoxides (also called leukotoxins; Figure 5 B) to their corresponding diols (Chacos et al., 1983; Halarnkar et al., 1989; Moghaddam et al., 1997; Yu et al., 2000) with biological functions of both the educts as well as the products. Therefore, possible roles of sEH in inflammation, blood pressure regulation and leukotoxin toxicity are indicated.

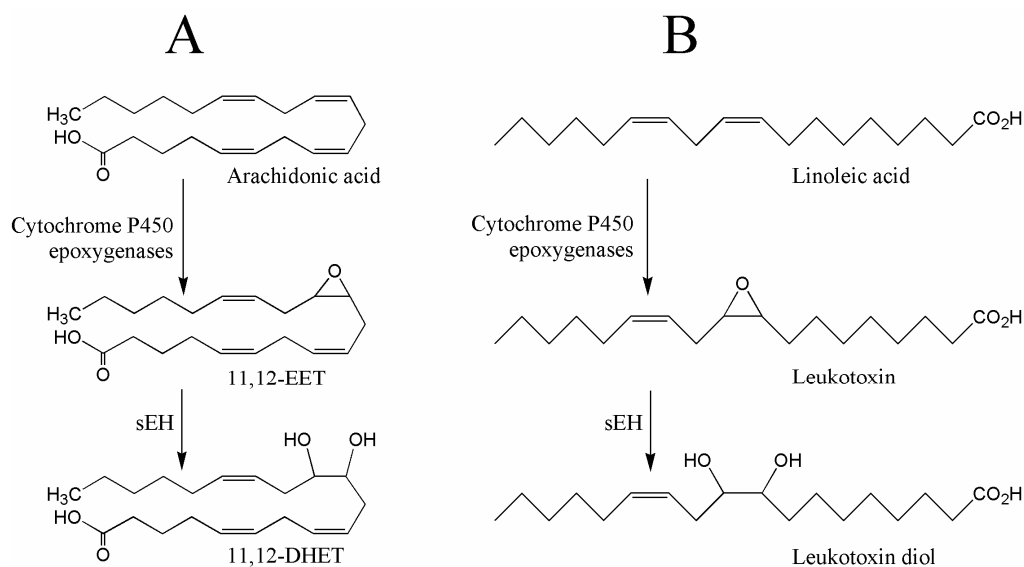


**Fig. 5** Endogenous metabolic pathways with sEH participation. **A** Conversion of the arachidonic acid-derived epoxide 11,12-EET to 11,12-DHET **B** Illustration of leukotoxin diol production from linoleic acid.

EETs affect blood pressure regulation as endogenous chemical mediators at the vascular, renal and cardiac level (Capdevila et al., 2000; Carroll and McGiff, 2000; Fleming, 2001). They induce vasodilation by activating  $\text{Ca}^{2+}$ -activated potassium channels, which results in hyperpolarization of the vascular smooth muscle. This way they produce vasorelaxation lowering blood pressure and alter myocardial perfusion (Harder et al., 1995; Campbell et al., 1996; Fisslthaler et al., 1999; Kroetz and Zeldin, 2002; Roman, 2002; Larsen et al., 2006). Furthermore, EETs were found to cause anti-inflammatory effects in endothelial cells (Node et al., 1999; Campbell, 2000; Liu et al., 2005b), effects



on smooth muscle migration (Sun et al., 2002), prostaglandin (PG) E<sub>2</sub> production (Fang et al., 1998), aromatase activity (Snyder et al., 2002) and Ca<sup>2+</sup> influx (Fang et al., 1999). Increased Ca<sup>2+</sup> entry (Graier et al., 1995; Mombouli et al., 1999) was observed in association with EETs as well as enhanced fibinolysis (Node et al., 2001) and a stimulation in tube formation (Munzenmaier and Harder, 2000). But functional effects can also be found in other tissues (Fitzpatrick et al., 1986; Seki et al., 1992; Wong et al., 1993; Peri et al., 1998; Chen et al., 1999; Lee et al., 1999; Lu et al., 2001a; Widstrom et al., 2001).

Dihydroxyeicosatrienoic acids (DHETs) represent the diols of EETs and are generally regarded as their inactivation products (Zeldin, 2001; Roman, 2002). Consequently, they display reduced activity in many systems compared to the respective corresponding epoxides, for example in the relaxation of the preglomerular vasculature (Imig et al., 1996) or the Ca<sup>2+</sup> uptake by porcine aortic smooth muscle cells and human coronary arterioles (Fang et al., 1999; Larsen et al., 2006). However, DHETs are also responsible for functional effects in other cases, such as the inhibition of the hydroosmotic action of arginine vasopressin in the kidney (Hirt et al., 1989) or the activation of the large conductance Ca<sup>2+</sup>-activated potassium channel of coronary artery myocytes in rat (Lu et al., 2001b). Besides, urinary DHETs are reported to act as modulators of renal water retention and are elevated in association with pregnancy-induced hypertension (Catella et al., 1990). Thus, DHETs serve as biomediators in some systems and are not only EET inactivation products (Spector et al., 2004).

The hydrolysis of epoxy-linoleate (leukotoxin) by sEH leads to a diol that disturbs membrane permeability and calcium homeostasis (Moghaddam et al., 1997). The result is inflammation regulated by nitric oxide synthase and endothelin-1 (Ishizaki et al., 1995a; Ishizaki et al., 1995b). Leukotoxin in micromolar concentrations has been associated with inflammation and hypoxia (Ozawa et al., 1986; Ozawa et al., 1991). In *in vitro* experiments it depresses mitochondrial respiration (Dudda et al., 1996) and evokes mammalian cardiopulmonary toxicity *in vivo* (Ozawa et al., 1986; Fukushima et al., 1988; Ishizaki et al., 1995a). The symptoms of leukotoxin toxicity resemble multiple organ failure and acute respiratory distress syndrome (ARDS) (Dudda et al., 1996). In both, *in vitro* and *in vivo* models, leukotoxin-mediated toxicity is dependent on epoxide hydrolysis (Moghaddam et al., 1997; Morisseau et al., 1999), implying sEH to be involved in the regulation of inflammation.

### *1.8 Soluble epoxide hydrolase as potential therapeutic target*

The biological role of sEH, including its substrates' and catalytic products' properties, as well as several recent observations suggest sEH as a potential therapeutic target.

To begin with, Sinal et al. (2000) reported that male sEH knockout mice show significantly lower blood pressure than wild type mice. Additionally, chemical inhibition of sEH resulted in blood pressure reduction in the spontaneously hypertensive rat (SHR) as well as in angiotensin II induced hypertension rat models (Yu et al., 2000; Imig et al., 2002; Imig et al., 2005). Therefore, treatment of hypertension by sEH inhibitors seems a promising therapeutic attempt. It has to be cautioned though, that the intracerebroventricular administration of the potent sEH inhibitor 12-(3-adamantane-1-yl-ureido)-dodecanoic acid (AUDA) increased blood pressure as well as heart rate in SHRs (Sellers et al., 2005) suggesting that peripheral and central control of blood pressure are influenced differently by EETs and sEH inhibitors. This observation demonstrates the need to understand which sEH inhibitors penetrate the blood / brain barrier.

sEH inhibitor treatment also increases EET levels in cell cultures and reduces indicator compounds for vascular inflammation (Slim et al., 2001; Davis et al., 2002; Liu et al., 2005b). This suggests that the treatment of several vascular inflammatory diseases including atherosclerosis and kidney failure is possible by sEH inhibition (Davis et al., 2002; Zhao et al., 2004). Furthermore, the chemical inhibition of sEH was shown to successfully treat acute systemic inflammation (Schmelzer et al., 2005). An endogenous mechanism, that is proposed to function in a similar way, is the increase of divalent cation metal concentrations, especially zinc, in the liver (Gaetke et al., 1997). Knowing that this cation inhibits sEH noncompetitively (compare to 2.1.6), the change in its concentration possibly represents a simple way to reduce sEH activity and thus to induce an anti-inflammatory process (Morisseau and Hammock, 2005).

Additionally and as mentioned before, leukotoxin diol is associated with inflammatory and toxic effects such as acute respiratory distress syndrome (ARDS) and multiple organ failure. By inhibiting sEH, this compound will not be generated anymore or only be produced to a lesser extent (Morisseau et al., 1999) stating that sEH represents a possible treatment for these diseases as well.

## 2 RNA interference

In 2002, an endogenous mechanism called RNA interference (RNAi) was entitled 'breakthrough of the year' by *Science* (Couzin, 2002). By then, the full importance and extent of this post-transcriptional gene silencing process, first observed in transgenic petunia plants but not yet understood at the time (Napoli et al., 1990; van der Krol et al., 1990), came into sight. Fire and coworkers (1998) were the first ones, who showed that double-stranded RNA (dsRNA) triggered the gene knockdown phenomenon in the nematode *Caenorhabditis elegans*. With this finding they initiated the discovery of the highly conserved endogenous RNAi pathway. Meanwhile, in the mid of 2006, many more details and properties of this mechanism are known and enable researchers in various fields to experimental approaches, which were impossible or at least hard to achieve and time-consuming only one decade ago.

The following paragraphs are intended to give a better understanding of the RNAi mechanism and its closely related processes with a focus on mammalian systems. Furthermore, they are meant to provide an overview of possibilities in research and therapeutic applications arising due to RNAi.

### 2.1 Molecular mechanism of RNAi

The RNAi pathway (Figure 6), which results in the post-transcriptional silencing of a specific gene, takes place in the cytosol (Zeng and Cullen, 2002). Even though some details of this endogenous mechanism are still unclear or can only be assumed at the moment, the overall procedure is understood.

RNAi is initiated by the enzymatic cleavage of precursor dsRNA molecules, homologous to the respective target gene. Dicer, a protein with RNase III-like enzyme activity (Bernstein et al., 2001), processes the dsRNA to short interfering RNA (siRNA) molecules. These are characterized by a 19-20 base pair (bp) stretch of the duplex region, a 2 nucleotide (nt) 3' overhang as well as a 5' phosphate and 3' hydroxy group on each strand (Hamilton and Baulcombe, 1999; Elbashir et al., 2001b). During the ATP-dependent (Nykänen et al., 2001) assembly of RISC (RNA-induced silencing complex), which presents a crucial multimeric protein complex in the RNAi pathway (Tuschl et al., 1999; Hammond et al., 2000), one double-stranded siRNA molecule is directionally incorporated while its passenger strand

(compare to Figure 6) is cleaved by a part of RISC (Matranga et al., 2005; Rand et al., 2005; Leuschner et al., 2006). This procedure is normally referred to as ‘RISC activation’.

The remaining guide strand of the siRNA, which is part of RISC, now serves as trigger molecule that sequence-specifically guides the binding of mRNA complementary to itself (Martinez et al., 2002a; Martinez and Tuschl, 2004). Once the Watson-Crick interactions between the two RNA strands are formed, endonucleolytic cleavage of the mRNA – in the middle of the guide strand (Elbashir et al., 2001b) – is induced (initial hypothesis and experiments by Montgomery et al., 1998; Tuschl et al., 1998; Hammond et al., 2000). The subsequent degradation of the remaining target mRNA pieces, which is only starting to be understood, guarantees the ultimate post-transcriptional gene silencing effect of this mechanism.

### 2.1.1 Dicer

The dsRNA-processing enzyme Dicer normally contains an N-terminal RNA helicase domain, a PAZ (Piwi/Argonaute/Zwille) domain, two RNase III domains, and a dsRNA binding domain (dsRBD) (Carmell and Hannon, 2004). Additionally, there are domains of unknown function, such as DUF283 in the human Dicer protein (see Hammond et al., 2005 and references therein).

Due to homology studies of related prokaryotic RNase III-type enzymes (Blaszczyk et al., 2001; Blaszczyk et al., 2004), Dicer was initially supposed to act as dimer (Zamore, 2001). However, more

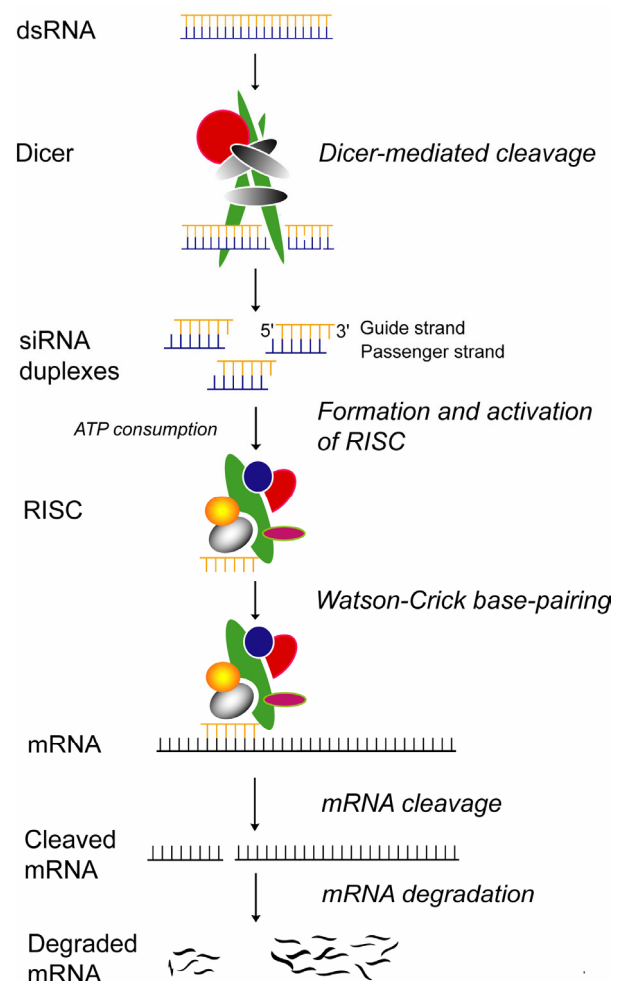


**Fig. 6** Schematic illustration of the RNAi mechanism.

recent results (Sun et al., 2004; Zhang et al., 2004a) suggest a different model of this enzyme's mode of action. Zhang and coworkers (2004a) proposed that the two RNase III domains of Dicer, with one cleavage site each, create a single active site by intramolecular dimerization (compare to Figure 7).

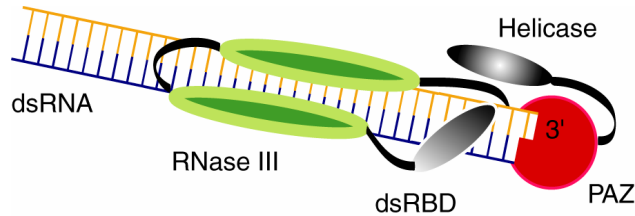


**Fig. 7** Model for Dicer activity essentially following Zhang and coworkers (2004a).

Each domain then cuts a single strand of the precursor dsRNA. By offsetting the two cutting sites by 2 nt, a terminus with a 2-nt 3' overhang is generated, which is characteristic for RNase III enzymes.

The PAZ domain was found to be able to bind single-stranded nucleic acids with 3' OH-groups or 2-nt nucleic acid 3' overhangs, both with a preference for RNA (Lingel et al., 2003; Song et al., 2003b; Yan et al., 2003; Lingel et al., 2004; Ma et al., 2004). Therefore, a combination of RNase III and PAZ in Dicer was suggested to act as molecular ruler granting a constant spacing between the cleavage sites in a Dicer-processed dsRNA (Zhang et al., 2004a). Macrae and coworkers (Macrae et al., 2006) proved this particular hypothesis.

The overall mode-of-action-theory for Dicer is supported by the observation that Dicer cleaves from the ends of dsRNA, producing constant sized siRNAs – in contrast to cutting dsRNA internally and producing multiple larger fragments (Zhang et al., 2002; Zhang et al., 2004a; Vermeulen et al., 2005). The dsRBD of Dicer would fit nicely into this suggested mechanism. It could bind blunt-ended dsRNA and thus assist the generation of the first 2-nt 3' overhang, which is then possible to be bound by PAZ (see Collins and Cheng, 2005 and references therein). Finally, the helicase domain of Dicer was proposed to unwind complex secondary structures of dsRNA prior to its processing by the corresponding RNase III activity (Zhang et al., 2002; Collins and Cheng, 2005). Nevertheless, the actual role of the helicase domain of Dicer, its dsRBD along with the function of other domains, like DUF283 in human Dicer, remains to be explored.

## 2.1.2 RISC

A minimal RISC only consists of the guide sequence of an siRNA and an Argonaute protein (Ago). Experiments revealed these two components as sufficient for minimal target mRNA cleavage activity (Rand et al., 2004; Rivas et al., 2005), which is often referred to as ‘Slicer activity’. Argonaute, member of a protein family that is conserved in most eukaryotic and several prokaryotic genomes, generally consists of an N-terminal domain, a PAZ domain, the ‘middle’ lac-Z-like domain and a C-terminal PIWI domain (Cerutti et al., 2000; Carmell et al., 2002). While N-terminal, Middle and PIWI domain form a bowl-like form with PIWI in the center of it, the PAZ domain is located above this structure (Collins and Cheng, 2005). Crystal structure studies of Argonaute family members from the archae bacteria *Pyrococcus furiosus* and *Archaeoglobus fulgidus*, their PIWI domain respectively, revealed an RNase H fold in this particular part of the protein (Parker et al., 2004; Song et al., 2004). RNase H endonuclease activity now is characterized by the cleavage of RNA of DNA/RNA duplexes, generating 5’ phosphate 3’ OH products employing a divalent metal as cofactor (Keck et al., 1998). However, in duplexes of short DNA and long RNA strands, RNase H is also able to cleave the RNA in the center of the DNA oligonucleotide – an activity that resembles the one of ‘Slicer’ greatly. This fact together with other observations and crystal structure investigations of (ds)RNA-complexed PIWI domains (Schwarz et al., 2004; Hammond, 2005; Ma et al., 2005a; Parker et al., 2005; Rivas et al., 2005) suggested the following scenario for the Slicer activity (see Figure 8): The 5’ phosphate of the siRNA guide strand is bound by the PIWI domain, the 3’ end is attached to the PAZ domain. The mRNA is cleaved by the RNase H fold of the PIWI domain in the middle of the siRNA guide strand.

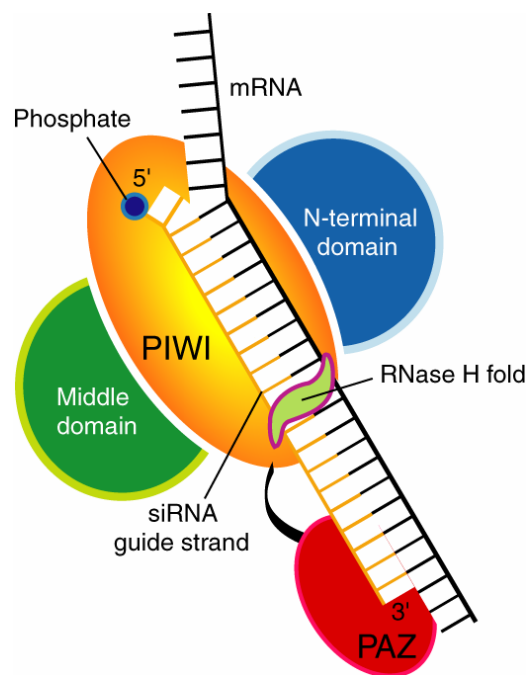


**Fig. 8** Model for Slicer activity of Argonaute in RISC. While the 5’ phosphate of the siRNA guide strand is bound by the PIWI domain, the 3’ end is attached to the PAZ domain. The mRNA is cleaved by the RNase H fold of the PIWI domain in the middle of the siRNA guide strand.

it away from the target mRNA strand. At the same time, the siRNA guide's 3' OH is bound by the Argonaute's PAZ domain (Martinez and Tuschl, 2004; Schwarz et al., 2004). The rest of the guide siRNA adopts a helical arrangement in a basic channel between the Mid and the PIWI domain and follows, after emerging from the cleft of Ago's bowl-like structure, along the PAZ domain. This allows target mRNA recognition and binding over the RNase H site of the protein resulting in the cleavage of the mRNA in the middle of the siRNA guide strand as well as a 5' phosphate and a 3' OH on the remaining RNA pieces (Carmell et al., 2002).

Interestingly, the number of distinct Argonaute proteins varies in different organisms. This phenomenon ranges from only one Ago in *Schizosaccharomyces pombe* to more than 20 in *Caenorhabditis elegans*. In *Arabidopsis thaliana*, 10 members were found to exist (Hunter et al., 2003), whereas 5 could be identified in *Drosophila melanogaster* (Williams and Rubin, 2002) and 8 in humans (Sasaki et al., 2003). However, most of these proteins are still to be functionally characterized by experiments. This is also the case for other identified members of the RISC complex. In *Drosophila melanogaster* for example, such RISC components are the RNA binding protein, the *Drosophila* homolog of the fragile X protein (dFXR), helicase proteins as well as Tudor-SN (Caudy et al., 2002; Ishizuka et al., 2002; Caudy et al., 2003). In human biochemical systems, interactions of AGO2/eIF2C2 (Argonaute2 – the only Argonaute of the closely related human Ago1-Ago4 possessing 'Slicer' activity (Hammond et al., 2001; Liu et al., 2004; Meister et al., 2004; Okamura et al., 2004; Rand et al., 2004); eukaryotic translation initiation factor 2C2) with FMRP (fragile X mental retardation protein – the human homologue of dFXR) have been observed (Jin et al., 2004). In this context, Meister and coworkers (Meister et al., 2005) also discovered the putative RNA helicase MOV10, and the RNA recognition motif-containing protein TNRC6B/KIAA1093.

### 2.1.3 RISC assembly

The question of how the double-stranded siRNA gets transferred from Dicer to RISC, and directionally integrated into the latter complex has been occupying scientists in this field for quite a while. If this problem was solved, the rational design of siRNAs would be an easy and save task, preventing time- and cost- intensive studies to discover highly functional siRNAs. Several recent experimental findings suggest that a complex of Dicer and at least one double-stranded RNA binding protein (TRBP and PACT in humans; Chendrimada et al., 2005; Lee et al., 2006b) binds the siRNA directionally (Khvorova et al., 2003; Schwarz et al., 2003; Tomari et al., 2004) and assembles with Ago2 (Doi et al., 2003; Kolb et al., 2005) and possibly other factors. During this process, the passenger strand of the siRNA gets cleaved (Matranga et al., 2005; Rand et al., 2005; Leuschner et al., 2006) in an Ago2-dependent manner (Miyoshi et al., 2005) and most likely discarded. Nevertheless, the detailed mechanism of this whole assembly process remains to be determined.

### 2.1.4 mRNA degradation

The mechanism of mRNA degradation after gene silencing by RNAi has only started to be understood. However, a recent study by Orban and Izaurralde (2005) in cells of *Drosophila melanogaster* provided key insights into this process. Essentially, they demonstrated that (a) RISC-degraded mRNA is processed without further deadenylation and decapping – in contrast to the major mRNA degradation pathways (reviewed in Parker and Song, 2004). This would point to a specific mRNA decomposition pathway of RNAi.

Furthermore, they showed that (b) the remaining capped 5' RNA fragment is degraded by the exosome (Orban and Izaurralde, 2005), which is a multimeric protein assembly containing 3'-to-5' exonucleases and known for its role in mRNA decay (reviewed in Parker and Song, 2004). In this context, (c) the Ski-complex with its components Ski2p, Ski3p and Ski8p proved essential for this particular degradation (Orban and Izaurralde, 2005). Moreover, there were indications, that (d) nonstop decay (NSD; a pathway, in which mRNAs without stop codon are degraded) occurs in case of the capped 5' RNA remnant of the RNAi process (Orban and Izaurralde, 2005). Ski7p now, a yeast protein that is required for 3'-to-5' mRNA decay (van Hoof et al., 2000; Araki et al., 2001) and interacting with



the exosome and the Ski complex, has been associated with mRNA NSD (van Hoof et al., 2002). Taking into account all these facts, Orban and Izaurralde (2005) proposed a model, in which an ortholog of this protein links a ribosome (at the 3' end of nonstop mRNA) with the Ski complex and exosome triggering the NSD of the 5' mRNA piece generated by RISC.

Finally, Orban and Izaurralde provided evidence that (e) the 3' fragment of the RISC-degraded mRNA is decomposed by means of XRN1 (Orban and Izaurralde, 2005), a 5'-to-3' exonuclease. XRN1 localizes in so-called mRNA decay foci or cytoplasmic bodies (Ingelfinger et al., 2002) that are also known as P-bodies or GW-bodies – an established place of mRNA degradation (Sheth and Parker, 2003; Cougot et al., 2004). In addition, there are findings, that Ago2 – one major component of RISC – localizes in the cytoplasmic bodies (Liu et al., 2005a; Sen and Blau, 2005). Considering all these results, it is likely that Argonaute and possibly other RISC components escorts the 3' mRNA fragment to the cytoplasmic bodies, where their degradation takes place.

## 2.2 RNAi in mammalian cells

Even though RNAi is an overall well conserved mechanism in higher eukaryotes, there are small differences in this pathway among organisms of distinct evolutionary levels. Consequently, before employing RNAi as research tool and considering it as potential therapeutic treatment for human kind, it is important to know more about its properties in mammals, mammalian cells respectively.

A key feature of RNAi in mammals is, that only dsRNA < 30 bp, such as synthetic siRNA duplexes (Caplen et al., 2001; Elbashir et al., 2001a), can initiate the silencing process. In case longer exogenous dsRNA gets introduced into the cytosol of mammalian cells, it turns on a number of mechanisms (compare to Figure 9) directed against viral infection – the major natural source of long cytosolic dsRNA. Activation of 2'-5'-oligoadenylate synthase as well as PKR (protein kinase R) are two well established viral defense mechanisms that are initiated in such a case leading to RNA degradation, inhibition of mRNA translation and finally apoptosis (reviewed in Wang and Carmichael, 2004). Additionally, it is also possible for viral dsRNA to bind to a toll-like receptor (TLR; a family of proteins, that recognize macromolecules common to pathogens) and thus initiate the interferon-I (IFN-I) system (Takeda and Akira, 2005). Experimental results point to TLR-3 (Sarkar et al., 2004; Takeda and

Akira, 2005) as binding partner causing this particular immune response. Moreover, there are indications for additional signaling pathways, e.g. involving RIG-1 (retinoic acid-inducible gene; Yoneyama et al., 2004), but detailed understanding of their regulation is lacking. Notably, the described innate viral defense mechanisms do not exist in evolutionary lower organisms such as *Caenorhabditis elegans* or *Drosophila melanogaster*. They deal with viruses by means of their RNAi pathway.

In this context it is worth mentioning that synthetic siRNAs and thus short dsRNAs are also able to induce a potent interferon response by means of binding to TLR-7, although in a sequence-dependent manner (Hornung et al., 2005).

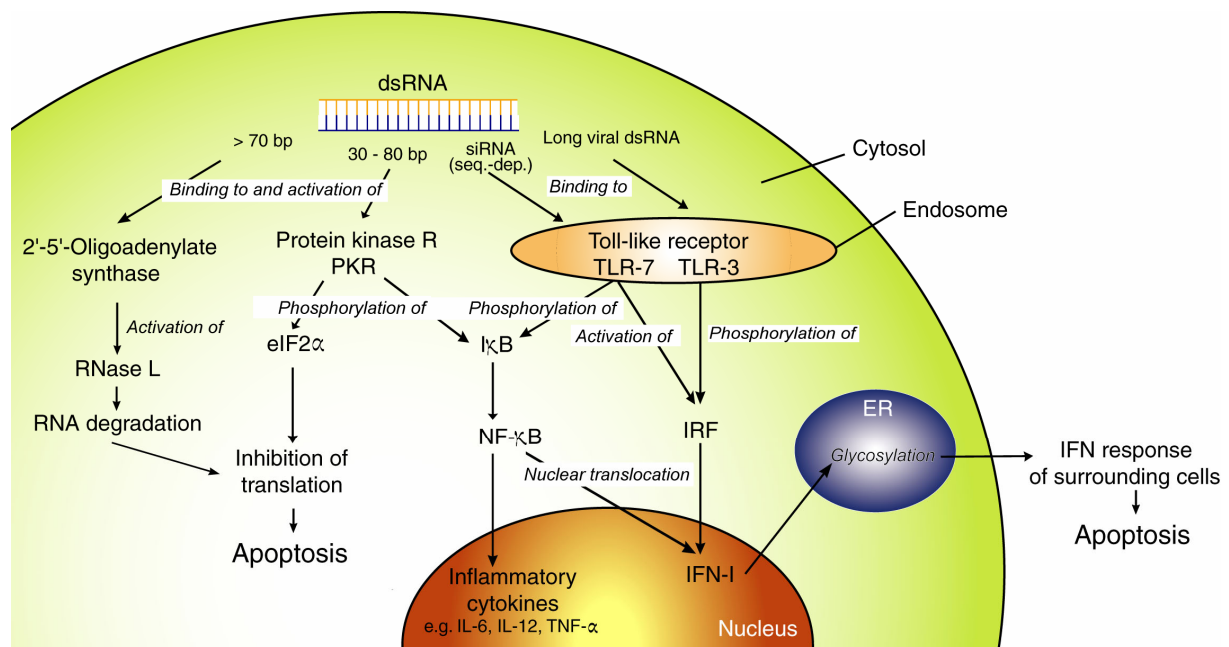


**Fig. 9** Schematic overview of mammalian responses to dsRNA in the cytosol besides RNAi. This illustration summarizes information and results from various sources (Sarkar et al., 2004; Wang and Carmichael, 2004; Hornung et al., 2005; Robbins and Rossi, 2005; Takeda and Akira, 2005). dsRNA longer than 70 bp can bind to **2'-5' oligo adenylate synthase**. This again activates RNase L leading to RNA degradation in the cytosol. Binding of 30-80 bp long dsRNA to **protein kinase R (PKR)** initiates phosphorylation of several cytosolic factors such as eIF2 $\alpha$  (eukaryotic transcription initiation factor 2 $\alpha$ ) and I $\kappa$ B. This process triggers the inhibition of further mRNA translation and thus protein production as well as transcription initiation of inflammatory cytokines and interferon-I (IFN-I) proteins via translocation of the transcription factor NF- $\kappa$ B to the nucleus. Furthermore, long viral dsRNA is recognized by **toll-like receptor 3 (TLR-3)** causing the nuclear translocation of IRF followed by the induction of the IFN-I system. Finally, binding of certain siRNA sequences to **TLR-7** leads to a potent IFN-I response. Moreover, the activation of this receptor is also known to induce the production of inflammatory cytokines. All of the here described signaling pathways consist of a multitude of intermediate steps and mediating compounds (mostly not displayed in this scheme), which are still not completely revealed and understood. (ER = endoplasmatic reticulum; IFN-I = interferon-I; IL = interleukin; IRF = interferon regulatory factor(s); seq.-dep. = sequence-dependent; TNF = tumor necrosis factor).

One could assume that, while exclusively employing synthetic siRNAs to achieve the silencing of a specific target gene, Dicer is not necessary to achieve this target. Nevertheless, there are observations, that RNAi is less effective in mammalian cells depleted for Dicer (Doi et al., 2003). Additionally, there is evidence, that dsRNA, which can be processed by Dicer – short hairpin RNA or siRNAs of about 27 nt – represents a clearly more effective RNAi trigger than regular siRNA duplexes of 21 nt length (Kim et al., 2005a; Siolas et al., 2005). Therefore, Dicer is bound to play an additional role in the RNAi game, which is in agreement with the hypothesis of Dicer being involved in RISC assembly (see above).

In humans and *Caenorhabditis elegans* only one Dicer enzyme has been identified for dsRNA processing (reviewed in Meister and Tuschl, 2004). In contrast, there are several organisms, which express more than one Dicer gene (Lee et al., 2004b; Xie et al., 2004). *Drosophila melanogaster* for example, holds two Dicer paralogues: Dicer-1 and Dicer-2 (Lee et al., 2004b). Furthermore, only Ago2 out of the closely related Ago1-4 displays ‘Slicer’ activity in humans. Ago1, Ago3 and Ago4 also associate with dsRNAs, but cannot cleave them (Liu et al., 2004; Meister et al., 2004). Taking into account these facts and the sophisticated antiviral response mechanisms in mammals, it is likely that their RNAi mechanism remained in a basic state or was optimized for a different assignment (e.g. gene regulation by microRNAs; see below).

Finally, it has to be noted that there is no amplification or spreading of siRNA molecules in mammalian cells. Therefore, RNAi effects in mammalian cell systems are only transient and depend on the proliferative state of the respective cells as well as the number of siRNA molecules introduced into their cytosol (Bartlett and Davis, 2006). Just as *Drosophila melanogaster*, mammalian species are deficient for RNA-dependent RNA polymerases (RDRPs or RDRs) or equivalent enzymes (Schwarz et al., 2002; Roignant et al., 2003; Stein et al., 2003). These particular proteins enable e.g. *Caenorhabditis elegans* to amplify and spread the RNAi signal within the organism facilitating a long lasting RNAi effect that can be passed on to the offspring (Grishok and Mello, 2002).

### 2.3 Original role of RNAi and closely related mechanisms

Over the last years, it became evident that various identified gene silencing phenomena in the nematode *Caenorhabditis elegans*, the fruit fly *Drosophila melanogaster*, as well as plants and fungi share a common basic mechanism (Hamilton and Baulcombe, 1999; Schmidt et al., 1999; Catalanotto et al., 2000; Fagard et al., 2000; Ketting and Plasterk, 2000; Aravin et al., 2001), which was possibly already present in the last common ancestor of eukaryotes (Cerutti and Casas-Mollano, 2006). Thus, post-transcriptional gene silencing (PTGS; de Carvalho et al., 1992), co-suppression (Napoli et al., 1990; van der Krol et al., 1990), quelling (Romano and Macino, 1992) and RNAi are all supposed to be variations of the same theme: the protection of the own genome against transposable elements and invasive nucleic acid parasites such as viruses (Jensen et al., 1999; Ketting et al., 1999; Tabara et al., 1999; Voinnet et al., 1999; Mourrain et al., 2000; Wu-Scharf et al., 2000).

The same purpose underlies some nuclear gene silencing pathways, which are related to RNAi by employing essential components of its machinery. **RNA-directed DNA methylation** (RdDM) for example provokes epigenic alterations by means of RNAi machinery located in the nucleus (Zilberman et al., 2003; Xie et al., 2004). First observed in plants (Wassenegger et al., 1994), it was found that dsRNA homologous to promoter regions can provoke the methylation of cytosines of these sequences (Cao et al., 2003; Aufsatz et al., 2004) resulting in relatively specific transcriptional gene silencing (Pelissier et al., 1999; Mette et al., 2000; Melquist and Bender, 2003). In human cells however, reports on the existence of this type of gene silencing are contradictory (Kawasaki and Taira, 2004; Morris et al., 2004; Svoboda et al., 2004) and need to be further explored and clarified.

The **assembly of heterochromatin** represents another regulatory pathway in the nucleus, which has recently been connected to RNAi. Heterochromatin – in contrast to euchromatin - is a gene-poor, cytologically visible but genetically rather inactive component of the nucleus. In many species, it surrounds the centromeric region of chromosomes and is also found near telomeres. At the DNA level, heterochromatin consists of degenerated retrotransposon sequences, long arrays of simple tandem repeats or a combination of the two (Hennig, 1999). Association with a methylated form of histone H3 and the heterochromatin protein 1 (HP1) are also characteristics for heterochromatic DNA (Bannister et al., 2001; Lachner et al., 2001; Muchardt et al., 2002). A whole range of reports indicate small dsRNAs

generated by Dicer as trigger molecules that guide methyltransferases to homologous sites in chromatin (Volpe et al., 2002; Saffery et al., 2003; Schramke and Allshire, 2003; Zilberman et al., 2003; Fukagawa et al., 2004; Lippman et al., 2004; Pal-Bhadra et al., 2004b; Kanellopoulou et al., 2005) – regardless if these sites are located in heterochromatic or euchromatic sites of the chromosome. Subsequent binding of repressive proteins such as HP1 or the polycomb complex (Pal-Bhadra et al., 1997; Pal-Bhadra et al., 2002) then leads to limited transcription of the respective DNA. On the other hand, a recent study (Wang et al., 2006) suggests that the RNAi machinery is not required for this mechanism in mammalian cells.

Moreover, the **elimination of excess DNA** has been found to utilize RNAi components. The phenomenon, which can be examined in ciliated protozoans during the sexual process of conjugation, is proposed to be triggered by micronuclear dsRNA. After Dicer-processing and export to the macronucleus, it supposedly directs methyltransferases to complementary DNA sequences. The RNA sequences, which cannot find a binding partner there are then assumed to migrate into the developing macronucleus and mark complementary sequences for subsequent excision (reviewed by Mochizuki and Gorovsky, 2004).

Finally, a connection between RNAi and **meiotic silencing**, a process where unpaired DNA is silenced during meiosis (Aramayo and Metzenberg, 1996; Shiu et al., 2001), was discovered in *Neurospora crassa* (Shiu et al., 2001; Shiu and Metzenberg, 2002; Lee et al., 2003a). The opposite effect, which is called **pairing-sensitive silencing**, was found in somatic cells of *Drosophila melanogaster* (Kassis, 1994) and as well connected to components of the RNAi machinery (Pal-Bhadra et al., 2004a). In this case, homozygous pairing of specific transgenes resulted in decreased expression levels in comparison to two scattered, non-allelic positions of the respective gene in the genome. Interestingly though, mutations in the relevant RNAi machinery genes ‘piwi’ and ‘homeless’ resulted in an increase of the silencing effect rather than a loss of it (Pal-Bhadra et al., 2004a).

In addition and in contrast to the above described nuclear regulatory processes, the RNAi machinery was found to be involved in the endogenous gene regulation pathway mediated by **microRNAs** (miRNAs). miRNAs are ~21 nt long RNA strands that were shown to influence critical developmental processes such as embryogenesis, organogenesis or growth (reviewed in Alvarez-Garcia

and Miska, 2005; Kidner and Martienssen, 2005). Moreover, misregulation of miRNAs is suspected to cause cancerous phenotypes since a large number of cancers display altered miRNA profiles (Lu et al., 2005) and miRNA overexpression lead to tumor development (He et al., 2005). miRNAs are common in worms and fruit flies as well as plants and vertebrates.

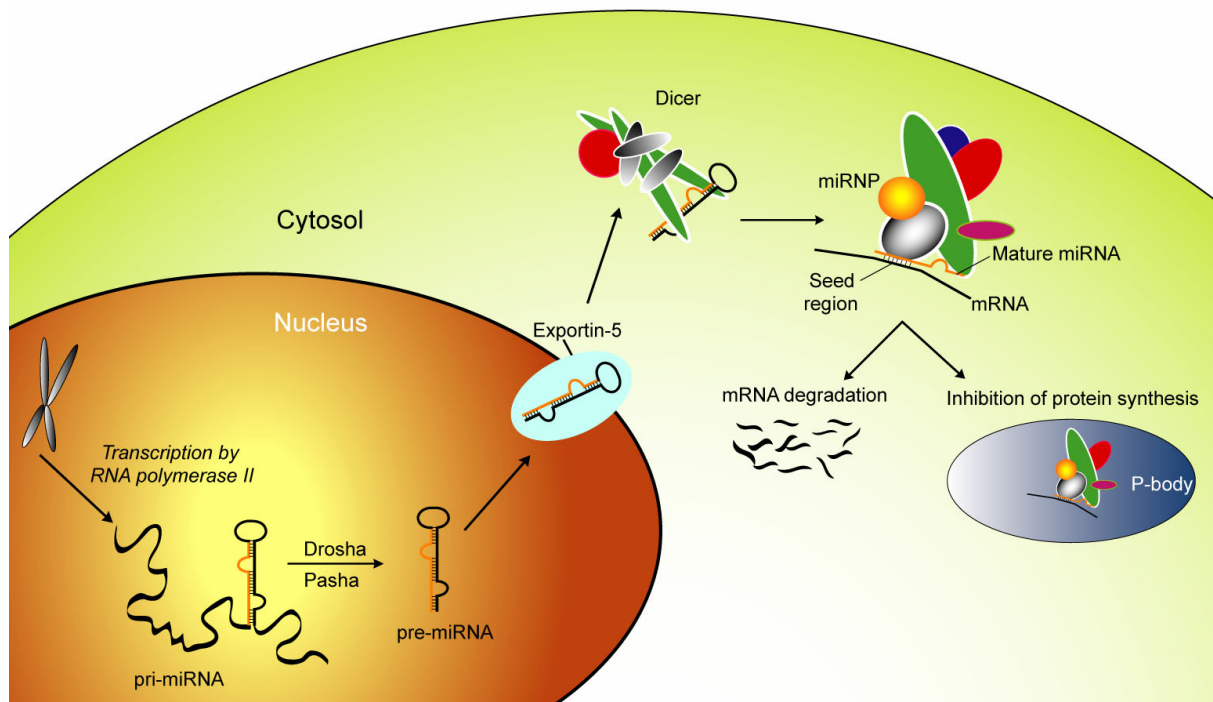


**Fig. 10** Scheme of miRNA biogenesis and function. See text for detailed explanation.

Biogenesis of miRNAs (see Figure 10) is initiated in the nucleus by transcribing non-coding or intronic sequences (Rodriguez et al., 2004) by RNA polymerase II (Cai et al., 2004; Lee et al., 2004a; Parizotto et al., 2004) resulting in the so-called pri-miRNA. Drosha, another RNase III-like enzyme that acts with the dsRBD Pasha, subsequently cuts out an ~70 nt precursor stem-loop structure termed pre-miRNA (Lee et al., 2002; Lee et al., 2003b; Denli et al., 2004; Gregory et al., 2004; Han et al., 2004; Landthaler et al., 2004; Zeng and Cullen, 2005; Zeng et al., 2005). After that, the hairpin-like RNA is specifically recognized and exported to the cytosol by means of Exportin-5 (Yi et al., 2003; Bohnsack et al., 2004; Lund et al., 2004; Zeng and Cullen, 2004), which was recently also shown to be essential for the RNAi mechanism (Ohrt et al., 2006). In the cytosol, Dicer processes the pre-miRNA (Grishok et al., 2001; Hutvagner et al., 2001; Lee et al., 2004b; Xie et al., 2004), just like other dsRNAs, to intermediate

duplex molecules of ~21 nt, which usually contain some mismatches. Subsequently, the mature single stranded miRNAs can be detected in multi-protein complexes called miRNPs (miRNA-containing ribonucleoprotein complex; Mourelatos et al., 2002). These greatly resemble RISCs in composition as well as function. miRNPs are then guided by their internal miRNAs to partially or fully complementary mRNA sequences. Once Watson-Crick base pairings are formed, the miRNAs trigger either the degradation of the respective mRNA or the inhibition of its translation. The latter process is connected to cytosolic P-bodies (Liu et al., 2005a; Pillai et al., 2005; Sen and Blau, 2005). However, it is not clear yet whether Ago proteins and miRNAs found in these RNA-rich structures are cause or consequence of the translational repression mediated by miRNAs (reviewed in Pillai, 2005).

In plants, miRNAs normally bind to a single, perfectly complementary site of target mRNA in either the coding or the 3' untranslated region (3' UTR) (Rhoades et al., 2002). In contrast, animal miRNAs were found to mostly bind to multiple sites in the 3' UTRs of mRNAs, which are only partially complementary. Hereby, nucleotides 2-8 in the 5' region of the mature miRNAs – the so-called 'seed region' – normally represent the core recognition sequence (Lewis et al., 2003; Brennecke et al., 2005; Lai et al., 2005; Lewis et al., 2005; Xie et al., 2005). Until recently it was assumed that the fate of an mRNA after binding to an miRNP was programmed by how many of its bases pair with the miRNA. If only the seed region was bound, translation would be repressed but the message would not be eliminated (Reinhart et al., 2000; Brennecke et al., 2003; Zeng et al., 2003). On the other hand, if miRNA and mRNA were perfectly complementary, the mRNA would be degraded (Yekta et al., 2004). Recent results however show that the picture is not that clear (reviewed in Du and Zamore, 2005; Pillai, 2005). Thus, many questions about the exact regulation, course and components of the miRNA pathway remain unanswered for now. Nevertheless, it became evident that this endogenous regulatory mechanism is an extremely important process, which may control as many as one third (Lewis et al., 2005; Xie et al., 2005) of protein-coding genes in man.

Taken together, major components of the RNAi machinery were found to be involved in a variety of different transcriptional and post-transcriptional silencing processes. It can even be assumed that mammalian organisms only maintained and refined the RNAi machinery to fine-tune gene expression in the cell, since they possess alternative viral defense mechanisms (see above). But are

these processes somehow connected? How does the RNAi machinery differentiate e.g. between the signals for RdDM and the assembly of heterochromatin? And when do miRNAs trigger mRNA degradation and when only translational repression? These and many more questions remain to be answered. Finally, it is important to remember that there are mechanisms for gene silencing via heterochromatin formation and DNA methylation in RNAi-enabled organisms, which are not connected with it (Tamaru and Selker, 2003; Chicas et al., 2004; Freitag et al., 2004; Jia et al., 2004; Goll and Bestor, 2005).

#### *2.4 Current role of RNAi in research*

Employment of RNAi in research offers the possibility of performing reverse genetic studies: By disrupting expression of a specific gene, conclusions on its function can be drawn. Therefore, right after its discovery, RNAi was used to specifically silence certain genes in *Drosophila melanogaster* (Kennerdell and Carthew, 1998; Misquitta and Paterson, 1999) and *Caenorhabditis elegans* (Powers et al., 1998) to determine and confirm their function in a fast and straight-forward manner. Particularly the latter organism is extremely advantageous for RNAi approaches, since the delivery of dsRNA can be as simple as soaking the worms in dsRNA solution (Tabara et al., 1998) or feeding them with bacteria expressing dsRNA (Timmons and Fire, 1998). In addition, the RNAi effect spreads systemically in it and is transmittable to the offspring (see above; Grishok et al., 2000). Consequently, the physiological impact of a target gene can be observed throughout the whole development of this model organism.

In mammalian cell systems, RNAi experiments are normally carried out by transfection / electroporation of synthetically (Caplen et al., 2001; Elbashir et al., 2001a) or enzymatically (Myers et al., 2003; Hagerkvist et al., 2005) generated siRNAs as well as by the introduction of vector-based systems into the cells (Brummelkamp et al., 2002a; Brummelkamp et al., 2002b; Paddison et al., 2002; Paul et al., 2002; Scherr et al., 2003). After entering and often under the regulation of the polymerase III promoters U6 or H1, such vectors (plasmids or viruses) express RNA strands that hybridize with themselves to form a hairpin-like structure. The resulting short hairpin RNAs (shRNAs; Paddison et al., 2002) are then processed by Dicer and provoke an RNAi effect just like siRNAs. Vector-based RNAi approaches provide the advantage of initiating a prolonged silencing effect in mammalian cells in



comparison to siRNAs, since in this case shRNAs are produced continuously. Alternatively, more recently developed viral vector systems hold the option of inducible shRNA expression, that can be ‘switched on’ e.g. by administration of chemical inducer such as doxycycline (Amar et al., 2006; Westerhout et al., 2006; Yu and McMahon, 2006). In addition, viral vectors are able to infect even primary cells (Stewart et al., 2003; Kao et al., 2004; Krick et al., 2005) and embryonic stem cells (Hoelters et al., 2005; Ikeda et al., 2005), facilitating reverse genetic analysis in challenging systems.

Testing of single gene functions by RNAi-mediated silencing was soon extended to high-throughput genome-wide approaches in whole organisms as well as cells (reviewed in Carpenter and Sabatini, 2004). Such large-scale RNAi screens employing siRNA and vector libraries have already lead to important findings including the identification of so-far unknown genes involved in NF- $\kappa$ B signaling (Lassus et al., 2002; Zheng et al., 2004), the p53 pathway (Martinez et al., 2002b; Berns et al., 2004; Lettre et al., 2004) and apoptosis (Aza-Blanc et al., 2003; Miyagishi et al., 2004). Furthermore, they are used for target identification and validation in drug discovery processes (reviewed in Chatterjee-Kishore and Miller, 2005). However, the experiments still suffer from insufficient knowledge about the design of effective and specific siRNA and shRNA sequences. False negative (e.g. inefficient sequence) as well as false positive (e.g. off-target effect) results can be provoked by inappropriate RNA trigger-molecules. Some rules for the rational design of siRNAs were revealed (Khvorova et al., 2003; Schwarz et al., 2003; Hsieh et al., 2004; Reynolds et al., 2004), but it is still necessary to evaluate 2 to 5 molecules for their effectiveness in mammalian systems. To circumvent this obstacle, siRNA libraries for large-scale screening contain at least two different siRNA sequences for targeting the same gene (Hsieh et al., 2004).

A promising method in the high-throughput analysis of gene function is the RNAi cell microarray principle (reviewed by Vanhecke and Janitz, 2005; Wheeler et al., 2005). Hereby, various siRNAs / shRNA vectors in combination with transfection reagents are spotted on glass slides and covered with a dense cell layer. Cells in contact with siRNAs get transfected (reverse transfection) and mostly display the desired RNAi effect. The slides can then be analyzed further, e.g. by immunochemical or staining procedures.

Finally, RNAi is used for *in vivo* reverse genetic studies in mammals. To start with, infection of embryonic stem cells or eight-cell embryos with an shRNA-expressing virus (e.g. lenti- or adenovirus) can create animals, in which the targeted gene is permanently silenced (Lois et al., 2002; Rubinson et al., 2003; Tiscornia et al., 2003). This represents an alternative to the extremely time-consuming and labor-intensive breeding of knockout animals. In addition, delivery of siRNAs eg. to the lung via intranasal administration (Zhang et al., 2004b) or to the liver, among others, via high-pressure, high-volume intravenous injection ('hydrodynamic delivery'; Lewis et al., 2002; McCaffrey et al., 2002; Song et al., 2003a) can provoke target gene knockdowns (for a review of *in vivo* RNAi experiments see Aigner, 2006).

It has to be noted, that RNAi is generally only able to knock *down* a specific target rather than to completely knock it out. The degree of down-regulation depends on the employed siRNA / shRNA sequence. This can be of advantage, if the analysis of a whole range of phenotypes due to different expression levels is desired (Hemann et al., 2003). However, if a complete removal of the gene function is intended, knockout of the target still remains the gold standard.

### *2.5 Potential of RNAi for therapeutic approaches*

Once RNAi could be initiated in mammalian cells, the possibility of employing this mechanism for human therapy emerged. The advantages of this approach are apparent: The specific and thus controllable knockdown of a gene by siRNAs is more potent and versatile than antisense or ribozyme (see Akashi et al., 2005 and references therein) approaches. With careful siRNA / shRNA design, single genes or even single alleles (single allele silencing has already been displayed, e.g. by Ding et al., 2003; Gonzalez-Alegre et al., 2003; Miller et al., 2003) can be silenced as well as whole gene families. Simultaneous silencing of several non-related targets within one treatment is also feasible. Moreover, RNAi-connected gene therapy approaches utilizing shRNA-producing viral vectors are as conceivable as the use of siRNAs as small molecule drugs.

However, there are several obstacles to overcome before routinely taking advantage of this endogenous mechanism in human therapy. The first and probably predominant problem is the delivery of siRNAs into the cytosol of target cells. In contrast to worm and fly cells (Tabara et al., 1998; Boutros

et al., 2004), almost all mammalian cells do not efficiently take up siRNAs – even those performing endocytosis like macrophages and dendritic cells. Nevertheless, there is evidence that cells of mucosal tissues such as lung and vagina represent exceptions to this rule (Zhang et al., 2004b; Bitko et al., 2005; Palliser et al., 2006). A multitude of strategies has been developed to improve the siRNA uptake of mammalian cells. This included complexing the duplexes with cationic lipids or polyethylenimines (PEIs; both used for *in vitro* transfection) as well as atelocollagen or linking them e.g. to cholesterol (Lorenz et al., 2004; Minakuchi et al., 2004; Zhang et al., 2004b; Urban-Klein et al., 2005; Santel et al., 2006; Zimmermann et al., 2006). Moreover, cationic peptides might be mixed with siRNAs to function correspondingly (Simeoni et al., 2003). Interestingly, a recent study also found the osmotic delivery of siRNAs to immune cells to be a valuable tool for the initiation of the RNAi effect (Aoki et al., 2006).

Electrical stimulation / electroporation (Kishida et al., 2004; Matsuda and Cepko, 2004; Golzio et al., 2005; Takabatake et al., 2005) as well as localized hydrodynamic delivery (Hagstrom et al., 2004; Hamar et al., 2004) have been employed successfully *in vivo* and should thus be considered to assist efficient local siRNA delivery. Yet, regular local administration such as injection also seems to work in several cases such as subcutaneous tumors (Takei et al., 2004; Yano et al., 2004) and eye therapy (Reich et al., 2003; Kim et al., 2004a; Tolentino et al., 2004). In contrast, the systemic delivery of RNAi effector molecules *in vivo* by means of the blood stream is disproportionately harder to achieve if viral vectors, which in general still need to be refined for human therapy, are not considered. In this case, the biggest issue is the problem of an extremely short half-life of siRNAs *in vivo* predominantly caused by kidney filtration or endogenous serum RNAses. Besides complexing the siRNAs or incorporating them into different particle types, which circumvents renal filtration, several modifications on the sugar backbone of the siRNAs themselves were found to prolong their half-life (Choung et al., 2006; Dande et al., 2006; Dowler et al., 2006; Kraynack and Baker, 2006; Prakash et al., 2006) or to even create fully functional single-stranded siRNAs (Hall et al., 2006). On top of that, antibody-mediated systemic delivery of siRNAs was proven to be feasible and target-specific (Song et al., 2005; Pirollo et al., 2006).

A very different approach to induce the RNAi effect was taken by Xiang and coworkers (2006): they developed a specific shRNA-expressing, non-pathogenic *Escherichia coli* bacterium and treated mice by oral or intravenous administration of these procaryotes. The study found specific gene silencing

in the murine intestinal epithelium and in human colon cancer xenografts and thus provided a novel method of non-viral vector-mediated gene silencing in mammals.

The excitement about the fast and relatively straight-forward development towards RNAi therapy is enormous. One reason for this is that particularly ‘non-drugable’ diseases like cancer, viral infections (e.g. HIV and hepatitis viruses) or neurological diseases such as amyotrophic lateral sclerosis (ALS) are possibly treatable by RNAi (reviewed in Uprichard, 2005; Dykxhoorn et al., 2006). Nevertheless, it has to be cautioned that there are still some safety issues to be considered and overcome. Most importantly, there are reports on off-target (down-regulation of non-target genes; Jackson et al., 2003; Saxena et al., 2003) as well as non-specific (interferon response – compare to Figure 9; Bridge et al., 2003; Sledz et al., 2003; Kariko et al., 2004; Hornung et al., 2005; Judge et al., 2005) effects due to siRNA introduction into cells, which are concerning. Cationic lipids and phage polymerase generated siRNAs were found to cause some of the non-specific effects (Kim et al., 2004b; Ma et al., 2005b), while others were shown to be sequence dependent (Hornung et al., 2005; Judge et al., 2005; Sioud, 2005). In addition, off-target effects were found to be caused by certain sequences (Birmingham et al., 2006; Fedorov et al., 2006), but could be avoided or at least be reduced by chemical modification of the siRNA in use (Fedorov et al., 2006; Jackson et al., 2006). Therefore, careful siRNA design along with extensive empirical tests of every single sequence and all delivery methods are still mandatory to circumvent avoidable risks. In addition, the natural properties of gene silencing by RNAi with incomplete target inhibition and an only transient effect emphasize the need for intense investigations.

Another safety concern is that when large amounts of siRNAs are introduced into cells, they might occupy all of the available RNAi machinery (Bitko et al., 2005). This could be the case if several genes were targeted simultaneously. Thus, Dicer and RISC might not be able to fulfill their natural assignment of gene regulation by miRNAs anymore, resulting in yet unpredictable consequences such as cancerous phenotypes (see above). Therefore, careful dosage studies have to be carried out to use as little siRNAs as possible, though this is likely to depend on the individual.

RNAi gene therapy mediated by viral vectors is still discussed controversially, because each kind of viral vector holds a whole set of different risks (Tomanin and Scarpa, 2004). However, if the gain in

health due to such treatment weighs out potential disadvantages, it should still be considered for systemic shRNA delivery.

In conclusion, RNAi represents a promising new therapeutic strategy; although right at the moment its applicability and potential success greatly depend on the targeted disease itself, the existence of an effective siRNA and the target tissue or organ. In this context, ocular diseases such as age-related macular degeneration (AMD) or diabetic retinopathy of the eye represent uncomplicated target diseases, since subretinal injection of siRNAs is easy to carry out and finding an effective siRNA is only a question of time. Thus, the RNAi therapy approach evolved quickly in this particular case and AMD patients have already been treated with siRNAs in a phase I clinical trial. The respective results are promising (Whelan, 2005). Findings and conclusions from this and coming studies (e.g. treatment of respiratory syncytial virus infection will supposedly be started in the first half of 2006 by Alnylam, Cambridge, MA, USA) as well as from experiments with non-human primates (Zimmermann et al., 2006) are invaluable for similar future investigations and will determine the applicability of RNAi as novel therapeutic strategy.

## EXPERIMENTAL PART

The experimental part of the present thesis consists, as indicated before, of two parts. First, the characterization of novel fluorescent substrates for sEH and the connected development of two potent inhibitor assay systems are presented. After that, experiments intended to post-transcriptionally silence sEH by RNAi as well as their respective outcome are reported.

### 1 Development of two novel fluorescence-based assay systems for sEH inhibitors

#### 1.1 Introduction and objective

Over the past few years the interest in chemical inhibitors of sEH increased due to their possible role in the treatment of inflammation, hypertension and renal damage caused by hypertension (Yu et al., 2000; Imig et al., 2002; Zhao et al., 2004; Imig et al., 2005; Schmelzer et al., 2005; Smith et al., 2005). Highly potent and selective inhibitors for sEH have been developed (Morisseau et al., 1999; Nakagawa et al., 2000; Morisseau et al., 2002; McElroy et al., 2003; Kim et al., 2004c; Kim et al., 2005b) and used to describe the biology associated with sEH (Morisseau and Hammock, 2005). While medicinal chemistry approaches were employed to increase their inhibitory activity and solubility (McElroy et al., 2003; Kim et al., 2004c; Kim et al., 2005b), the latest reported compounds still do not possess physical properties to produce a successful pharmaceutical (Lipinski et al., 2001). For example, the sEH inhibitor AUDA (12-(3-adamantane-1-yl-ureido)-dodecanoic acid) is only 30% orally available and thus can only work with careful formulation. This is, in part, due to suboptimal pharmacokinetic properties (Watanabe et al., 2006). Therefore, while urea-based compounds are good sEH inhibitors *in vitro* and valuable experimental tools, they should be improved toward higher biological availability and stability for future *in vivo* drugs that can be administered orally with simple formulations. Consequently, there is need for novel sEH inhibitor structures and optimized urea, amide and carbamate inhibitors. This fact will require screening of large compound libraries on one hand, as well as rational improvements of known structures – perhaps in combination with combinatorial chemistry and thus large numbers of molecules to test – on the other.

To select structures leading to potent sEH inhibitors, it is necessary to have robust and sensitive enzymatic screening tools in hand. A rapid kinetic spectrophotometric assay employing recombinant sEH and carried out in 96-well microtiter plates was used to develop the first generation of sEH inhibitors (Dietze et al., 1994; Morisseau et al., 1999). However, this assay was not sensitive enough to distinguish among the best compounds based on their  $IC_{50}$  values (Kim et al., 2004c; Kim et al., 2005b) and therefore will be of little use in the quest for enhanced inhibitory molecules. Moreover, the aqueous instability of this photometric substrate (4-nitrophenyl-*trans*-2,3-epoxy-3-phenylpropyl carbonate or NEPC; Dietze et al., 1994) requires short incubation time and it can thus not be employed in long-term assay systems as often in use for screening large compound libraries (Davydov et al., 2004; Soriano et al., 2006). Besides the photometric inhibitor test system, several sensitive radiochemical and chromatographic assays have been developed (Borhan et al., 1995). Unfortunately though, they are too slow, costly and labour intensive to screen larger amounts of compounds.

In summary, to discover new and optimize known inhibitory structures of sEH, novel enzymatic screening tools for sEH inhibitors were required. Ideally, there should be two new assay systems: (a) one, which would be fast and effortless in execution as well as more sensitive than NEPC to separate the most potent sEH inhibitors by their  $IC_{50}$ s and (b) one, which could be used for screening large compound libraries to find new inhibitory structures in a high-throughput manner. In order to develop these systems, a series of novel fluorescent substrates for sEH (see Figure 11) were designed, synthesized and kindly provided by Dr. Paul D. Jones. In this study, these compounds were examined for their aqueous solubility and stability as well as for kinetic properties in combination with several recombinant sEHs. By means of this acquired knowledge, suitable substrates for the intended assays were selected and the corresponding assay conditions were optimized. Finally, the newly developed tests to determine potent sEH inhibitors were validated and a possible stop solution for the high-throughput screen assay was investigated.

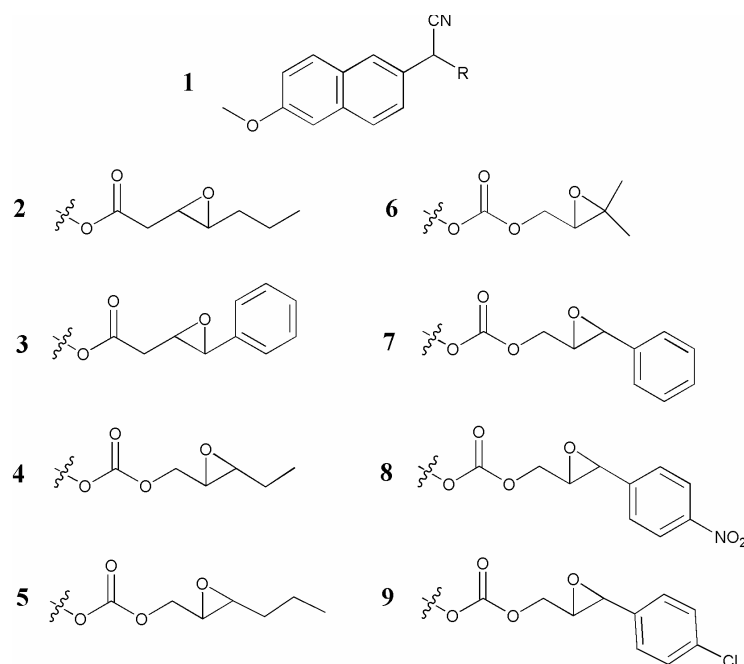


**Fig. 11** Novel fluorescent substrates for sEH. All compounds have the chemical motive **1** in common while various ester or carbonate groups holding an epoxide each complete the structures (**2** through **9**). These variable molecule parts are positioned at the 'R' moiety of the basic structure. (R = rest)

### 1.2 Reaction mechanism and synthetic properties of fluorescent sEH substrates

$\alpha$ -Cyanoesters and -ethers are basically non-fluorescent. Yet the cleavage of these molecules by esterases and P450s, respectively, can result in the formation of highly fluorescent aldehydes (Shan and Hammock, 2001; Wheelock et al., 2003; Zhang et al., 2003; Huang et al., 2005a; Huang et al., 2005b; Kang et al., 2005; Huang et al., 2006). The novel substrates for sEH shown in Figure 11 consist of  $\alpha$ -cyanoester and  $\alpha$ -cyanocarbonate epoxides. They were designed to follow the same mechanistic degradation pathway as reported by Dietze et al. (1994) for NEPC. However, in this case 6-methoxy-2-naphthaldehyde, which is characterized by a large Stokes' shift (Shan and Hammock, 2001), was selected as reporter molecule (Jones et al., 2005) in analogy to the above mentioned substrates for esterases and P450s.

In brief, NEPC as well as the new fluorescent substrates are hydrolyzed by sEH resulting in their corresponding diols. The reaction is followed by a consecutive intramolecular cyclization of the compounds. In case of NEPC, this leads to the release of 4-nitrophenol, which is utilized as a spectrophotometric reporter molecule. On the other hand, cleavage of the novel fluorescent substrates



causes the liberation of a cyanohydrin, which – under basic conditions – very rapidly decays to the highly fluorescent 6-methoxy-2-naphthaldehyde (see Figure 12).

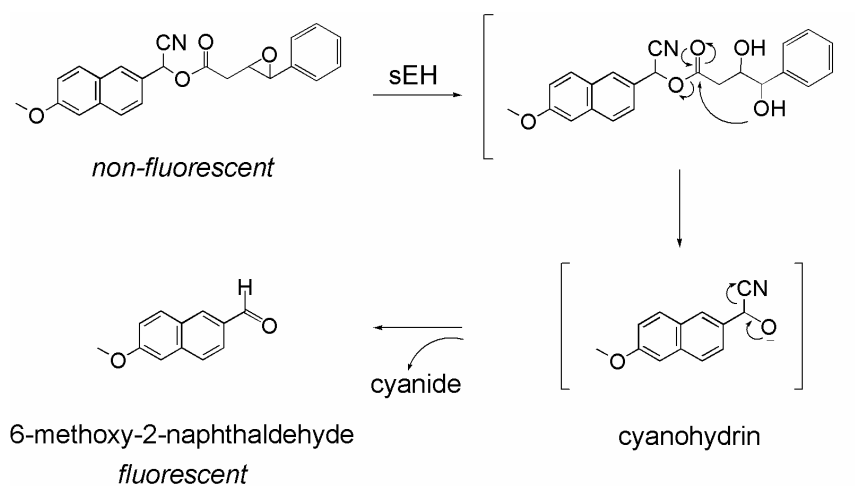


**Fig. 12** Reaction mechanism of novel fluorescent substrates for sEH - ester **3** serves as example.

The fluorescent substrates of the present study were produced in a racemic synthesis (Jones et al., 2005), since it has been reported previously that only little difference can be observed between (+)-NEPC and (-)-NEPC (Dietze et al., 1994). Furthermore, due to the lack of enantiomeric preference of mammalian sEH, only *trans*-epoxides were included in this study (Jones et al., 2005)

### 1.3 Materials and methods

#### 1.3.1 Chemicals and reagents

Chemicals and reagents were purchased from Sigma Chemical (St. Louis, MO, USA) unless otherwise indicated. The solvents 1-propanol, 2-propanol, acetonitrile, dioxane, dimethyl formamide (DMF), DMSO, tetrahydrofuran (THF), ethanol (95%) and methanol as well as hydrogen peroxide, hydrochloric acid and 2-[bis(2-hydroxyethyl)amino]-2(hydroxy-methyl)-1,3-propanediol (BisTris) were obtained from Fisher Scientific Co. (Pittsburgh, PA, USA). One hundred percent ethanol was acquired from Gold Shield Chemical Co. (Hayward, CA, USA). All of the substances were of at least enzymatic grade. 6-Methoxy-2-naphthaldehyde was purchased from Avocado Research Chemicals (Heysham, UK).

Fluorescent substrates for sEH were synthesized as described in Jones et al. (2005) and, while not in use, stored as 100x dimethyl sulfoxide (DMSO) stocks at -20°C.

### 1.3.2 Enzymes

Recombinant sEH from human (Beetham et al., 1993), mouse (Grant et al., 1993), rat (Knehr et al., 1993), potato (Stapleton et al., 1994) and mouse-eared cress (Kiyosue et al., 1994) were kindly provided by Dr. Christophe Morisseau. They were produced in a baculovirus expression system and purified by affinity chromatography as previously described (Wixtrom et al., 1988; Morisseau et al., 2000). Enzyme preparations were at least 97% pure as confirmed by SDS-PAGE and scanning densitometry. Esterase or glutathione *S*-transferase activities, which may interfere with sEH assays of the present study, could not be detected. Protein concentrations of the recombinant sEH preparations were determined by BCA assay using albumin standard for calibration (both products from Pierce, Rockford, IL, USA). Porcine liver esterase was purchased from Sigma Chemical (St. Louis, MO; USA).

### 1.3.3 Buffer

The buffer utilized in this enzymological study was BisTris with an ionic strength of 25 mM, supplemented with 0.1 mg bovine serum albumin (BSA) fraction V per ml of buffer and prepared with water filtered through a MilliQ reagent water system (Millipore Corp., Bedford, MA, USA). Since the buffer was employed at different pHs, pH-adjustment with HCl was required.

### 1.3.4 Standardization curves

Fluorescence and absorbance are determined in relative fluorescence units (RFU) and optical density (OD), respectively. Thus for quantification purposes, standardization curves – acquired under the respective assay conditions – were necessary to convert the obtained values into moles of fluorophore and moles of chromophore, respectively.

For this purpose, stock solutions of the fluorescent reporter molecule 6-methoxy-2-naphthaldehyde in dimethyl sulfoxide (DMSO) were prepared at known concentrations (0.01 – 10 mM) and diluted (ratio 1:25 v/v) with buffer (pH 6.5, 7.0, 7.5 and 8.0). Subsequently, 50 µl of these mixtures

were added to 150  $\mu\text{l}$  of the same buffer in a black 96-well polystyrene microtiter plate (Greiner Bio-One, Longwood, FL, USA). Thus, final assay volume was 200  $\mu\text{l}$ , DMSO concentration was 1% (v/v) and final concentrations of the reporter molecule ranged between 0.1 and 100  $\mu\text{M}$ .

Fluorescence measurements were carried out with two different fluorescence plate readers, because the two assay systems were developed employing two separate machines. The settings of the SpectraFluor Plus plate reader (Tecan, Research Triangle Park, NC, USA) were the following: excitation wavelength 330 nm (band width = 20 nm), emission wavelength 465 nm (band width = 20 nm), manual gain 60, integration time 40  $\mu\text{s}$ , number of flashes 3, and temperature 30°C. The SpectraMax M2 microplate reader (Molecular Devices, Sunnyvale, CA, USA) had the following setup: excitation wavelength 316 nm, emission wavelength 460 nm (cutoff 455 nm), 3 reads per well. In this case, fluorescence readings were acquired at room temperature which was  $23 \pm 2^\circ\text{C}$ .

A similar experiment was carried out for the colorimetric reporter molecule of NEPC, 4-nitrophenol. Stock solutions of this chemical at known concentrations were prepared in 100% ethanol, diluted (1:12.5 and 1:25 v/v) with buffer at pH 7.0 and added to the same buffer in a clear polystyrene 96-well plate (ThermoLabsystems, Franklin, MA, USA) as already described. This resulted in final ethanol concentrations of 2% and 1% as well as to 4-nitrophenol concentrations of 0.2-200  $\mu\text{M}$  and 0.1-100  $\mu\text{M}$ . Absorbance measurements were taken with the SpectraMax 340PC<sup>348</sup> microplate spectrophotometer (Molecular Devices, Sunnyvale, CA, USA) at 405 nm and 30°C.

Correlations between moles of 6-methoxy-2-naphthaldehyde and RFU as well as 4-nitrophenol quantity and OD were calculated by linear regression using Origin 6.1 (Microsoft, Redmond, WA, USA). Measurements were carried out in at least three replicates and linear regression was performed with at least five datum points resulting in correlation coefficients of at least 0.97.

### 1.3.5 Determination of aqueous solubility

Fluorescent substrates were observed to display low solubility in aqueous solutions. Therefore, their apparent limit of solubility (LS) was determined experimentally. DMSO stock solutions of compounds **2** through **9** were prepared at the following concentrations: 10, 7.5, 5, 2.5, 1.5, 1.0, 0.75, 0.5, 0.25, 0.1 and 0.05 mM. First, these solutions were diluted 1:25 (v/v) in buffer (pH 7.0). Then 50  $\mu\text{l}$  of the

resulting mixtures were added in triplicate to 150  $\mu$ l of the buffer in a clear 96-well styrene flat-bottom microtiter plate (ThermoLabsystems, Franklin, MA, USA; final DMSO stock concentration in assay volume was 1%). Insolubility of the substrates was indicated by the increase in turbidity in aqueous solution and determined by measuring absorbance at 800 nm using a SpectraMax 340PC<sup>384</sup> microplate spectrophotometer (Molecular Devices, Sunnyvale, CA, USA) at 30°C.

### 1.3.6 Determination of aqueous stability

One mM stock solutions of all fluorescent substrates were prepared in DMSO and diluted 1:25 (v/v) in buffer (pH 6.5, 7.0, 7.5 and 8.0). Fifty  $\mu$ l of these mixtures were then added to 150  $\mu$ l of the same buffer in a black 96-well microtiter plate (Greiner Bio-One, Longwood, FL, USA). The hydrolysis of the substrates was recorded using a SpectraFluor Plus fluorescence plate reader (Tecan, Research Triangle Park, NC, USA) by measuring the fluorescence signal of 6-methoxy-2-naphthaldehyde for 10 min every 30 s at 30°C employing the above mentioned settings. To test aqueous stability for pH dependency at pH 6.5, 7.0, 7.5 and 8.0, measurements were taken in triplicate. Assays to assess the hydrolysis rates of the different substrates at pH 7.0 were conducted in at least thirty replicates. In both cases, rates of hydrolysis were determined by linear regression analysis of the linear part of each hydrolysis graph.

Additionally, an experiment to directly compare aqueous stability of NEPC and one of the less stable fluorescent substrates was performed. For this purpose, 2.5 and 2.0 mM solutions of NEPC in 100% ethanol as well as 2.0 and 0.5 mM stocks of compound **7** in DMSO were produced and diluted as described above. Exception here was the 2.5 mM stock solution of NEPC, which was diluted first 1:12.5 (v/v) to achieve inhibitor assay conditions. In this case, the final solvent content was 2%. Experiments to determine the aqueous stability of NEPC were performed in clear polystyrene 96-well microtiter plates (ThermoLabsystems, Franklin, MA, USA). Absorbance readings were carried out at 405 nm in a SpectraMax 340PC<sup>384</sup> microplate spectrophotometer (Molecular Devices, Sunnyvale, CA, USA) for 10 min every 30 s at 30°C. 6-methoxy-2-naphthaldehyde appearance was monitored for 10 min every 30 s with a SpectraFluor Plus plate reader (Tecan, Research Triangle Park, NC, USA) as already explained. Hydrolysis rates were again determined by linear regression.

### 1.3.7 Determination of specific activity

One millimolar fluorescent substrate stock solutions in DMSO were pre-diluted as described above and 50  $\mu\text{l}$  of the resulting mixture was added to 150  $\mu\text{l}$  of previously incubated (5 min at 30°C) enzyme solution in a black 96-well microtiter plate (Greiner Bio-One, Longwood, FL, USA;  $[\text{S}]_{\text{final}} = 10 \mu\text{M}$ ). Enzyme solutions consisted of purified recombinant sEH from cress, potato, rat, mouse or human sEH as well as porcine liver esterase in buffer (pH 7.0) at various quantities (human sEH: 0-1.2  $\mu\text{g}/\text{well}$ , mouse sEH: 0-3.6  $\mu\text{g}/\text{well}$ , rat sEH: 0-1.7  $\mu\text{g}/\text{well}$ , cress sEH: 0-3.5  $\mu\text{g}/\text{well}$ , potato sEH: 0-0.8  $\mu\text{g}/\text{well}$ , porcine liver esterase: 0-0.3  $\mu\text{g}/\text{well}$ ). Subsequently, appearance of the fluorescent reporter molecule was monitored using a SpectraFluor Plus fluorescence plate reader (Tecan, Research Triangle Park, NC, USA) and the corresponding settings. Measurements were performed for at least 10 min every 30 s at 30°C. These tests were carried out in triplicate at least.

Initial velocities of substrate turnover were determined by linear regression and only further considered if  $r^2$  was  $> 0.9$ . Mean velocities, corrected for the respective mean background hydrolysis rates (reaction without enzyme, carried out in at least fifteen replicates), were then plotted versus the corresponding protein concentrations. Specific enzyme activities were determined by linear regression of the linear portion of these curves containing at least four datum points. Exceptions were specific activities of potato sEH and porcine liver esterase for compound **6**. For the plant enzyme, substrate turnover above background was only significant for the three highest protein concentrations (in this case,  $r^2$  values were not considered). Thus, specific activity determination could only be conducted with three datum points. In case of porcine liver esterase, only initial velocities of the three lowest enzyme concentrations were taken into account for linear regression analysis, due to the obviously non-linear tendency of the remaining datum points.

### 1.3.8 Determination of $K_m$ , $V_{\text{max}}$ and $k_{\text{cat}}$

The assays to determine the Michaelis-Menten parameters  $V_{\text{max}}$  and  $K_m$  were carried out similar to the determination of specific enzyme activity. However, instead of varying the enzyme concentration per well, these were kept constant (cf. Table 1 for final enzyme concentrations) and substrate concentrations were varied. Therefore, substrate stock solutions were prepared in DMSO and pre-diluted as described

above. Fifty  $\mu\text{l}$  of these solutions were then added to 150  $\mu\text{l}$  of pre-incubated (5 min at 30°C) enzyme-buffer (pH 7.0) mixtures in black 96-well polystyrene plates (Greiner Bio-One, Longwood, FL, USA) in at least triplicate. Final substrate concentrations were 25, 15, 10, 7.5, 5, 2.5, 1, and 0.5  $\mu\text{M}$ . Fluorescence measurements were taken every 30 s for 10 min with a SpectraFluor Plus plate reader (Tecan, Research Triangle Park, NC, USA) and the described settings.

**Table 1** Final enzyme concentrations employed in the determination of the Michaelis-Menten parameters.  $[\text{E}]_{\text{final}}$  in nM.

	Human sEH	Mouse sEH	Rat sEH	Cress sEH	Potato sEH
<b>2</b>	9.4	11.5	27.3	48.9	37.9
<b>3</b>	2.8	6.9	5.5	6.5	9.1
<b>4</b>	9.4	16.4	27.3	16.3	37.9
<b>5</b>	2.8	6.9	9.1	10.9	37.9
<b>6</b>	141.7	345.3	273.4	326.0	227.3
<b>7</b>	2.8	6.9	20.5	24.4	37.9
<b>8</b>	5.7	13.8	8.2	48.9	11.4
<b>9</b>	5.7	13.8	8.2	4.9	4.5

Initial velocities ( $v$ ) of the 6-methoxy-2-naphthaldehyde appearance were determined by linear regression analysis and only considered if  $r^2 > 0.9$ . Exception here were reactions of potato sEH with compound **3**, in which case velocities with  $r^2$  values of greater than 0.85 were taken into account as well. Resulting velocities of corresponding reactions were then, corrected for self-hydrolysis rates, averaged and plotted as  $1/v$  versus  $1/[\text{S}]_{\text{final}}$ . Subsequently, linear regression analysis was performed with at least four datum points, resulting in  $K_m/V_{\text{max}}$  values that represent the slopes of the obtained lines. Additionally, the specificity constants for all substrate-enzyme combinations were obtained by applying the following formula:

$$k_{\text{cat}}/K_m = \frac{(K_m/V_{\text{max}} \times 60)^{-1}}{\text{protein amount of reaction}} \quad \begin{array}{l} k_{\text{cat}}/K_m \text{ in } \text{s}^{-1} \mu\text{M}^{-1} \\ K_m/V_{\text{max}} \text{ in } \text{nmol}/\text{min} \\ \text{protein amount in } \text{nmol} \end{array}$$

### 1.3.9 Optimization of detection of 6-methoxy-2-naphthaldehyde

The subsequently described long-term assay system, intended for high-throughput screens of large compound libraries, was intended to be conducted at room temperature and measurements were intended to be taken with a SpectraMax M2 plate reader (Molecular Devices, Sunnyvale, CA, USA). This prerequisite and the option of this particular machine to scan fluorescent spectra suggested the new determination of excitation and emission maxima of 6-methoxy-2-naphthaldehyde under assay conditions. Therefore, 200  $\mu$ l of a 10  $\mu$ M 6-methoxy-2-naphthaldehyde solution in buffer (pH 7.0, including 1% (v/v) DMSO) were added to a black polystyrene 96-well microtiter plate (Greiner Bio-One, Longwood, FL, USA) in five replicates. The excitation and emission spectra scans were conducted in an iterative procedure at room temperature with scanning steps as small as 1 nm in a range of at least 20 nm.

### 1.3.10 Assay optimization

After selecting a substrate for each type of assay (compound **7** for a fast and sensitive continuous test and **3** for an endpoint assay suitable for compound screening in a high-throughput format), the conditions for both systems were optimized using checkerboard assays. These tests should facilitate to find combinations of substrate and enzyme concentrations, which would result in high sensitivity in case of the kinetic system as well as steady-state-like conditions during the endpoint assay.

Consequently, combinations of various enzyme and substrate concentrations were tested in black polystyrene 96-well plates (Greiner Bio-One, Longwood, FL, USA) employing BisTris buffer at pH 7.0. After a 5-min incubation of the respective enzyme solution, reactions were started by addition of pre-diluted substrate as described before. The **kinetic assay** was optimized with human sEH amounts of 0-354 ng/well, and mouse sEH quantities of 0-1079 ng/well, respectively. The corresponding substrate concentrations of compound **7** ranged between 0 and 10  $\mu$ M. Reporter molecule appearance at 30°C was monitored for 10 min every 30 s with a SpectraFluor Plus plate reader (Tecan, Triangle Research Park, NC; settings as described before). **Endpoint assay** optimization was performed at room temperature with human sEH amounts of 0-219 ng/well and concentrations of substrate **3** between 0 and 50  $\mu$ M. In this case fluorescence was detected for 2 h every 3 min utilizing a SpectraMax M2 microplate

reader (Molecular Devices, Sunnyvale, CA, USA) and the earlier mentioned instrument setup. These investigations were performed under room temperature conditions. Subsequently, selected concentrations of enzyme and substrate were evaluated in quadruplicate.

### 1.3.11 Assay validation

Inhibitor assays were carried out in order to test and validate the optimized novel fluorescent assay systems and to compare them with other methods.

In case of the **continuous kinetic assay** employing substrate **7**,  $IC_{50}$ s of sEH inhibitors were determined as it follows: enzymes (0.88 nM for murine and 0.96 nM for human sEH) were incubated with inhibitors ( $[I] = 0.5$ -10,000 nM) for 5 min in buffer (pH 7.0) at 30°C prior to substrate introduction ( $[S]_{\text{final}} = 5 \mu\text{M}$ ; 1% (v/v) final DMSO concentration per well). Soluble epoxide hydrolase activity was measured with a SpectraFluor Plus plate reader (Tecan, Longwood, FL, USA) as described earlier monitoring the appearance of the reporter molecule for 10 min every 30 s.  $IC_{50}$ s are inhibitor concentrations that reduce enzyme activity by 50%. These values were determined by regression of at least five datum points with a minimum of two points in the linear region of the curve on either side of the  $IC_{50}$ s. The curve was generated from at least three separate runs, each in triplicate. Results are given as means  $\pm$  standard deviation.

In case of the **endpoint assay**, inhibitor potencies were tested in three complementary ways (a-c). First,  $IC_{50}$ s of sEH inhibitors were determined employing the endpoint assay system (3 nM final enzyme concentration; 50  $\mu\text{M}$  final substrate concentration; 200  $\mu\text{l}$  total assay volume in black 96-well polystyrene microtiter plates from Greiner Bio-One, Longwood, FL, USA). For one set of experiments (a), serial dilutions of inhibitor in triplicate as well as their vehicle DMSO (in seven replicates for maximum activity) were incubated with enzyme solution for 10 min at room temperature. At the same time, buffer (pH 7.0) was incubated with DMSO as well as inhibitor (eight replicates each) in order to determine the substrate's self-hydrolysis. After addition of compound **3**, reporter group appearance was monitored continuously at room temperature for 60 min every 3 min with a SpectraMax M2 fluorescence plate reader (Molecular Devices, Sunnyvale, CA, USA) and detection settings as indicated above. Substrate turnover rates were determined by SoftMax Pro 4.7 (software of the SpectraMax M2



plate reader) and further used for  $IC_{50}$  calculations. These again included linear regression analyses employing at least three datum points (corresponding to the substrate turnover rates) in the linear range of the resulting inhibition curve (between 20 and 80% enzyme activity reduction). After that, the concentration at which sEH activity only displayed 50% of its maximum was determined by means of the obtained regression curve.

In a separate but similar approach (b), experiments to reveal the  $IC_{50}$ s of the same inhibitors were conducted exactly as described for the endpoint assay system in at least five replicates. The only difference was the detection method, which consisted only of a single fluorescence measurement after 60 min with a SpectraMax M2 plate reader (Molecular Devices, Sunnyvale, CA, USA).  $IC_{50}$  calculations were carried out as per above, setting the mean level of fluorescence from reactions without enzyme as 100% inhibition and the one of reactions without inhibitor as 0%.

These two types of experiments (a and b) were conducted to compare actual  $IC_{50}$  values of the endpoint system to the kinetic fluorescent system as well as to tests performed with NEPC and *t*DPPO. In addition, they were supposed to test both detection variants to be applicable. However, a further set of experiments (c) was carried out to evaluate the endpoint assay system for robustness. Therefore, enzyme solutions (final enzyme concentration was again 3 nM) were incubated with five already characterized inhibitors (Morisseau et al., 1999; Morisseau et al., 2002; McElroy et al., 2003) at one concentration each (final concentrations of inhibitors: 10  $\mu$ M CEU, 0.1  $\mu$ M CHU, 10  $\mu$ M DCU, 0.1  $\mu$ M CDU and 0.1  $\mu$ M AUDA) or DMSO for 10 min in quadruplicate. Additionally, buffer at instead of enzyme solution was incubated with DMSO to determine substrate self-hydrolysis. After addition of substrate **3** (final concentration 50  $\mu$ M; total assay volume 200  $\mu$ l), the black 96-well polystyrene plates (Greiner Bio-One, Longwood, FL, USA) were sealed and kept in darkness at room temperature. After 1 h, fluorescent signal was acquired once with a SpectraMax M2 plate reader (Molecular Devices, Sunnyvale, CA, USA) employing the earlier mentioned settings. After a further 30-min incubation, measurements were repeated. This assay evaluation was performed with 4 plates per day on 3 consecutive days to be able to reveal variations within a plate as well as from plate to plate and from day to day.

### 1.3.12 Evaluation of candidate stop solutions

Performance flexibility of a high-throughput assay is supposed to increase with the employment of a stop solution. In order to test several chemicals as stop solutions for the above described endpoint assay system ultimately intended to be performed in a high-throughput manner, reactions were set up employing optimized conditions (see above). After 1 h of reaction time in darkness and at room temperature, 50  $\mu$ l the potential stop solutions were added to the reactions as well as – for comparison reasons – 50  $\mu$ l of buffer (pH 7.0). Candidate solutions were 1-propanol, 2-propanol, acetonitrile, saturated ammonium sulphate solution, 10% (v/v) bleach in water, 5% (w/w) borax in water, 25% dioxane in water, DMF, DMSO, ethanol (95%), 30% H<sub>2</sub>O<sub>2</sub>, saturated solution of iodine in H<sub>2</sub>O, methanol, 5% (v/v) morpholine in water, 50% polyethylene glycol in water, 10% (w/w) SDS in water, 0.5% sodium azide in water, 10% (v/v) THF in water, and 1 M solutions of zinc nitrate and zinc sulphate in water. Subsequently, the fluorescent signals of all reactions were monitored every min for at least 10 min using a SpectraMax M2 microplate reader (Molecular Devices, Sunnyvale, CA, USA) and detection settings as described before. For the initial screen of compounds, reactions were carried out without replicates, whereas the later experiments with zinc sulphate and zinc nitrate solutions of various concentrations were conducted in triplicate. The resulting data were further analyzed relatively to the respective reference – the variant where buffer was added to the reaction instead of a candidate stop solution. Hydrolysis rates were determined by linear regression analyses employing the plate reader's software SoftMax Pro 4.7 (Molecular Devices, Sunnyvale, CA, USA). Fluorescence levels were compared by taking in account the first acquired fluorescent signals after stop solution addition.

In a further step, the impact of Zn(NO<sub>3</sub>)<sub>2</sub> and ZnSO<sub>4</sub> on the fluorescent signal of 6-methoxy-2-naphthaldehyde was evaluated. Therefore, calibration curves of this substance were obtained as described above. Subsequently, 50  $\mu$ l of buffer (pH 7.0), or 1 M solutions of Zn(NO<sub>3</sub>)<sub>2</sub>, ZnSO<sub>4</sub> respectively (both dissolved in water), were added to a set of standard solutions (250  $\mu$ l final assay volume), resulting in data for three distinct standardization curves containing seven datum points each. Single fluorescence readings were taken again with a SpectraMax M2 microplate reader (Molecular Devices, Sunnyvale, CA, USA) and the corresponding detection setup. Subsequently, data were analyzed by linear regression analyses.

### 1.4 Results

Physical, chemical and enzyme-kinetic properties of the fluorescent substrates were examined first to find the most suitable substrate(s) for subsequent assay development.

#### 1.4.1 Aqueous solubility

To determine aqueous solubility of compounds **2** through **9**, various concentrations of DMSO stock solutions per substrate were diluted in assay buffer (pH 7.0) with a final DMSO concentration of 1%. The absorbance of these solutions at 800 nm was examined in a clear 96-well microtiter plate.

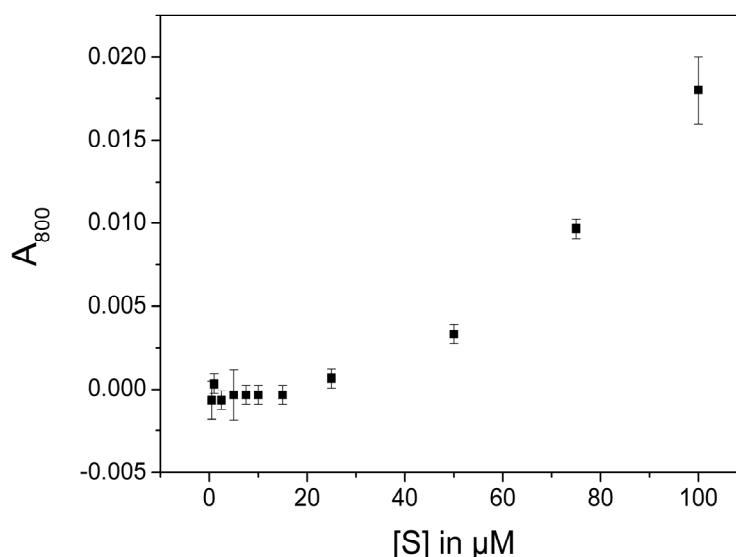


**Fig. 13** Determination of aqueous solubility for compound **2**. The presented absorbance data correspond to mean values  $\pm$  standard deviation ( $n=3$ ).

In this experiment, detected absorbance represents turbidity of the solution and thus substrate precipitation, which only occurs above the apparent limit of solubility (LS) of a chemical (see Figure 13 as data example from the present study). A range for this value was determined for each fluorescent substrate (see Table 2). At the upper concentration limit of this range, absorbance was first observed to rise above background, whereas the lower concentration limit did not display significant turbidity.

Table 2 identifies compound **3** as most soluble substrate under the employed experimental conditions. It is still in solution at a concentration of 50  $\mu\text{M}$ . Least soluble were compounds **7** and **9**, which were both found to precipitate in aqueous solution above a concentration of 15  $\mu\text{M}$ .

**Table 2** Determined concentration range for the apparent LS of fluorescent substrates **2** through **9**.

Compound	Lower LS [ $\mu\text{M}$ ]		Upper LS [ $\mu\text{M}$ ]
<b>2</b>	25	$\leq$ LS $\leq$	50
<b>3</b>	50	$\leq$ LS $\leq$	75
<b>4</b>	25	$\leq$ LS $\leq$	50
<b>5</b>	25	$\leq$ LS $\leq$	50
<b>6</b>	25	$\leq$ LS $\leq$	50
<b>7</b>	15	$\leq$ LS $\leq$	25
<b>8</b>	25	$\leq$ LS $\leq$	50
<b>9</b>	15	$\leq$ LS $\leq$	25

#### 1.4.2 Aqueous stability

Aqueous stability of all fluorescent compounds was first investigated for pH dependency. This examination, the following auto-hydrolysis tests as well as the specific activity determinations were carried out with a final substrate concentration of 10  $\mu\text{M}$

to ensure complete solubility of all substrates. In general, it could

be observed that, with increasing pH in the range between 6.5 and 8.0, hydrolysis rates increased correspondingly. Figure 14 demonstrates this finding for compound **5**. High standard deviations originate mostly from measurements taken close to the detection limit.

Additionally, self-hydrolysis was determined at pH 7.0 in at least 30 replicates. This high number was employed to achieve lower standard deviations and thus more reliable values for the comparison of all substrates. Figure 15 displays the hydrolysis rates for compounds **2** through **9**.

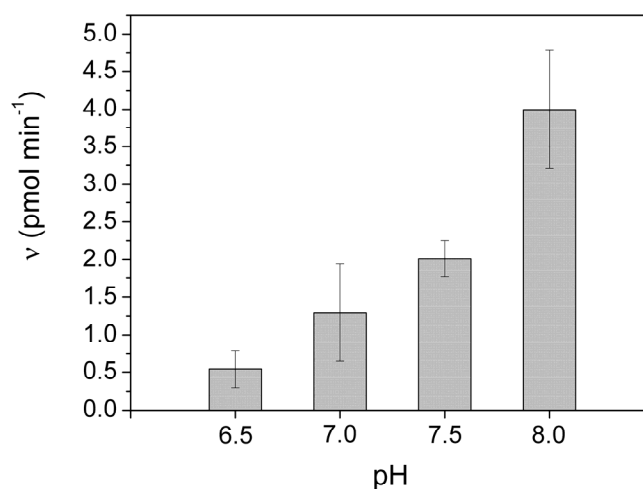


**Fig. 14** Aqueous stabilities of compound **5** at different pH values. Data are shown as mean values  $\pm$  standard deviation ( $n=3$ ).

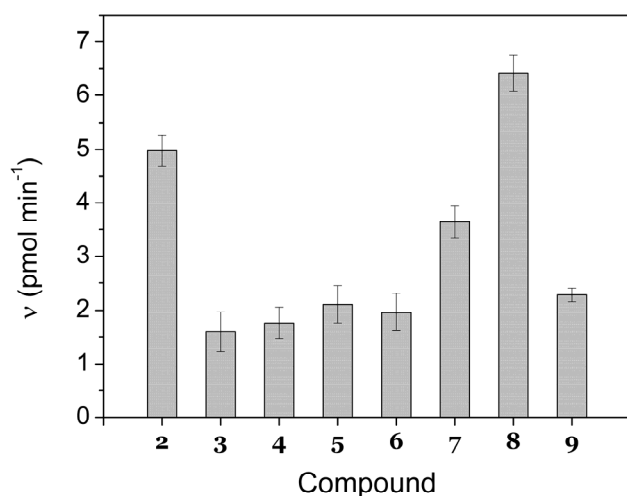


**Fig. 15** Self-hydrolysis rates of fluorescent substrates. Data correspond to means  $\pm$  standard deviation ( $n \geq 30$ ).

This chart reveals compounds **8**, **2** and **7** as least stable under the test conditions, whereas compounds **3** through **6** as well as compound **9** show comparatively low self-hydrolysis rates. Interestingly, the aqueous stability of all compounds is rather different: substrate **8**, as least stable, decays about four times faster than the most stable one (compound **3**).

Furthermore, an investigation was carried out to compare aqueous stabilities of NEPC and compound **7** at different pHs. Substrate **7** was chosen for the development of a kinetic assay in order to subsequently test sEH inhibitor potencies in a fast and highly sensitive way. Thus, the stability comparison was conducted at final substrate concentrations as employed in the optimized inhibitor assays (50  $\mu\text{M}$  for NEPC and 5  $\mu\text{M}$  for substrate **7**) as well as at the same substrate concentrations (20  $\mu\text{M}$ ) to directly compare hydrolysis rates. The results of this study are shown in Figure 16. Based on the comparison of both substances at the same final concentration, NEPC is clearly less hydrolytically stable. This statement holds true for assay conditions with an increased NEPC concentration and a decreased concentration of compound **7**.

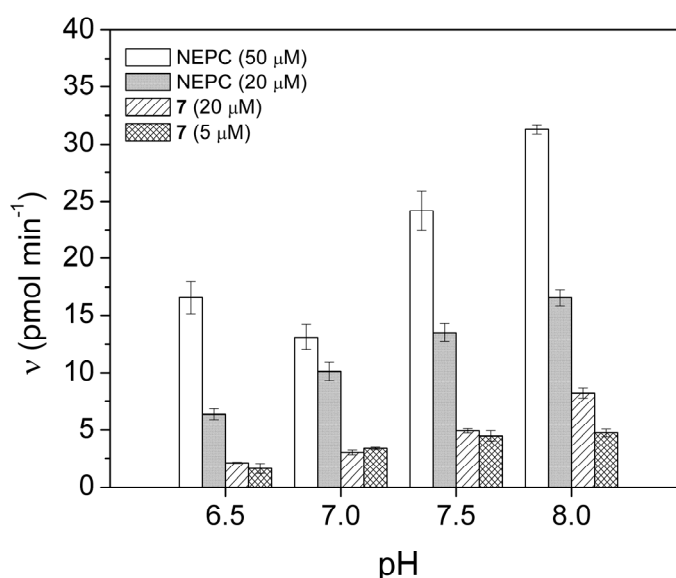


**Fig. 16** Aqueous stability of NEPC and substrate **7** at two concentrations each. Values represent means  $\pm$  standard deviation ( $n \geq 3$ ).

## 1.4.3 Specific activities

Specific activities of substrates **2** through **9** (see Table 3) were determined for several recombinant soluble epoxide hydrolases as well as for porcine liver esterase to obtain a first evaluation of the enzymes' substrate selectivity. In addition, these tests enabled to select a suitable enzyme concentration for subsequent experiments determining the Michaelis-Menten parameters  $K_m$ ,  $V_{max}$  and  $k_{cat}$ .

**Table 3** Specific activities of recombinant soluble epoxide hydrolases and porcine liver esterase for compounds **2** through **9** in  $\text{nmol min}^{-1} \text{mg}^{-1}$ . Specific activities are given as slopes  $\pm$  standard error determined by linear regression analysis.

Compound	Human sEH	Mouse sEH	Rat sEH	Cress sEH	Potato sEH	Porcine liver esterase
<b>2</b>	522 $\pm$ 5	275 $\pm$ 4	305 $\pm$ 8	423 $\pm$ 7	597 $\pm$ 25	6347 $\pm$ 486
<b>3</b>	729 $\pm$ 96	214 $\pm$ 63	461 $\pm$ 9	743 $\pm$ 121	279 $\pm$ 19	1956 $\pm$ 92
<b>4</b>	358 $\pm$ 16	125 $\pm$ 32	178 $\pm$ 16	430 $\pm$ 41	169.5 $\pm$ 0.1	3568 $\pm$ 126
<b>5</b>	785 $\pm$ 104	254 $\pm$ 45	635 $\pm$ 33	935 $\pm$ 74	279 $\pm$ 8	2138 $\pm$ 90
<b>6</b>	12.0 $\pm$ 0.4	8.31 $\pm$ 0.05	19.5 $\pm$ 1.1	48.8 $\pm$ 1.4	27.2 $\pm$ 0.4	1713 $\pm$ 167
<b>7</b>	2647 $\pm$ 167	586 $\pm$ 66	599 $\pm$ 58	1768 $\pm$ 51	401 $\pm$ 5	1939 $\pm$ 32
<b>8</b>	614 $\pm$ 19	760 $\pm$ 40	382 $\pm$ 2	441 $\pm$ 70	248 $\pm$ 15	833 $\pm$ 25
<b>9</b>	699 $\pm$ 10	924 $\pm$ 16	458 $\pm$ 13	964 $\pm$ 134	660 $\pm$ 19	1036 $\pm$ 10

Porcine liver esterase displays relatively high specific activities with all the tested substrates. Particularly ester **2** was found to be turned over with very high preference, whereas compound **8** and **9** were favoured least.

All examined recombinant soluble epoxide hydrolases show their lowest specific activities with compound **6**. The observed values are roughly at least one order of magnitude lower than all other specific activities determined.

Both plant enzymes display a preference for substrate **9**. But whereas potato sEH shows an increased specific activity value only with ester **2** and carbonate **7**, cress sEH is not very selective and exhibits elevated specific activities for all compounds except substrate **6**. Particularly high values for cress sEH were found with substance **7** (about two to four fold higher than with the other substrates).

Mouse sEH clearly prefers the aryl carbonates **7**, **8** and **9** with its highest specific activity for compound **9**. However, preferences of rat sEH could be observed for compound **5** and **7**. Human sEH displayed extremely high specific activity in combination with chemical **7**, although high numbers could also be determined for substrates **3**, **5**, and **9**. It should be noted that human sEH generally showed relatively high specific activities in comparison to the other tested sEH.

All tested soluble epoxide hydrolases – in contrast to porcine liver esterase – favour (mostly around twice as much) compound **5** compared to structure **4**. This fact suggests a general selectivity of sEHs for longer chained substances. Additionally, it is interesting to see that only the potato enzyme clearly prefers the alkyl ester **2** over the alkyl carbonates **4** and **5**. The other enzymes either favoured the alkyl carbonate **5** or displayed no obvious preference.

Finally, it is remarkable that out of the five soluble epoxide hydrolases, three exhibit the same order in substrate selectivity for the aryl carbonates **7**, **8** and **9**. The human as well as the rat and the cress enzyme prefer compound **7** over **9** and favour substrate **8** least. However, highest specific activities for mouse and potato sEH in combination with these three substances were examined for aryl carbonate **9**. The same groupings of the recombinant enzymes were found when considering only esters **2** and **3**. The mouse as well as the potato enzyme displayed a preference for the alkyl ester **2**, while the other recombinant sEHs showed higher specific activities for the ester with the terminal phenol group.

#### 1.4.4 Michaelis-Menten parameters

The Michaelis-Menten parameters  $K_m$ ,  $V_{max}$  and  $k_{cat}$  characterize enzyme-substrate interactions regarding substrate turnover and enable a direct comparison between them. In the present study, these values should assist and facilitate the selection of suitable substrates for the new inhibitor assay systems as well as allow conclusions about steady-state conditions of the respective enzyme-substrate reactions.

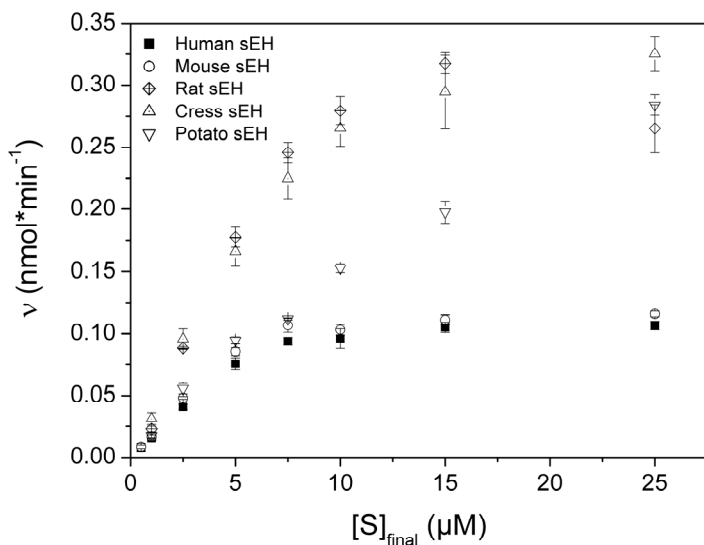


**Fig. 17** Enzyme kinetics of compound **7** in combination with various recombinant sEHs. Data are shown as average velocities  $\pm$  standard deviation ( $n=4$  for human and mouse sEH;  $n=3$  for cress, rat and potato sEH).

When plotting the resulting initial velocities of these enzymatic reactions versus the corresponding substrate concentrations (see Figure 17 for compound **7**), the values for certain substrates are found to reach saturation with increasing concentrations. Moreover, they do not follow a hyperbolic curve shape as expected according to the theory of enzyme kinetics. In case of substrate **7** for example, this phenomenon starts around a substrate concentration of 10  $\mu\text{M}$  suggesting a de facto lower LS than experimentally determined before: the apparent LS for substrate **7** was found to be between 15 and 25  $\mu\text{M}$  (see above).

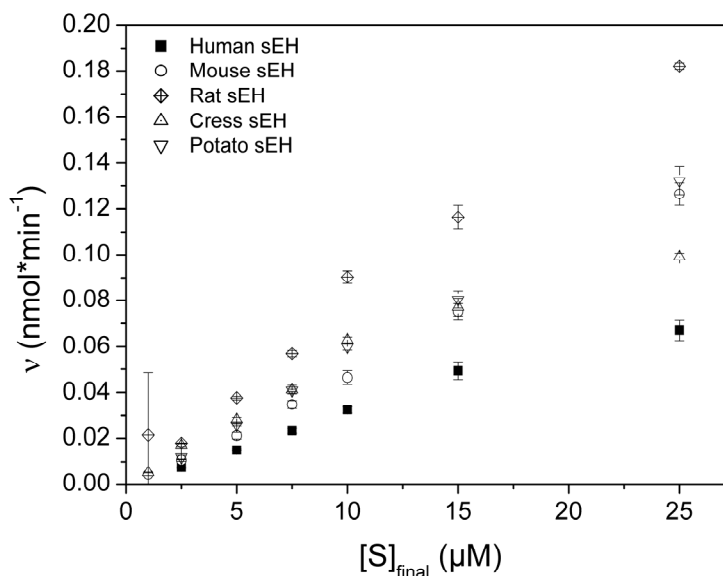


**Fig. 18** Enzyme kinetics of compound **4** in combination with various recombinant sEHs. Data represent average velocities  $\pm$  standard deviation ( $n=4$  for human and mouse sEH;  $n=3$  for cress, rat and potato sEH).

In order to determine the Michaelis-Menten parameters for substrates **2** through **9**, enzyme activities were monitored in dependence of varying substrate concentrations following the appearance of 6-methoxy-2-naphthaldehyde. It should be noted that measurements were only conducted up to final substrate concentrations of 25  $\mu\text{M}$  to ensure complete solubility of most substrates.



Additionally, other substrate-enzyme combinations do not reach saturation conditions with the maximal employed substrate concentration (25  $\mu\text{M}$ ; see Figure 18 for compound **4**) indicating a  $V_{\text{max}}$  value significantly above the highest determined initial velocity. In these cases, examinations employing higher substrate concentrations will possibly lead to results similar to the ones for substrate **7** (see Figure 17) pointing again to solubility limitations of the compounds in aqueous solutions. Therefore, one would not gain further information from such additional experiments.

Overall, the described results made it impossible to directly and accurately determine the Michaelis-Menten parameters  $K_m$ ,  $V_{\text{max}}$  and  $k_{\text{cat}}$ . However, application of the Lineweaver-Burk transformation to the data revealed good correlation of at least four datum points when performing linear regression analysis. The slopes of the corresponding regression lines represent the respective values for  $K_m/V_{\text{max}}$  and are listed in Table 4.

**Table 4**  $K_m/V_{\text{max}}$  values of combinations between several sEHs and fluorescent substrates **2** through **9**. Results were obtained by linear regression analyses of Lineweaver-Burk plots. Numbers are given as means  $\pm$  standard deviation (n=4 for human and mouse sEH; n=3 for cress, rat and potato sEH) in  $\text{min } \mu\text{M nmol}^{-1}$ .

Substrate	Human sEH	Mouse sEH	Rat sEH	Cress sEH	Potato sEH
<b>2</b>	95.4 $\pm$ 7.0	94.9 $\pm$ 3.9	140.0 $\pm$ 4.3	152.8 $\pm$ 3.7	181.8 $\pm$ 0.3
<b>3</b>	256.9 $\pm$ 8.4	256.7 $\pm$ 7.0	200.8 $\pm$ 26.7	172.7 $\pm$ 9.0	365.9 $\pm$ 25.8
<b>4</b>	324.2 $\pm$ 11.8	229.6 $\pm$ 13.2	159.9 $\pm$ 23.3	182.4 $\pm$ 6.0	206.3 $\pm$ 17.5
<b>5</b>	152.1 $\pm$ 7.1	131.6 $\pm$ 3.6	100.1 $\pm$ 4.7	77.6 $\pm$ 6.7	157.3 $\pm$ 8.4
<b>6</b>	493.8 $\pm$ 8.5	239.7 $\pm$ 7.2	251.5 $\pm$ 2.1	104.5 $\pm$ 8.8	882.2 $\pm$ 53.4
<b>7</b>	53.5 $\pm$ 6.9	55.4 $\pm$ 7.0	24.1 $\pm$ 0.5	20.2 $\pm$ 2.0	52.6 $\pm$ 8.2
<b>8</b>	26.6 $\pm$ 0.9	18.2 $\pm$ 0.5	19.4 $\pm$ 2.0	30.3 $\pm$ 1.7	60.7 $\pm$ 4.1
<b>9</b>	39.5 $\pm$ 8.9	21.7 $\pm$ 1.6	45.2 $\pm$ 5.4	35.0 $\pm$ 2.9	131.8 $\pm$ 5.1

When analyzing the data from Table 4, it becomes obvious that compounds **7**, **8** and **9** generally display low  $K_m/V_{\text{max}}$  values pointing to either a comparably low  $K_m$  or a high  $V_{\text{max}}$ , which are both advantageous for rapid kinetic assays. On the other hand, comparably high quotients were determined

for compound **6** reacting with potato, human and rat sEH. This phenomenon is also seen for substrate **3** particularly in combination with the potato enzyme.

$K_m/V_{max}$  values from Table 4 were converted to the respective specificity constants  $k_{cat}/K_m$ , which describe the rate of product formation by the enzyme. The results of these calculations are presented in Table 5.

**Table 5**  $k_{cat}/K_m$  values of substrates **2** through **9** in combination with various soluble epoxide hydrolases. Numbers are given as means  $\pm$  standard deviation (n=4 for human and mouse sEH; n=3 for cress, rat and potato sEH) in  $s^{-1} \mu M^{-1}$ .

Substrate	Human sEH	Mouse sEH	Rat sEH	Cress sEH	Potato sEH
<b>2</b>	0.093 $\pm$ 0.007	0.076 $\pm$ 0.003	0.022 $\pm$ 0.001	0.011 $\pm$ 0.000	0.012 $\pm$ 0.000
<b>3</b>	0.115 $\pm$ 0.004	0.047 $\pm$ 0.001	0.077 $\pm$ 0.010	0.074 $\pm$ 0.004	0.025 $\pm$ 0.002
<b>4</b>	0.027 $\pm$ 0.001	0.022 $\pm$ 0.001	0.019 $\pm$ 0.003	0.028 $\pm$ 0.001	0.011 $\pm$ 0.001
<b>5</b>	0.194 $\pm$ 0.009	0.092 $\pm$ 0.002	0.091 $\pm$ 0.004	0.099 $\pm$ 0.009	0.014 $\pm$ 0.001
<b>6</b>	0.00119 $\pm$ 0.00002	0.00101 $\pm$ 0.00003	0.00121 $\pm$ 0.00001	0.0025 $\pm$ 0.0002	0.00042 $\pm$ 0.00002
<b>7</b>	0.556 $\pm$ 0.073	0.220 $\pm$ 0.029	0.168 $\pm$ 0.004	0.170 $\pm$ 0.017	0.042 $\pm$ 0.006
<b>8</b>	0.554 $\pm$ 0.018	0.332 $\pm$ 0.010	0.527 $\pm$ 0.052	0.056 $\pm$ 0.003	0.121 $\pm$ 0.008
<b>9</b>	0.387 $\pm$ 0.084	0.279 $\pm$ 0.020	0.227 $\pm$ 0.025	0.489 $\pm$ 0.039	0.139 $\pm$ 0.005

As expected from enzymological theory, their order corresponds roughly to the one of the specific activities from Table 3. For example, the highest  $k_{cat}/K_m$  value for human sEH was obtained for substrate **7**, which was found earlier to display the highest specific activity at 10  $\mu M$  substrate concentration. The lowest numbers for human sEH were acquired by employing compounds **6**, **4** and **2** (in this order) which is true for both, the quotient  $k_{cat}/K_m$  as well as the observed specific activities.

In case of mouse sEH, compounds **7**, **8** and **9** are characterized by the highest  $k_{cat}/K_m$  values as well as the highest specific activities. Nevertheless, it should be noted that the order among these values differed for both parameters.

### 1.4.5 Excitation and emission maximum of 6-methoxy-2-naphthaldehyde

Scanning 6-methoxy-2-naphthaldehyde under assay conditions for its excitation and emission maximum with a SpectraMax M2 microplate reader revealed 316 nm as excitation and 460 nm as emission maximum. Subsequently, these wavelengths were employed when monitoring the turnover of the fluorescent substrates with this particular instrument.

### 1.4.6 Assay optimization

In this study, the development of two novel test systems for sEH inhibition was intended: one rapid, highly sensitive, continuous assay and one endpoint assay, suitable to screen large compound libraries. After the selection of appropriate fluorescent substrates for both systems, substrate and enzyme concentrations were optimized employing checkerboard assays. Hereby, a series of different enzyme concentrations was tested in a matrix with various final substrate concentrations, enabling to optimize these two assay parameters at once.

In case of the **rapid continuous assay**, which was intended to be performed with mouse as well as human sEH, the following requirements to the system were defined in advance: (a) enzyme

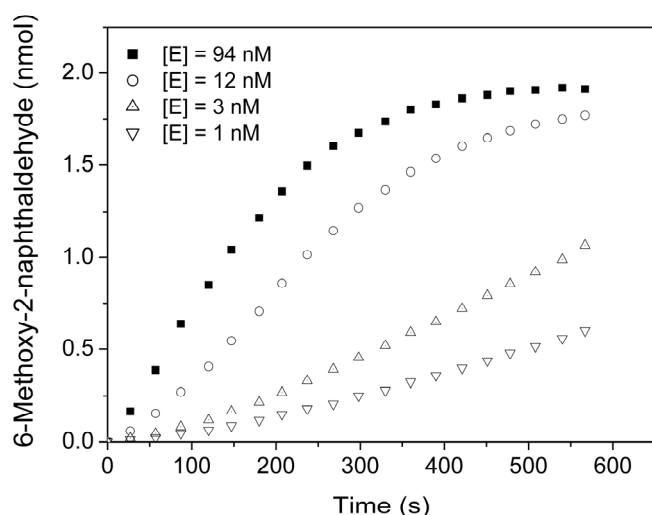


**Fig. 19** Appearance of 6-methoxy-2-naphthaldehyde over time in reactions with various concentrations of human sEH and substrate **7** at 10  $\mu$ M. This chart illustrates the observed lag times of reactions employing low enzyme concentrations.

concentrations should be as small as possible in order to obtain maximal assay sensitivity, (b) the enzymatic substrate turnover rate was supposed to be c. 10 times above the self-hydrolysis rate to obtain a broad separation band between these two values also contributing to high assay sensitivity, and finally (c) the substrate turnover rate was required to be constant over the duration of the assay, which was set at 10 min. Useful concentrations for substrate **7** – the selected compound for the

continuous assay – and sEH were found to be 5  $\mu\text{M}$  and 1 nM, which holds true for both, the murine as well as the human enzyme. Interestingly, this optimization experiment also revealed increasing lag times of the here monitored reactions with decreasing concentrations of sEH (see Figure 19). For the optimized kinetic assay concentrations, a lag time of approximately 2 min was observed.

In case of the **endpoint assay**, it was intended (a) to obtain a very stable and reproducible assay, which is usually achieved with high substrate concentrations, and (b) to assure a constant substrate turnover rate over a time period of at least 1 h. Both conditions imply (c) to use a comparably low enzyme concentration (in this case human sEH only) to ensure substrate excess and thus steady-state-like reaction conditions throughout the assay. On the other hand, it was planned (d) to achieve a final signal to background ratio of 4 to 5 employing lowest possible protein concentrations that would enhance assay sensitivity.

**Table 6** Results of the checkerboard assay for the optimization of human sEH and compound **3** concentrations. The three numbers given for each combination of concentrations represent – from top to bottom – (a) the squared linear correlation coefficient  $r^2$  analyzing reporter molecule appearance for 60 min reaction time, (b) the ratio of fluorescent signal to background after 60 min and (c) the percentage of compound **3** turned over after 60 min.

[ <b>3</b> ] ( $\mu\text{M}$ )	[human sEH] (nM)											
	26.1	13.1	6.5	3.3	2.6	1.6	1.3	0.8	0.7	0.4	0.3	0
50	0.838	0.991	0.997	0.998	0.998	0.998	0.999	0.998	0.998	0.998	0.996	0.976
	12.4	10.8	7.3	4.3	3.8	2.6	2.3	1.8	1.6	1.4	1.3	1.0
	86	74	48	26	22	14	11	8	7	5	4	2
45	0.818	0.990	0.997	0.997	0.997	0.997	0.997	0.997	0.997	0.995	0.995	0.928
	22.3	20.2	12.9	7.2	5.7	4.0	3.1	2.4	2.0	1.7	1.4	1.0
	95	86	54	28	21	14	10	7	5	4	3	0.5
40	0.791	0.988	0.997	0.998	0.998	0.997	0.998	0.998	0.997	0.997	0.996	0.947
	23.6	22.1	15.3	8.4	6.8	4.6	3.4	2.8	2.3	1.8	1.7	1.0
	100	94	64	33	26	17	11	8	6	4	3	1
35	0.730	0.952	0.997	0.998	0.997	0.997	0.997	0.996	0.997	0.996	0.997	0.953
	23.0	21.7	16.5	9.3	7.5	5.0	3.8	2.9	2.5	2.0	1.6	1.0
	100	97	73	40	31	19	14	10	8	6	4	1
30	0.671	0.932	0.997	0.998	0.998	0.997	0.997	0.998	0.998	0.996	0.997	0.887
	24.0	23.4	19.9	11.2	8.8	5.8	4.6	3.4	2.8	2.2	1.9	1.0
	100	62	53	29	22	4	10	7	5	4	3	1
25	0.579	0.841	0.985	0.998	0.998	0.998	0.998	0.998	0.997	0.997	0.996	0.889
	20.9	20.3	19.0	11.7	9.7	6.0	4.8	3.5	2.9	2.2	1.8	1.0
	100	100	97	58	47	28	21	14	11	7	6	1
20	0.521	0.761	0.937	0.815	0.998	0.998	0.998	0.998	0.998	0.997	0.997	0.963
	20.4	18.3	18.3	7.3	11.0	7.4	5.4	4.2	3.2	2.5	2.1	1.0
	100	100	100	41	60	39	28	20	14	10	8	1
15	0.474	0.701	0.874	0.998	0.998	0.998	0.998	0.998	0.998	0.998	0.998	0.958
	19.1	18.6	17.3	14.8	11.9	7.6	5.7	4.2	3.4	2.5	2.3	1.0
	100	100	100	100	80	50	36	25	19	13	11	2

The results of the checkerboard assay, summarized in Table 6, suggest a combination of 3 nM final human sEH concentration and 50  $\mu\text{M}$  final concentration of compound **3**, which was selected as substrate for this system. These concentrations meet all mentioned requirements and were even found to maintain a constant substrate turnover rate for 90 min (compare to Figure 20): linear regression analysis of the reporter molecule appearance over this time period displayed a squared correlation coefficient of 0.994 and after 90 min only about 30% of the total substrate amount was consumed. Therefore, endpoint readings of the developed inhibitor test can be taken any time between 60 and 90 min after the reaction is started by substrate addition, still ensuring steady-state-like conditions and a constant substrate turnover rate.

Finally, the results of this checkerboard assay allow an analysis of the correlation between enzyme amount and initial velocity of the corresponding enzymatic substrate turnover. In theory, these two parameters should be linearly correlated at a certain substrate concentration. In case of human sEH in combination with a substrate **3** concentration of 50  $\mu\text{M}$ , the linear

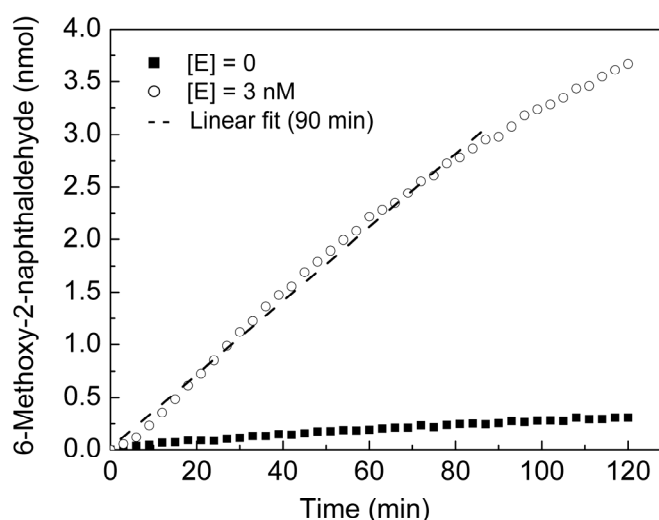


**Fig. 20** Time course of normalized 6-methoxy-2-naphthaldehyde appearance for optimized endpoint assay conditions ( $[E]_{\text{final}} = 3 \text{ nM}$ ;  $[S]_{\text{final}} = 50 \mu\text{M}$ ; 200  $\mu\text{l}$  assay volume) in comparison to self-hydrolysis of compound **3**. The dashed line exemplifies the linear regression analysis result after 90 min of enzymatic reaction ( $r^2=0.994$ ).

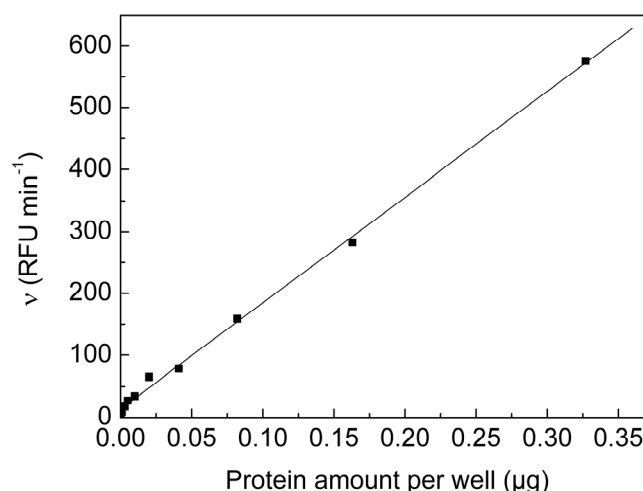


**Fig. 21** Increase of initial velocity  $v$  caused by increasing human sEH amounts per well at a compound **3** concentration of 50  $\mu\text{M}$ .

regression analysis (illustrated in Figure 21) confirmed this theory ( $r^2=0.998$ ).

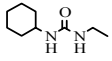
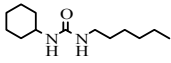
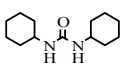
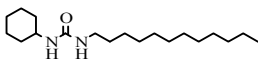
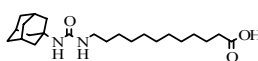
#### 1.4.7 Inhibitor assays and assay validation

Experiments to determine the  $IC_{50}$ s of characterized sEH inhibitors were carried out employing fluorescent substrates **3** and **7** in kinetic as well as endpoint assays. These experiments were conducted to compare the potencies of both assay systems with already existing tests and thus to validate them.

Table 7 summarizes main assay conditions as well as the results of the investigations.

In these tests, the sEH inhibitor CEU clearly displays the highest  $IC_{50}$  values within all fluorescent assay systems. Thus, among the tested inhibitors this chemical showed least impact on sEH activity. On the other hand, assays employing human sEH revealed AUDA as most potent substance. Nevertheless, mouse sEH was inhibited best by CDU. Assays carried out with substrate **3** did not display significant differences between the  $IC_{50}$ s of CHU and DCU. However, assays utilizing substrate **7** clearly identified CHU as the more potent inhibitor. Most importantly, all employed test systems ranked the examined structures due to their  $IC_{50}$  values correspondingly and were able to differentiate between the best inhibitors.

**Table 7** Assay conditions and  $IC_{50}$  values of sEH inhibitors determined with the new assay systems that employ substrates **7** and **3**. Numbers are given as average of at least three replicates in nM  $\pm$  standard deviation.

Substrate		<b>7</b>	<b>7</b>	<b>3</b>	<b>3</b>
Enzyme		Mouse sEH	Human sEH	Human sEH	Human sEH
[S] <sub>final</sub> ( $\mu$ M)		5	5	50	50
[E] <sub>final</sub> (nM)		1	1	3	3
Detection mode		Continuous	Continuous	Continuous	Endpoint
	CEU	> 100000	7500 $\pm$ 130	9800 $\pm$ 2700	39600 $\pm$ 4300
	CHU	75 $\pm$ 8	25.0 $\pm$ 0.1	29 $\pm$ 13	33 $\pm$ 3
	DCU	240 $\pm$ 20	52 $\pm$ 1	33 $\pm$ 7	35 $\pm$ 4
	CDU	17 $\pm$ 3	7.0 $\pm$ 0.2	19 $\pm$ 2	8.1 $\pm$ 0.5
	AUDA	27 $\pm$ 1	3.2 $\pm$ 0.1	4.6 $\pm$ 0.6	5.5 $\pm$ 0.5

In case of the endpoint assay system, it was particularly important to test and evaluate its stability, reproducibility and suitability for high-throughput performance. Therefore, an experiment was carried out that investigated the five inhibitors – in quadruplicate and at one concentration each covering a wide range of inhibitory potencies – for their sEH inhibition strength. The experiment was repeated four times per day on three consecutive days. This way, intra- and inter-plate variations as well as day-to-day discrepancies should be revealed and the assay's accuracy and precision could be investigated. Additionally, the experiment tested for differences between reaction times of 60 and 90 min. However, the results after 60 and 90 min of incubation time were similar and therefore Table 8 only displays those of the longer incubation time.

Variations within a plate can be studied best by analyzing standard deviations of replicates, relative standard deviations (standard deviation divided by the corresponding absolute value) respectively. The described assay validation showed relative standard deviations within the plates to range between 0.3 and 6.2%. The averaged relative standard deviation of all acquired values was 2.4% and thus comparatively low. Daily inter-plate variations, judged by their coefficient of variation (CV; another expression for relative standard deviation), were found to be below 6.2% testifying high assay precision (cf. Table 8).

As shown in Table 8, the assay gives good accuracy on the first day (above 95%), but the values slowly decrease over the next two days to reach only 60% for CEU on day 3. In general, absolute inhibition values were also found to decrease over the three days of investigation. Finally, the  $Z'$  factor was calculated to quantify assay performance. This statistical parameter indicates the robustness of assays and thus their suitability for high-throughput screening (Zhang et al., 1999). In case of the endpoint assay, values between 0.7 and 0.8 were found. Except for DCU, whose inhibitory impact on the activity of human sEH was extremely high and the corresponding fluorescent signal therefore too close to the blank,  $Z$  values (Zhang et al., 1999) between 0.6 and 0.8 were calculated. This implies that the endpoint assay has a separation band comprised between 0 and 90% of inhibition in which it can differentiate inhibitors from each other.

**Table 8** Precision and accuracy data as well as  $Z'$  values acquired from the fluorescent endpoint system validation. Mean accuracy was determined by calculating the ratio of the determined inhibition percentage, divided by the nominal value, and multiplying it with 100%. Precision or CV (coefficient of variation) values represent standard deviations of fluorescent signal, divided by the mean fluorescent signal of maximum enzyme activity, and multiplied by 100%.  $Z'$  was calculated as previously described (Zhang et al., 1999).

	Nominal inhibition (%)	Day 1		Day 2		Day 3		Interday precision <sup>b</sup> (CV, %)
		Mean accuracy <sup>a</sup> (%)	Precision <sup>a</sup> (CV, %)	Mean accuracy <sup>a</sup> (%)	Precision <sup>a</sup> (CV, %)	Mean accuracy <sup>a</sup> (%)	Precision <sup>a</sup> (CV, %)	
Blank	-		3.4		2.2		3.4	4.6
Control	-		4.6		7.3		6.7	6.2
Inhibitor								
CEU	5	95.2	5.2	71.3	3.9	59.0	3.5	5.0
CHU	35	97.9	3.7	92.4	2.0	70.0	6.2	5.7
CDU	55	99.9	2.5	95.0	3.9	88.6	2.6	5.7
AUDA	65	98.9	3.5	98.9	2.2	87.1	2.5	6.0
DCU	95	98.6	2.8	99.8	3.0	98.3	2.9	4.9
$Z'$		0.8 <sup>c</sup>		0.8 <sup>c</sup>		0.7 <sup>c</sup>		0.7 <sup>d</sup>

<sup>a</sup> Intraday (n = 16). <sup>b</sup> Intraday (n = 48). <sup>c</sup> Intraday average (n = 4). <sup>d</sup> Interday average (n = 12).

#### 1.4.8 Evaluation of stop solutions

The search for an appropriate stop solution was carried out in order to increase flexibility of the fluorescent endpoint assay employing compound **3**. If it was possible to stop an ongoing substrate hydrolysis reaction and conserve the current signal by means of an appropriate solution, the endpoint assay could potentially be interrupted any time between 60 to 90 min after substrate addition. And most importantly, the quantification of the fluorescent signal could be achieved independently from the assay starting time, which would significantly improve the adaptability of the system.

In order to identify a suitable substance for this purpose, various chemicals and solutions were tested for their potential (a) to block the interaction between human sEH and substrate **3** as well as (b) to inhibit further self-hydrolysis and (c) to conserve or enhance existing fluorescence. In an initial screen,



substrate hydrolysis rates as well as fluorescence levels after addition of candidate solutions were compared to the respective values after buffer addition. Results of this investigation were classified with the terms *constant* (difference to the reference value  $\pm 10\%$ ), *slightly elevated / reduced* (10 to 20% variation relative to the reference), *elevated / reduced* (20-50% above / below the reference value), or *significantly elevated / reduced* ( $> 50\%$  difference to the reference value) and are summarized in Table 9.

**Table 9** Qualitative influence of stop solutions on enzymatic hydrolysis rate and fluorescence level under endpoint assay conditions. After 60 min of incubation at room temperature in the dark, 50  $\mu\text{l}$  of stop solution were added to the enzymatic reaction (200  $\mu\text{l}$ ) and the fluorescent signal was monitored for 10 min. Variations were classified with the terms *constant* (difference to the reference value  $\pm 10\%$ ), *slightly elevated / reduced* (10 to 20% variation relative to the reference), *elevated / reduced* (20-50% above / below the reference value), or *significantly elevated / reduced* ( $> 50\%$  difference to the reference value).

Stop solution	Hydrolysis rate	Fluorescence level
1-propanol	constant	slightly elevated
2-propanol	constant	slightly elevated
acetonitrile	reduced	elevated
ammonium sulphate (saturated solution)	reduced	constant
bleach (10% in H <sub>2</sub> O)	significantly reduced	constant
borax (5% in H <sub>2</sub> O)	elevated	elevated
dioxane (25% in H <sub>2</sub> O)	reduced	elevated
DMF	elevated	slightly elevated
DMSO	significantly elevated	slightly elevated
ethanol (95%)	elevated	elevated
H <sub>2</sub> O <sub>2</sub> (30%)	elevated	reduced
saturated iodine solution in H <sub>2</sub> O	significantly reduced	constant
methanol	significantly elevated	slightly elevated
morpholine (5% in H <sub>2</sub> O)	constant	slightly reduced
PEG (50% in H <sub>2</sub> O)	elevated	elevated
SDS (10% in H <sub>2</sub> O)	significantly reduced <sup>a</sup>	reduced
sodium azide (0.5% in H <sub>2</sub> O)	reduced	slightly reduced
THF (10% in H <sub>2</sub> O)	reduced	slightly elevated
zinc nitrate (1 M in H <sub>2</sub> O)	significantly reduced	reduced
zinc sulphate (1 M in H <sub>2</sub> O)	significantly reduced	elevated

<sup>a</sup> Basically no slope was detectable at the same fluorescence level; however, the fluorescence level dropped during detection.

Solutions that significantly reduced substrate turnover in this context were 10% (v/v) bleach in water, a saturated iodine solution in water, 10% SDS in water as well as aqueous zinc nitrate and zinc sulphate solutions. However, only the latter two salts were able to decrease substrate decomposition rates as much as  $\sim 90\%$  in comparison to the reference value. Therefore, further investigations were conducted employing these two substances in aqueous solution.

In order to confirm the results of the initial screen and to find a suitable concentration of a possible stop solution, the same experiment was carried out with several concentrations of zinc sulphate and zinc nitrate in triplicate. Table 10 lists the results of this investigation.

**Table 10** Influence of different concentrations of  $\text{ZnSO}_4$  and  $\text{Zn(NO}_3)_2$  on hydrolysis rate and fluorescence level of ongoing reactions between human sEH and compound **3**. Zinc salts were employed as aqueous stop solutions after 1 h of enzymatic reaction and results were set relative to the reference obtained by buffer addition. Values are displayed as means  $\pm$  standard deviation (n=3).

Final concentration of stop solution ( $\mu\text{M}$ )	Relative hydrolysis rate (% of reference value)		Relative fluorescence level (% of reference value)	
	$\text{ZnSO}_4$	$\text{Zn(NO}_3)_2$	$\text{ZnSO}_4$	$\text{Zn(NO}_3)_2$
200	11 $\pm$ 4	3 $\pm$ 2	126 $\pm$ 1	63 $\pm$ 2
100	10 $\pm$ 4	12 $\pm$ 2	118 $\pm$ 5	86 $\pm$ 5
50	22 $\pm$ 7	19 $\pm$ 4	129 $\pm$ 5	102 $\pm$ 4
25	33 $\pm$ 7	28 $\pm$ 2	115 $\pm$ 5	107 $\pm$ 5
10	35 $\pm$ 5	34 $\pm$ 8	117 $\pm$ 5	110 $\pm$ 2
5	26 $\pm$ 5	26 $\pm$ 4	110 $\pm$ 6	107 $\pm$ 3
1	51 $\pm$ 3	51 $\pm$ 4	106 $\pm$ 1	108 $\pm$ 1
0.5	64 $\pm$ 1	63 $\pm$ 2	106 $\pm$ 3	103 $\pm$ 0

The two zinc salt solutions decreased the hydrolysis rate of compound **3** by human sEH relative to buffer with increasing concentrations. Satisfying hydrolysis reductions were obtained with concentrations of 100 and 200  $\mu\text{M}$  in case of both chemicals. However, they displayed contrary impacts on the fluorescent signal of the reporter molecule. Zinc sulphate was found to relatively enhance the fluorescent signal, whereas zinc nitrate reduced it – both again in dependence of their final concentration.

Finally, the direct influence of zinc sulphate and zinc nitrate on the fluorescent signal of 6-methoxy-2-naphthaldehyde was determined. Therefore, 1.0 M solutions of these chemicals as well as buffer were added to several standard solutions (final concentration of the zinc salts was 200  $\mu\text{M}$ ) of the fluorescent molecule and the resulting standardization curves were compared (see Figure 22). All curves were obtained

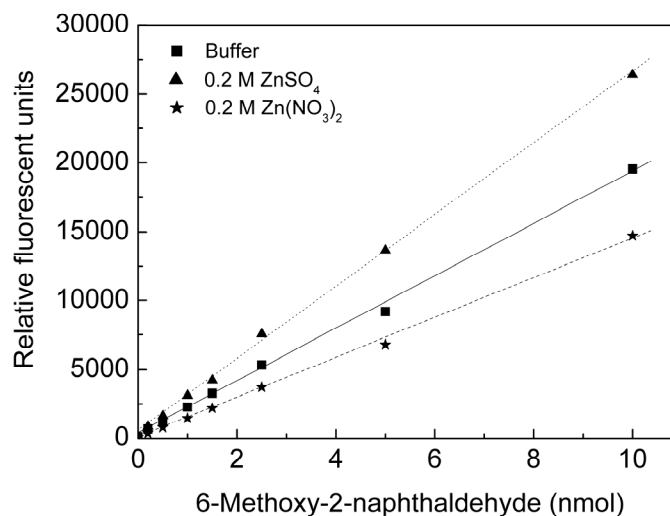


**Fig. 22** Influence of  $\text{ZnSO}_4$  and  $\text{Zn}(\text{NO}_3)_2$  at 0.2 M on the fluorescent signal of 6-methoxy-2-naphthaldehyde.

by linear regression and displayed  $r^2$  values of at least 0.994. The conversion factors from RFU into nmol of fluorescent 6-methoxy-2-naphthaldehyde, represented by the slopes of the obtained lines, differed notably: buffer addition led to a value of 1901 RFU/nmol  $\pm$  a standard error of 63 RFU/nmol, whereas slopes of  $2611 \pm 86$  RFU/nmol and  $1446 \pm 42$  RFU/nmol were found for zinc sulphate and zinc nitrate.

## 1.5 Discussion

### 1.5.1 Aqueous solubility and stability

Solubility of the fluorescent substrates in aqueous solution was generally found to be poor. With the exception of ester **3**, all examined compounds displayed apparent limits of solubility below 50  $\mu\text{M}$ . On the other hand, bi-linear regression analysis revealed an apparent LS of compound **3** of  $58 \pm 7$   $\mu\text{M}$  (mean  $\pm$  standard deviation;  $n=3$ ) implying its complete aqueous solubility at a concentration of 50  $\mu\text{M}$ . Overall, this result is surprising, because carbonate compounds, like the majority of the tested substrates, are generally known to display better aqueous solubility than esters. In addition, NEPC as well as *t*DPPO, both sEH substrates used at an assay concentration of 50  $\mu\text{M}$  (Dietze et al., 1994; Borhan et al., 1995; Morisseau et al., 1998), are clearly more soluble than the majority of the fluorescent compounds.

Furthermore, aqueous stability of all substrates was investigated. Hereby, it was examined in dependence of pH first. The compounds were generally shown to hydrolyze faster with increasing pH within a pH range of 6.5 to 8.0. This result was not surprising, due to the higher amounts of OH<sup>-</sup>-ions in solutions of more basic pH. These anions are expected to attack the carbonate / ester moiety of the compounds inducing intramolecular cyclization of the fluorescent substrates without enzyme (compare to Figure 12). Therefore, the more OH<sup>-</sup>-ions there are in the solution and thus the higher the pH, the faster an auto-hydrolysis of the investigated substrates occurs. This experimental outcome strongly suggested the choice of a comparably low pH for further investigations and applications in order to stop self-hydrolysis as much as possible. Moreover, it was found earlier that sEH achieves maximum activity between pH 7.0 and 7.5 (Wixtrom and Hammock, 1985). Taking into account these two facts, pH 7.0 was selected for further experiments.

When comparing the aqueous stability of all fluorescent substrates at pH 7.0, the aryl carbonates **7**, **8** and **9** as well as ester **2** displayed higher hydrolysis rates than compounds **3** through **6**. However, a low self-hydrolysis rate is favourable with respect to further applications. The lower it is, the more sensitive will a future assay potentially be. Statistically, substrates **3**, **4**, **5** and **6** do not differ in their aqueous stability. However, on average compound **3** was found to be most stable in aqueous solution.

The comparison between the aqueous stabilities of the fluorescent substrates with the one of NEPC clearly shows that the latter structure hydrolyses faster. Compound **7** represents one of the less stable substrates in the investigated series of compounds. Nevertheless, it decays approximately three to four times slower in aqueous solution at pH 7.0 than NEPC at the same concentration. This fact implicates future assays utilizing the fluorescent substrates to potentially be more sensitive than an assay with NEPC. They will enable to employ smaller amounts of enzyme while maintaining a useful signal-to-background ratio.

### 1.5.2 Specific activities and Michaelis-Menten parameters

Specific activity of an enzyme-substrate combination is an expression for the selectivity of this enzyme for the analyzed substrate. A high specific activity allows to employ little enzyme and therefore results in high sensitivity of an assay.

Compound **6**, the only tri-substituted epoxide in this series of fluorescent substrates, exhibits the lowest specific activities for all tested recombinant soluble epoxide hydrolases. This result can be explained by the steric congestion around the epoxide of this particular structure. It most likely represents a hindrance for reaching the enzyme's catalytic site in its L-shaped hydrophobic tunnel (Argiriadi et al., 1999; Argiriadi et al., 2000). Furthermore, this finding is consistent with the earlier observation that sEH generally prefers di-substituted epoxides over tri-substituted ones (Wixtrom and Hammock, 1985; Morisseau et al., 2000).

Dietze and coworkers (1994) reported that, with the murine system, carbonate structures were more active as substrates than the corresponding esters. This observation holds only partially true for the fluorescent compounds characterized in this work. In the comparison between ester **3** and the corresponding carbonate **7**, the carbonate exhibits more than twice the specific activity of the ester. However, the specific activity of ester **2** in the murine system can statistically not be distinguished from the one of its corresponding carbonate **5**. It has to be noted that the epoxide functionalities of the carbonate structures were further away from their keto-groups in comparison to the respective esters. However, this was also the case in the study of Dietze et al. (1994).

The latter study also demonstrated that the specific activity of murine sEH for the aryl-epoxy ester 4-nitrophenyl *trans*-3,4-epoxy-4-phenylbutanoate (NEB) was roughly four times higher than for the alkyl-epoxy ester 4-nitrophenyl *trans*-3,4-epoxyhexanoate (NEH). This finding could not be confirmed in the present study. Substrate **3**, an aryl-epoxy ester, was statistically indistinguishable from substrate **2**, an alkyl-epoxy ester, with regard to its specific activity. However, compound **2** had a longer alkyl chain on its right-hand side than the corresponding NEH. This fact is likely to increase the specific activity value relative to the respective aryl-epoxy ester, because it was found in the present study that soluble epoxide hydrolase in general is more selective for longer chained substrates (see above).

Porcine liver esterase represents a mixture of numerous hybrids of at least three protein subunits (Heymann and Junge, 1979) and is known to hydrolyze a wide range of substrates. When Dietze and coworkers (1994) tested its specific activity with NEPC, they found a value of  $4.61 \mu\text{mol min}^{-1} \text{mg}^{-1}$ . Not surprisingly and consistent with these earlier findings, this commercial enzyme preparation also displayed high specific activities with basically all fluorescent compounds. The conditions in the study of Dietze and coworkers ( $25^\circ\text{C}$  assay temperature; phosphate buffer pH 6.4; final substrate concentration  $50 \mu\text{M}$ ) were quite different from the ones in the present examination ( $30^\circ\text{C}$  assay temperature; BisTris buffer pH 7.0; final substrate concentration  $10 \mu\text{M}$ ). Additionally, differences in the enzyme preparations are likely. Nevertheless, it can still be argued that compound **2** showed a specific activity ( $6.3 \mu\text{mol min}^{-1} \text{mg}^{-1}$ ) comparable to NEPC. Overall, the high specific activities of the fluorescent substrates in analogy to the findings of Dietze et al. (1994) strongly suggest that they are not useful for testing sEH activities in crude extract preparations of cells or tissues – at least due to their high reactivity with esterases. Employment of these compounds to determine sEH activity requires at least partially purified enzyme, and / or judicious use of enzyme inhibitors for proper performance.

Catalytic reactions between enzymes and substrates generally follow Michaelis-Menten kinetics and can thus be characterized by the parameters  $K_m$ ,  $V_{\text{max}}$  and  $k_{\text{cat}}$  independently from their respective concentrations. However, in the present study it was not possible to determine these values directly and accurately – mainly due to the low aqueous solubility of the substrates. Nevertheless,  $k_{\text{cat}}/K_m$  quotients, which are obviously also independent from enzyme and substrate concentrations, could be obtained. Therefore, it is possible to directly compare the tested enzyme-substrate combinations with previously examined ones. A  $k_{\text{cat}}/K_m$  value, the so-called catalytic efficiency, represents the apparent second-order rate constant and describes the conversion of free enzyme and substrate into enzyme and product. Therefore, the higher this number, the faster a reaction is supposed to take place and the higher the preference of an enzyme for the respective substrate. Values of this quotient for the sEH substrates *t*DPPO and NEPC, which were extracted from literature (Morisseau et al., 1998; Morisseau et al., 2000), are listed in Table 11.

**Table 11**  $k_{\text{cat}}/K_m$  values for various recombinant sEH enzymes with *t*DPPO and NEPC obtained from earlier studies. Quotients are given in  $\text{s}^{-1} \mu\text{M}^{-1}$ .

	Human sEH	Mouse sEH	Rat sEH	Cress sEH	Potato sEH
<i>t</i> DPPO <sup>a</sup>	0.694	4.186	1.739	0.209	0.573
NEPC <sup>b</sup>	2.556	3.310	nd	nd	nd

<sup>a</sup> Calculated from  $k_{\text{cat}}$  and  $K_m$  values determined by Morisseau et al. (2000).

<sup>b</sup> Calculated from  $k_{\text{cat}}$  and  $K_m$  values determined by Morisseau et al. (1998).  
nd, not determined.

From the values in Tables 11 and 5 it is apparent that the surrogate substrate *t*DPPO, which was developed for murine soluble epoxide hydrolase (Borhan et al., 1995), is turned over roughly 10 to 15 times faster by mouse sEH than its favoured fluorescent substrates **8** and **9**. Human, rat and potato sEH still prefer *t*DPPO in comparison to the substrates of the present study – although to a lesser extent. Only considering this fact, assays utilizing the fluorescent substrates in combination with recombinant sEHs are unlikely to achieve higher sensitivity than the *t*DPPO assay. This is particularly the case, since *t*DPPO is very stable in aqueous solution and its turnover is quantified radiometrically, and thus with a more sensitive detection system than the fluorescent substrates.

Nevertheless,  $k_{\text{cat}}/K_m$  quotients of cress sEH display a preference of this plant enzyme for compound **9** when compared to *t*DPPO. It would be very interesting to test the fluorescent substrates with other recombinant plant sEHs, e.g. from oilseed rape (*Brassica napus*; Bellevik et al., 2002), soybean (*Glycine max*; Blee and Schuber, 1992) or common tobacco (*Nicotiana tabacum*; Guo et al., 1998), to find out if these enzymes shared the preference of the investigated ones for this fluorescent substrate.

Finally, Morisseau and coworkers (1998) found  $k_{\text{cat}}/K_m$  values of the human and the murine recombinant enzyme with NEPC of 2.6 and 3.3  $\text{s}^{-1} \mu\text{M}^{-1}$ , respectively (compare to Table 11). Thus, fluorescent substrates **3** and **7** which were selected for the development of inhibitor assays (see below) were hydrolyzed five (fifteen) or even twenty (sixty) times slower than NEPC by human (mouse) sEH (refer to Table 5). However, this can and will be compensated by the clearly lower auto-hydrolysis rates of the new substrates and the much higher sensitivity of the employed fluorescence detection system versus the spectrophotometric one of NEPC.

### 1.5.3 Assay development

The purpose of the previous substrate characterization was the selection of suitable substrates for the development of a fast continuous kinetic assay as well as a long-term high-throughput-suitable endpoint assay. Both of those tests were supposed to determine sEH inhibitor potencies for human sEH and in case of the continuous assay also for the murine enzyme. However, each one was developed with a different application in mind.

#### 1.5.3.1 Substrate selection

The main aim of developing a new and **rapid continuous kinetic assay** for sEH with one of the fluorescent substrates was to achieve more sensitivity in comparison to the spectrophotometric NEPC assay, maintaining the latter test's fast execution and data acquisition. An improved system was highly desirable, because – as already mentioned – the latter method was no longer able to distinguish between the most potent sEH inhibitors (Kim et al., 2004c; Kim et al., 2005b) and could therefore not contribute to their refinement. Additionally, the IC<sub>50</sub> tests utilizing the *t*DPPO system are too costly and time consuming to be conducted for larger numbers of inhibitors.

The theory teaches that sensitivity within an enzyme assay is achieved – among others – by employing a substrate, which the enzyme of interest highly favours. This preference is indicated by a high specific activity or a high  $k_{\text{cat}}/K_{\text{m}}$  value. The higher either of these numbers, the less amount of enzyme needs to be employed and thus the more sensitive will a later inhibitor assay potentially be. Moreover, enzyme-substrate interactions that are characterized by high specific activity occur faster than the ones with low specific activity when carried out with the same enzyme amount. Therefore, if these values are found to be high, a potential later assay would also be comparably fast in execution.

When selecting a suitable compound for this particular application, specific activities of human sEH – as ultimate target for the inhibitors to test – were considered first. In case of compound **7** this parameter was found to be well (at least three times) above the ones of the other substrates. In addition, mouse sEH also displayed an acceptable specific activity with this chemical. Consequently, substrate **7** was selected for the development of a fast continuous kinetic assay despite its comparatively low solubility and high self-hydrolysis rate. Particularly the latter parameter is of significance as well when



high assay sensitivity is desired, but it has been shown that compound **7** decays much slower than NEPC. Therefore, it could still be considered to improve the spectrophotometric assay.

In a separate approach, a **long-term endpoint assay** was supposed to be developed that should enable the screening of large compound libraries for unknown pharmacophores of human sEH inhibitors. In this case, stability and reproducibility of a future assay were emphasized, whereas the sensitivity requirement was still important but not predominant. High stability in a rate-dependent enzyme assay is achieved first of all by the employment of a high substrate concentration, which is ideally chosen to be three times above the  $K_m$  constant of the enzyme-substrate interaction. The explanation for this requirement is found in the enzyme kinetics theory of Michaelis and Menten (see Figure 23 for illustration). At high substrate concentrations (when the respective compound is in high abundance compared to product or enzyme), substrate turnover rates – or velocities – approach  $V_{max}$  and are very stable. Under such conditions, small variations in enzyme amount or other assay conditions such as temperature and pH should not influence the velocity significantly, resulting in a stable and reproducible assay. However, the present study found all tested fluorescent compounds to be comparably insoluble in aqueous solution with compound **3** as most soluble of them. Thus, this structure could be employed with the highest concentration in a future assay.

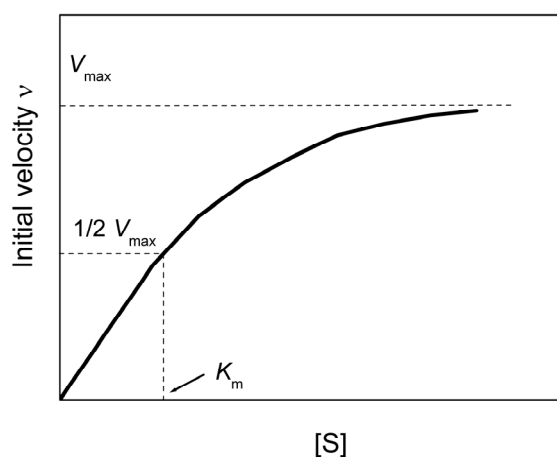


**Fig. 23** Schematic plot of initial velocity  $v$  versus substrate concentration  $[S]$  following the theory of Michaelis-Menten. ( $V_{max}$  = maximal velocity;  $K_m$  = Michaelis-Menten constant)

Additionally, in particular for a desired long-term endpoint assay, as usually employed in high-throughput test systems (Davydov et al., 2004; Soriano et al., 2006), it would be advantageous if the utilized substrate was characterized by high aqueous stability. On one hand, this condition contributes to maintain the substrate abundance during an enzymatic reaction and thus steady-state-like conditions. On the other hand, a low self- or background hydrolysis rate allows the employment of only little enzyme to

detect signal over background. This once more increases the sensitivity of a future assay. Compound **3** showed highest aqueous stability among the tested fluorescent compounds of the present study.

Put together, these findings favoured compound **3** as substrate in combination with human sEH for an endpoint assay employing long incubation times and thus for a high-throughput screen assay. Its comparatively high solubility and low auto-hydrolysis rate will allow a near steady-state reaction for long reaction times using comparatively low enzyme concentrations. This again will decrease total cost and increase sensitivity for the screening of chemical libraries. Additionally, the mid-range  $k_{cat}/K_m$  value of the combination human sEH / compound **3** ensures the respective enzymatic reactions to occur neither too slow nor too fast. The first option would cause a too narrow separation band between maximum and minimum enzyme activity, whereas the second could interfere with the relatively long reaction time and the steady-state-like condition of the reaction. However, both prospects should and could be avoided with the selection of compound **3**.

#### 1.5.3.2 Assay optimization

During the optimization process, assay conditions were investigated and / or maintained that would result in the desired properties of the respective future inhibitor test system.

As mentioned before, pH was kept constant at 7.0 for both assay developments to avoid self-hydrolysis (and therefore background signal) as much as possible. Total assay duration and enzyme-inhibitor incubation times were fixed as well. The continuous assay was decided to monitor substrate turnover every 30 s for no longer than 10 min in order to sustain its intended rapid execution. On the other hand, the endpoint assay was set up for a reaction time of 1 h as a compromise between enzyme activity decay (human sEH half life is > 8h at 25°C under the employed assay conditions; Morisseau et al., 2000) and sensitivity increase over time as well as to simplify its execution. Moreover, incubation of enzyme with inhibitor was decided to happen for 5 min at 30°C within the rapid system employing compound **7**, which is in accordance with the NEPC assay. For endpoint assays employing compound **3**, 10-min incubations were thought to be appropriate when considering this assay's ultimate application of compound library screening. This way, slower binding inhibitors were supposed to be detected as well, and later automatization enabling high-throughput screening was thought to be simplified.

When designing the latter test system, high emphasis was put on it being uncomplicated and undemanding in execution. This again recommended room temperature conditions for this application. On the other hand, the kinetic assay and its optimization experiments were carried out at 30°C in accordance with the NEPC assay (Morisseau et al., 1998) and in order to provide stable reaction conditions for this more sensible test. Both assay types were optimized utilizing human sEH since this is the protein which inhibitors should eventually be effective with. Moreover, Gomez and coworkers (2006) only recently emphasized the importance of employing human sEH and not the murine enzyme when screening inhibitory structures for therapeutic treatments in humans, due to alternative inhibitor binding orientations in both proteins. Nevertheless, in case of the rapid kinetic assay a useful mouse sEH concentration was determined to be able to further compare inhibitor potencies in both mammalian systems.

As soon as compound **7** was selected for a fast continuous kinetic assay, it became clear that, due to its low aqueous solubility, such an assay could never be carried out at substrate concentrations well above its  $K_m$  with human and murine sEH. Therefore, substrate abundance conditions that would grant stable and reproducible results were not possible with this substrate. However, if a combination of enzyme and compound **7** fulfilled all required conditions mentioned earlier – in brief, a minimal enzyme concentration causing a constant turnover rate well above background over a period of 10 min– it was assumed that this assay would still be very useful for ranking extremely potent inhibitors, which were indistinguishable with the previous NEPC assay. Applicable concentrations of substrate **7** and enzyme were found to be 5  $\mu$ M and 1 nM for both, the mouse as well as the human sEH. With a two orders of magnitude lower final enzyme concentration, the fluorescent continuous kinetic assay promised a clearly higher sensitivity in comparison to the NEPC system (Morisseau et al., 1998; Morisseau et al., 1999; Morisseau et al., 2002; McElroy et al., 2003). However, it should be noted that this assay design will be able to rank compounds according to their inhibitory potency but potentially not reveal reproducible  $IC_{50}$  numbers. Additionally, the observed lag time of about two min under optimized kinetic assay conditions – a phenomenon that was already noted by Dietze and coworkers (1994) reporting the development of the photometric substrate NEPC – allowed initial velocities of substrate hydrolysis only to be taken into account after this time had passed.

With the decision for substrate **3** to be used in a later endpoint assay, it was possible to employ a final substrate concentration as high as 50  $\mu\text{M}$ . This corresponds to the one of NEPC in the absorbance-based inhibitor assay as well as to the employed *t*DPPO concentration (Borhan et al., 1995; Morisseau et al., 1998; Morisseau et al., 1999; Morisseau et al., 2002; McElroy et al., 2003). Human sEH at 3 nM in combination with this substrate concentration met all the earlier stated requirements for the endpoint assay – briefly, the maintenance of a constant substrate turnover over a period of 1 h with minimal enzyme amount, resulting in a final fluorescent signal around 4 times above background. It even sustained a constant substrate turnover rate over a period of 90 min enabling to take measurements between 60 and 90 min. This circumstance clearly improves the assay's flexibility and contributes to its simplicity in execution. Moreover, the optimized enzyme concentration is once more well below the one of the NEPC assay while both test systems employ the same substrate concentrations. Therefore, the optimized endpoint assay conditions imply improved sensitivity in comparison to the spectrophotometric assay as well as the system's reproducibility.

#### 1.5.3.3 Confirmation of epoxide hydrolysis as rate-limiting step

To be able to employ the fluorescent substrates **3** and **7** in any kind of rate-dependent assay, it is crucial to prove the formation of 6-methoxy-2-naphthaldehyde to fully depend on the epoxide hydrolysis (compare to Figure 12). In case this was not the rate-limiting factor of the substrates' reaction mechanism, extreme care would be needed for interpreting results of such an assay.

The mechanism of the fluorescent substrate decomposition basically occurs in three steps: epoxide hydrolysis, intramolecular cyclization and conversion of the cyanohydrin into 6-methoxy-2-naphthaldehyde (compare to Figure 12). The conversion of cyanohydrin to the fluorescent reporter molecule has already been displayed to basically occur instantly (Shan and Hammock, 2001). However, the cyclization of the hydrolyzed epoxide (the diol) resulting in cyanohydrin needed to be excluded as rate-limiting step of the reaction mechanism as well. In case of the **rapid continuous assay**, this was attempted by comparing the disappearance of compound **7** in an optimized enzymatic reaction to the rate of 6-methoxy-2-naphthaldehyde appearance. If those two rates were found to be equal, epoxide hydrolysis could be assumed to be rate-limiting under the employed conditions. However, if epoxide

hydrolysis and thus disappearance of compound **7** was found to occur at a higher rate than reporter molecule appearance, cyanohydrin formation would be restricting product formation. Unfortunately, all attempts to detect these rates employing HPLC methods failed, due to the decomposition of the chemical during the HPLC runs. However, taking a closer look again at the data obtained from the determination of specific activities, it can be observed that enzyme activities approached saturation with increasing concentrations of human and mouse sEH (data not shown). However, epoxide hydrolysis should in theory increase proportionally with enzyme concentration. Therefore, the observed saturation in substrate turnover can be ascribed to the fact that this reaction step, at high concentrations of enzyme, occurs faster than the later diol cyclization. The observed maximal hydrolysis rates can thus be interpreted as approximations of the respective cyclization and cyanohydrin formation rate. Non-linear regression analysis revealed these values to be around  $410 \text{ pmol min}^{-1}$  for compound **7**. However, optimized conditions for the kinetic assay employing compound **7** correspond to hydrolysis rates of  $33 \text{ pmol min}^{-1}$  in case of human sEH and  $7 \text{ pmol min}^{-1}$  for mouse sEH based on the specific activities reported in Table 3. When comparing these numbers, it becomes apparent that epoxide hydrolysis by sEH occurs significantly slower than the cyanohydrin formation under optimized assay conditions, establishing the latter reaction step as rate-limiting.

In case of the **endpoint system**, optimized substrate and enzyme concentrations force the epoxide hydrolysis by human sEH to be the rate-limiting step of the reaction mechanism as well. During the checkerboard assay, linear increase of the initial substrate turnover rate was demonstrated with increasing human sEH amounts up to  $0.33 \text{ }\mu\text{g/well}$  at  $50 \text{ }\mu\text{M}$  substrate concentration (compare to Figure 21). This represents roughly ten times more protein than utilized in the optimized test system. If either the intramolecular cyclization or the cyanohydrin conversion step was the rate-limiting reaction, the increase in initial velocity would approach saturation at a certain protein concentration (see above) and thus not be constant anymore.

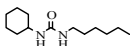
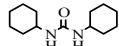
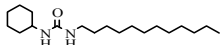
Put together, optimized assay conditions of the rapid kinetic system as well as of the endpoint assay guarantee the epoxide hydrolysis to be rate-limiting and thus the assays to result in valid information.

## 1.5.3.4 Inhibitor potency tests and assay validation

In order to test and confirm the applicability of the newly developed assays, inhibitory potencies of already characterized structures were re-evaluated with the novel systems. These structures were selected to cover a wide range of  $IC_{50}$ s. For comparison reasons, Table 12 lists previously determined  $IC_{50}$ s of the inhibitors, which were obtained by the spectrophotometric NEPC as well as the radiometric *t*DPPO assay (Morisseau et al., 1999; Morisseau et al., 2002; McElroy et al., 2003). Furthermore, the Table sums up the corresponding assay conditions.

The fluorescent continuous assay employing mouse sEH (compare to Table 7) ranks the investigated inhibitors in analogy to the *t*DPPO system, whereas this order diverges slightly when the same structures are tested with the NEPC system. On the other hand, the relative ranking of CHU and DCU differs when comparing the radioactive and the optically based assays carried out with the human enzyme. These observations prove a general difficulty in relating  $IC_{50}$  values to inhibitory potency of chemicals, since these constants are evidently dependent on their determination method. This fact is supported by the ten to twenty times higher absolute  $IC_{50}$ s of CDU and AUDA obtained by means of the radioactive-based determination in comparison to the fluorescence-based one.

**Table 12** Previously (see text) determined  $IC_{50}$  values for selected sEH inhibitors and employed assay conditions. Data are shown as means  $\pm$  standard deviation in nM.

Enzyme		Mouse sEH	Mouse sEH	Human sEH	Human sEH
Substrate		NEPC	<i>t</i> DPPO	NEPC	<i>t</i> DPPO
[S] <sub>final</sub> ( $\mu$ M)		50	50	50	50
[E] <sub>final</sub> (nM)		100	8	200	16
Inhibitor					
	CEU	51700 $\pm$ 700	nd	42200 $\pm$ 2000	nd
	CHU	110 $\pm$ 30	55 $\pm$ 3	70 $\pm$ 20	221 $\pm$ 2
	DCU	90 $\pm$ 10	81.8 $\pm$ 0.7	160 $\pm$ 10	63 $\pm$ 0.3
	CDU	50 $\pm$ 10	9.8 $\pm$ 0.4	100 $\pm$ 10	85.2 $\pm$ 0.5
	AUDA	50 $\pm$ 10	18 $\pm$ 1	100 $\pm$ 10	69 $\pm$ 2

Nevertheless, all fluorescent assays were, in contrast to the NEPC assay, able to differentiate between the most effective inhibitors CDU and AUDA in accordance with the relative ranking of the *t*DPPO system fulfilling the previously stated sensitivity requirements. Additionally, the respective numbers obtained from all fluorescent assay variants resembled each other greatly, suggesting the continuous assay with compound **7** not only to be able to rank inhibitors but also to result in more or less valid absolute  $IC_{50}$ s.

As already mentioned before, the fluorescent assay carried out with compound **3** could statistically not differentiate  $IC_{50}$  values of CHU and DCU. This might, on one hand, be assigned to high standard deviations resulting from the low replicate number of 3 in case of the continuous detection mode. On the other hand and more importantly, it should be noted that incubation times of enzyme and inhibitor were higher when utilizing substrate **3** (10 min versus five in all other mentioned systems). This has already been shown to influence absolute  $IC_{50}$  values (Morisseau et al., 1998). Therefore, if DCU binds to human sEH more slowly than CHU but with the same affinity, the observed  $IC_{50}$ s are easy to explain. This is of course not significant for a screening assay system and can be addressed, if necessary, by direct comparison of the compounds utilizing e.g. the *t*DPPO assay.

The endpoint assay validation, which was conducted by means of four experiments each on three consecutive days, sufficiently established the reliability and reproducibility of this test system. Daily as well as overall accuracy and precision values were satisfying. However, a loss of accuracy over the test period due to decreased absolute inhibition values was observed, suggesting this phenomenon to be caused by continuous inhibitor decay. Suboptimal storage conditions for the corresponding solutions – at room temperature and unprotected from light – possibly caused their decomposition and thus the accuracy deficit on day 3 of the investigation. The  $Z'$  value, which characterizes the quality of an assay and evaluates its suitability for high-throughput screening (Zhang et al., 1999), was found to range between 0.7 and 0.8 for this test system. With an ideal  $Z'$  of 1 and excellent values ranging between 0.5 and 1, these numbers imply a large separation band between maximal signal and background as well as excellent reproducibility of the endpoint assay. Therefore, its suitability for future high-throughput screens of large compound libraries was confirmed.

#### 1.5.3.5 Stop solution

The search for an appropriate stop solution, which could be utilized in the described fluorescent endpoint assay, was carried out in order to increase this system's flexibility in performance and adaptability to automated high-throughput screening. In brief, solutions suitable for this task are required to interrupt the ongoing substrate decomposition conserving or enhancing the present fluorescent signal.

Candidate stop solutions were selected due to the following facts: soluble epoxide hydrolase activity is known to be sensitive to organic solvents as well as oxidants (Wixtrom and Hammock, 1985; Draper and Hammock, 1999). Furthermore, zinc was identified not only to be able to inhibit the epoxide hydrolase but also the phosphatase activity of sEH (Draper and Hammock, 1999; Newman et al., 2003). Finally, substances commonly known to denature (SDS) or precipitate (ammonium sulphate) proteins in general were tested.

Concentrations of 100 and 200  $\mu\text{M}$  zinc sulphate were found to drastically decrease substrate turnover down to 10% in comparison to buffer addition. Furthermore, they not only conserved but enhanced the fluorescent signal of 6-methoxy-2-naphthaldehyde – in contrast to zinc nitrate. This rather surprising finding, which is expressed by increased conversion factors of fluorescent signal into mols of compound, will most likely enhance assay sensitivity by boosting the fluorescent signal and can thus improve assay performance even more. Therefore, if the necessity for a stop solution should occur, zinc sulphate at a final concentration of 100 to 200  $\mu\text{M}$  is highly recommended – possibly combined with a reduction in temperature. However, the time span in which fluorescent signal can / has to be determined after stop solution addition is still to be determined. Furthermore, it should be considered that the addition of stop solution represents one extra step for the assay, increasing its labour and cost requirements.

Data presented in this dissertation were generated without stop solutions to simplify the assay and because the plate design provided internal controls.



#### 1.5.4 Further applications for the novel fluorescent sEH substrates

In the present study, the development of novel fluorescence-based assay systems to investigate sEH inhibitors is described. While this use is important, the employed technology could be extended to other applications. It could be used in combination with other epoxide hydrolases or other enzymes that hydrolyze epoxides to diols (Arand et al., 2005). Additionally, the substrates should be excellent for the analysis of some GSTs. Furthermore, because the substrates contain an ester or carbonate function, esterases or lipases could also hydrolyze these compounds and yield a fluorescent response (Shan and Hammock, 2001; Wheelock et al., 2003). Results of the present study testing porcine liver esterase as well as sEH from rat, cress and potato in combination with the fluorescent sEH substrates underline the latter option.

Epoxide hydrolases, especially from microorganisms, are used for the production of chiral epoxides (de Vries and Janssen, 2003). If used as a competitive substrate, the fluorescent endpoint assay developed in this paper could be easily employed to screen libraries of pure oxirane enantiomers and to determine the enantio-selectivity of a particular enzyme.

The cyanohydrin re-arrangement concept used for the sEH substrates of this study leading to the formation of a fluorescent aldehyde has also been employed for esterases and P450 assay development (Zhang et al., 2003; Huang et al., 2005a; Kang et al., 2005; Huang et al., 2006). This concept can be extended by means of other fluorescent aldehydes acting as reporter molecules to shift excitation and emission maxima. Alternatively, the assay can be set up to yield an absorbance or luminescent signal.

#### 1.6 Conclusion

In summary, the present study characterizes a series of novel fluorescent substrates for the enzyme soluble epoxide hydrolase. Their reaction mechanism is based on the addition of water by the enzyme, the subsequent cyclization of the resulting diol to form a cyanohydrin, and finally the liberation of the fluorescent reporter molecule 6-methoxy-2-naphthaldehyde.

Two assay systems for different applications were developed and evaluated with these compounds. A rapid continuous kinetic assay employing substrate **7** was designed in order to be able to rapidly and rather inexpensively differentiate between inhibitors that were kinetically indistinguishable

with a previously reported spectrophotometric assay (Dietze et al., 1994; Kim et al., 2004c; Kim et al., 2005b). In addition, an undemanding and highly reproducible endpoint assay utilizing compound **3** was created intended for future screens of compound libraries. Both systems were evaluated in comparison to existing methods and found to reflect the results determined by means of the so far most sensitive sEH substrate *t*DPPO – a determination method that is costly and time intensive. Moreover, accuracy and precision of the endpoint assay performance as well as its suitability for high-throughput screening were shown to be respectable. The new assays employ 30 to 100 times less enzyme than the existing economical, absorbance-based rapid assay with NEPC and were therefore able to differentiate inhibitors that could not be ranked in an inexpensive way before. Finally, zinc sulphate at final concentrations above 0.1 M was provided as potential stop solution for the endpoint assay system.

The novel fluorescent assay systems will be invaluable tools for the improvement of known as well as for the discovery of new sEH inhibitors advancing and facilitating the development novel drugs for the treatment of vascular and inflammatory diseases.

## 2 Cellular inhibition of sEH by RNA interference and potential role in therapy

### 2.1 Introduction and objective

Soluble epoxide hydrolase (sEH; EC 3.3.3.2) is a new drug target. Its natural role is to catalyze the addition of a water molecule to an epoxide, which leads to the formation of the compound's corresponding diol (Oesch, 1973). If sEH is inhibited, epoxyeicosatrienoic acids (EETs), its predominant endogenous substrates, will accumulate. These compounds are known to provoke vasodilatory as well as anti-inflammatory effects in mammals (Harder et al., 1995; Campbell et al., 1996; Node et al., 1999; Campbell, 2000; Liu et al., 2005b; Larsen et al., 2006). Therefore, it is not surprising that chemical inhibition of sEH in rodent models was found to trigger successful treatment of hypertension (Yu et al., 2000; Imig et al., 2002; Imig et al., 2005) and inflammatory diseases (Schmelzer et al., 2005; Smith et al., 2005) as well as protection against renal damage caused by hypertension (Zhao et al., 2004; Imig et al., 2005). Furthermore, sEH inhibitors were suggested as potential therapeutic agents for ischemic stroke (Dorrance et al., 2005).

Highly potent inhibitors for sEH have been developed (Morisseau et al., 2002; McElroy et al., 2003; Kim et al., 2004c; Kim et al., 2005b). However, while these substances proved extremely useful for research purposes, their physical properties suggest that they cannot be turned into a practicable pharmaceutical (Watanabe et al., 2006) due to suboptimal pharmacokinetic properties (Lipinski et al., 2001). Therefore, alternative and / or complementary therapy options should be considered.

RNA interference (RNAi) is a recently discovered endogenous mechanism leading to the specific post-transcriptional down-regulation of target genes. First reported in *Caenorhabditis elegans* (Fire et al., 1998), it soon could also be initiated in mammalian cells by 19-25 bp (base pair) short, double-stranded RNAs (dsRNAs) that possess 2-base overhangs at the 3'-end of each strand (Caplen et al., 2001; Elbashir et al., 2001a). These particular duplex molecules called short interfering RNAs (siRNAs) are able to circumvent the initiation of several mammalian antiviral mechanisms, which are normally set off by dsRNA > 30 bp (reviewed in Wang and Carmichael, 2004). After the introduction of an siRNA into a cell, it gets directionally incorporated into a protein complex called RISC (RNA

induced silencing complex), while its so-called passenger strand is cleaved (Matranga et al., 2005; Leuschner et al., 2006). After that, the remaining siRNA guide strand mediates mRNA recognition by means of Watson-Crick base-pairing and RISC proceeds with the cleavage of the complementary mRNA, which causes the specific post-transcriptional down-regulation of the respective gene (for a review of the RNAi machinery and mechanism see Collins and Cheng, 2005). Rapidly it became obvious that this phenomenon would prove very helpful not only as reverse genetic tool for basic research, but also for drug target identification and validation (reviewed in Ito et al., 2005; Chatterjee-Kishore and Miller, 2005). On top of that, it holds potential for the actual treatment of diseases (reviewed in Dykxhoorn et al., 2006; Uprichard, 2005). The potential advantages of this approach are obvious: the (a) selective, (b) highly potent and (c) versatile abolishment of a target gene, a group of related genes respectively, by means of (4) an endogenous mechanism. The first phase I clinical trial of an siRNA-therapeutic directed against age-related macular degeneration (AMD) was carried out with promising initial results (Whelan, 2005) confirming the significance of RNAi for novel therapy approaches on the post-transcriptional level.

The above facts suggest that RNAi could represent an alternative and / or complementary approach to chemical inhibition of sEH with potential for therapy and the herein presented study might be a first step toward this big target. This report documents the search for an appropriate human cell culture model expressing sEH. Furthermore, the *in vitro* knockdown of human sEH by siRNAs as well as the time- and dose-response of this effect are demonstrated. Finally, the current potential for RNAi as therapy approach for the inhibition of sEH will be discussed.

## 2.2 Materials and methods

### 2.2.1 Chemicals and reagents

Chemicals and reagents were purchased from Sigma Chemical (St. Louis, MO, USA) unless otherwise indicated. The <sup>3</sup>H-labeled sEH substrate *trans*-1,3-diphenylpropene oxide (*t*DPPO) was synthesized and purified as described before (Borhan et al., 1995).

### 2.2.2 Cell lines

Cell lines were received from various sources. 22RV1, LNCaP, TCC-SUP, T24, 5637 and SCaBER were generously provided by Ruth L. Vinall (Department of Urology, UC Davis, CA, USA). Raji, Ramos, SU-DHL-4, SU-DHL-6, B35M, Jurkat and DU-145 cells were kind gifts from Alan Epstein, MD, PhD (USC, Keck School of Medicine, Los Angeles, CA, USA) and Gerald DeNardo, MD (UC Health Center, Sacramento, CA, USA). T47-D and 293 cells were gratefully obtained from the UC Davis Cancer Center (Sacramento, CA, USA) thanks to the help of Ralph De Vere White. SIK cells were a kind gift from Robert Rice (Department of Nutrition, UC Davis, CA). HepG2 cells were purchased from ATCC (Manassas, VA, USA).

### 2.2.3 Determination of specific sEH activity of different cell lines

Several human cell lines were tested for their specific sEH activity with the surrogate substrate *t*DPPO. Therefore, frozen pellets of  $\sim 10^6$ - $10^7$  cells were lysed in 1-2 ml of lysis buffer (20 mM sodium phosphate buffer pH 7.4, supplemented with 5 mM ethylenediaminetetraacetic acid (EDTA), 1 mM phenylmethylsulphonylfluoride (PMSF), 1 mM dithiothreitol (DTT) and 0.01% (v/v) Tween 20). Subsequently, the suspensions were diluted at least 10-fold with 100 mM sodium phosphate buffer (pH 7.4) including 0.1 mg/ml bovine serum albumin (BSA) fraction V. Addition of 1  $\mu$ l of 5 mM *t*DPPO in 100% ethanol to 100  $\mu$ l of the diluted cell lysates, or – as positive and negative control – to the same amount of 100 mM sodium phosphate buffer including BSA, started the conversion of the substrate to the corresponding diol (Borhan et al., 1995). The reaction, which was carried out at 30°C for 30 or 60 min in triplicate, was stopped by adding 60  $\mu$ l of methanol. Furthermore, 250  $\mu$ l of isoctane were

added to separate the highly water-soluble reaction product and the original *t*DPPO substrate. Thus, the latter compound was extracted into the organic phase, following Borhan et al. (1995). Alternatively, hexanol extraction was carried out to examine the cells' glutathione *S*-transferase activity due to the following circumstance: while isooctane partitions the epoxide into the hyperphase leaving the sEH-derived diol in the aqueous one, hexanol extracts both, the epoxide and the diol leaving the glutathione conjugate. In case of the positive control, buffer samples were not extracted at all. Forty  $\mu$ l of the remaining aqueous reaction phase in 1 ml of scintillation solution (Fisher Scientific Co., Pittsburg, PA, USA) were then analyzed by liquid scintillation counting (LSC) using a Wallac 1409 Liquid Scintillation Counter (Wallac Inc., now Perkin Elmer Life Sciences, Wellesley, MA, USA). Protein concentrations of at least 10-fold diluted cell lysates (dilution with 100 mM sodium phosphate buffer pH 7.4, no BSA addition) were determined employing the BCA assay as well as albumin standard for calibration (both products from Pierce, Rockford, IL, USA).

Specific activities of cell lines were calculated employing the following formula:

$$\text{Specific sEH activity} = \frac{\text{LSC}_{10} - \text{MIN}}{\text{MAX}} \times \frac{5 \text{ nmol}}{t \times m} \times \frac{\text{Dilution factor}}{0.907}$$

$\text{LSC}_{10}$  = liquid scintillation counts of isooctane extracted *t*DPPO reaction

MIN = mean liquid scintillation counts of hexanol extracted reactions

MAX = mean liquid scintillation counts of positive controls

m = protein amount per reaction in mg

t = reaction time in min

1/0.907 = correction factor (Borhan et al., 1995)

#### 2.2.4 Cell culture

The human prostate carcinoma cell line 22RV1 was cultured in RPMI 1640 medium including 25 mM HEPES (Mediatec Cellgro™, Herndon, VA, USA) and supplemented with 10 % fetal bovine serum premium (FBS; Cambrex, Walkersville, MD, USA). Cells were incubated at 37°C in a humidified atmosphere enriched with 5% CO<sub>2</sub>. They were routinely passaged twice a week at 80-95% confluency utilizing trypsin-EDTA (Gibco®, Invitrogen, Carlsbad, CA, USA).

### 2.2.5 Optimization of electroporation

Electroporation conditions for 22RV1 cells were optimized following the procedure suggested by amaxa biosystems Inc. (Gaithersburgh, MD, USA) employing their Nucleofector technology. In brief,  $1 \times 10^6$  cells per reaction were resuspended in three different electroporation buffers (R, T, and V) and mixed with 2  $\mu\text{g}$  of the mammalian expression vector maxGMP (amaxa Inc., Gaithersburgh, MD, USA) that codes for green fluorescent protein (GFP). Eight different electroporation programs each (A-23, A-27, T-20, T-27, T-16, T-01, G-16 and O-07) or no electroporation at all were then tested in combination with the three electroporation buffers resulting in 27 differently treated variants. After electroporation, cells were immediately diluted with 37°C warm serum-free RPMI 1640 medium. After a 15 min incubation at 37°C, cells of one reaction were plated in one well of a 6-well tissue culture-treated polystyrene plate (Falcon™, BD Biosciences, Bedford, MA, USA). After 24 h under regular cell culture conditions, cells were analyzed for electroporation efficiency. This investigation was carried out by randomly choosing 100 cells per variant and visually examining them for GFP expression employing an inverted fluorescent microscope equipped with a IMT2-DMB dichroic mirror unit (Olympus IMT-2, Olympus Corp., Melville, NY, USA) and along with an attached digital camera (Olympus MicroFire, Olympus Corp., Melville, NY, USA). The percentage of cells that expressed GFP was then determined.

### 2.2.6 siRNAs and RNAi experiments

Four siRNAs directed against human sEH and therefore called siHsEH 1-4 were designed by and purchased from Dharmacon, Inc. (Chicago, IL, USA). Sense and antisense sequences of these short double-stranded RNAs are listed in Table 13. Additionally, a non-targeting siRNA sequence (siCONTROL #1) and a fluorescence-tagged siRNA effective against cyclophilin B (siGLO Cyclophilin B siRNA) were acquired as controls from the same source.

Lipid-mediated transfection experiments were carried out utilizing the X-tremeGENE siRNA transfection reagent (Roche Applied Sciences, Indianapolis, IN, USA). One day before transfection,  $2.5 \times 10^5$  cells per well were seeded in a 6-well tissue culture plate. Before transfection, medium was exchanged. Transfection was performed with 0.74  $\mu\text{g}$  of siRNAs complexed with 3.7  $\mu\text{l}$  of the transfection reagent in Opti-MEM (Gibco®, Invitrogen, Carlsbad, CA, USA) following the

recommendations of the transfection reagent's manufacturer. This resulted in a final siRNA concentration of 100 nM per well as recommended by the siRNA-synthesizing company. In addition, cells were treated with Opti-MEM with and without transfection reagent only to reveal their impact on human sEH expression. Medium was exchanged 6 h after transfection to avoid cell toxicity effects due to the transfection reagent.

**Table 13** siRNA sequences of the present study directed against human sEH. Sequences were provided by Dharmacon, Inc. (Chicago, IL, USA) and are given in 5'-3' direction.

siRNA	Sense sequence	Antisense sequence
siHsEH 1	gaaaggcuauggagagucauu	ugacucuccauagccuuucuu
siHsEH 2	guacauggcucucuucuuacuu	guagaagagagccauguacuu
siHsEH 3	gaauccagcuucucauuacuu	guauugagaagcuggauucuu
siHsEH 4	gcacuuugacuuccugauuuu	uaucaaggaagucaagugcuu

Electroporation experiments employed the Nucleofector technology (amaxa, Inc., Gaithersburg, MD, USA). Therefore, 22RV1 cells were grown up to 80-90% confluency. After trypsin-EDTA treatment,  $1 \times 10^6$  cells were resuspended in 100  $\mu$ l of electroporation solution V and mixed with the respective siRNA amount (normally 2  $\mu$ g; exception were dose-response experiments). Subsequently, the Nucleofector program T-27 was executed. After the actual electroporation, cells were allowed to recover as described above. However, after the 15-min incubation, 100  $\mu$ l per electroporated cell sample were seeded in one well of a 24-well tissue culture-treated plate for mRNA expression analysis and the remaining cells in a 6-well plate (both plate types: Falcon™, BD Biosciences, Bedford, MA, USA) in order to examine sEH activity later on. Medium was exchanged twice around 8 h after seeding to remove dead cells. Forty-eight h after electroporation, cells were analyzed for the RNAi effect. Exceptions were samples for the time-response investigation. All described RNAi investigations targeting human sEH were performed in three independent experiments.



### 2.2.7 sEH activity determination of siRNA-treated cells

The medium was completely removed from siRNA-treated cells in the 6-well plates and 500  $\mu$ l of lysis buffer (20 mM sodium phosphate buffer pH 7.4, supplemented with 5 mM ethylenediaminetetraacetic acid (EDTA), 1 mM phenylmethylsulphonylfluoride (PMSF), 1 mM dithiothreitol (DTT) and 0.01% (v/v) Tween 20) were added per well. After a 5-min incubation of the cells in this solution, they could be completely detached by pipetting. Suspensions were transferred to 1.5 ml tubes (ISC BioExpress, Kaysville, UT, USA) and stored at  $-80^{\circ}\text{C}$  for at least 1 day to completely destroy all cells. Lysates were thawed on ice and centrifuged with maximum speed at  $4^{\circ}\text{C}$  using an Eppendorf 5415C microcentrifuge (Eppendorf, Westbury, NY, USA). The undiluted supernatant was then analyzed in triplicate for sEH activity by means of the *t*DPPO assay as described above. Relative enzyme activity was calculated via the ratio “LSC of cells treated with targeting-siRNAs / LSC of cell lysates treated with non-targeting siRNA”. Hereby each of the three LSC per ‘silenced’ variant was divided by each of the corresponding negative control numbers, which resulted in 9 values per sample.

### 2.2.8 RNA extraction and RT-PCR

Total-RNA extraction of 22RV1 cells was carried out using TRIzol (Invitrogen, Inc., Carlsbad, CA, USA) following the manufacturer’s instructions. RNA of one sample was recovered in 7-10  $\mu$ l of molecular biology-grade water and transcribed using the “Transcriptor First Strand cDNA Synthesis Kit” (Roche Applied Sciences, Indianapolis, IN, USA). Therefore, 6  $\mu$ l of total RNA were mixed with 0.5  $\mu$ l anchored-oligo(dT)<sub>18</sub> primer, incubated for 10 min at  $65^{\circ}\text{C}$ , then placed on ice. After that, 3.5  $\mu$ l of a mixture of reaction buffer, RNase inhibitor, dNTPs and reverse transcriptase were added following the manufacturer’s instructions. Samples were then transcribed for 1 h at  $50^{\circ}\text{C}$  and subsequently heated up to  $85^{\circ}\text{C}$  in order to inactivate the employed enzyme.

### 2.2.9 Quantitative PCR

Human sEH expression of all samples was quantified relative to the one of human glyceraldehyde-3-phosphate dehydrogenase (GAPD) employing a LightCycler® instrument and the LightCycler® “FastStart DNA Master<sup>PLUS</sup> SYBR Green I” kit (Roche Applied Sciences, Indianapolis, IN, USA)

following the manufacturer's instructions unless indicated otherwise. All DNA oligonucleotides were employed at final concentration of 1  $\mu$ M in the PCR reactions. Primer sequences for human sEH were 5'-ccactaccggcttatgaaa-3' and 5'-ttcagattagccccgatgtc-3' resulting in a 426 bp long product. GAPD amplification was carried out with the following primers: 5'-gagtcaacggatttgctgct-3' and 5'-ggaggcattgctgatgatct-3'. In this case, PCR amplicates were 434 bp long. All primers were purchased from MWG Biotech, Inc. (High Point, NC, USA) in 'high purity salt free' quality. Both genes were amplified per sample with the following PCR program: (1) pre-incubation for 10 min at 95°C to activate the polymerase; (2) 10 s at 95°C for denaturing the double-stranded DNA, pursued by 3 s at 57°C in order to anneal the primers and 20 s at 72°C for the elongation process. During another 2 s at 72°C, fluorescence detection was carried out. Step (2) was repeated 40 times. Afterwards, a melting curve analysis was carried out. In order to determine PCR efficiency for both genes, serial dilutions (dilution factor 10) of cDNA from untreated 22RV1 cells were produced and amplified in triplicate. cDNA samples from siRNA-treated cells were 10x diluted with molecular biology-grade water and 5  $\mu$ l were used for the subsequent PCR. Expression analysis of human sEH as well as GAPD per cDNA sample was performed in triplicate. In addition, a calibrator was amplified per PCR run without replicate. Relative expression levels of human sEH were calculated as it follows:

$$\text{Relative mRNA level} = \frac{E_{\text{HsEH}}^{\text{CP}_{\text{HsEH}}(\text{C}) - \text{CP}_{\text{HsEH}}(\text{S})} \times E_{\text{GAPD}}^{\text{CP}_{\text{GAPD}}(\text{C}) - \text{CP}_{\text{GAPD}}(\text{S})}}{E_{\text{HsEH}}^{\text{CP}_{\text{HsEH}}(\text{C}) - \text{CP}_{\text{HsEH}}(\text{N})} \times E_{\text{GAPD}}^{\text{CP}_{\text{GAPD}}(\text{C}) - \text{CP}_{\text{GAPD}}(\text{N})}} 100\%$$

$E_{\text{HsEH}}$  = Efficiency of human sEH amplification, which in this case was found to be 1.99

$E_{\text{GAPD}}$  = Efficiency of GAPD amplification, which in this case was determined as 1.89

$\text{CP}_{\text{HsEH}} / \text{CP}_{\text{GAPD}}$  = Crossing point; PCR cycle number at which the respective gene amplification could be detected above threshold

C = Callibrator; cDNA sample of untreated 22RV1 cells at 1:100 dilution

S = Sample; cDNA sample of cells treated with human sEH-targeting siRNAs

N = Negative control; cDNA sample of cells treated with non-targeting siRNAs

Hereby, each possible combination of results was calculated yielding 81 values per sample.

## 2.3 Results

### 2.3.1 Expression of sEH by human cell lines

The knockdown of sEH by RNAi was considered as potential alternative to its chemical inhibition in the treatment of vascular and inflammatory diseases. Therefore, initial *in vitro* experiments to test the hypothesis that siRNAs could down-regulate the respective human enzyme by RNAi were intended. However, this plan raised the necessity of a suitable cell model expressing sEH in sufficient and thus detectable amounts. Thus far, no human cell system is reported that would fulfill this requirement (Hammock et al., 1997). Nevertheless, several human cell lines were tested for this particular property and results of the investigation are shown – in part – in Figure 24.

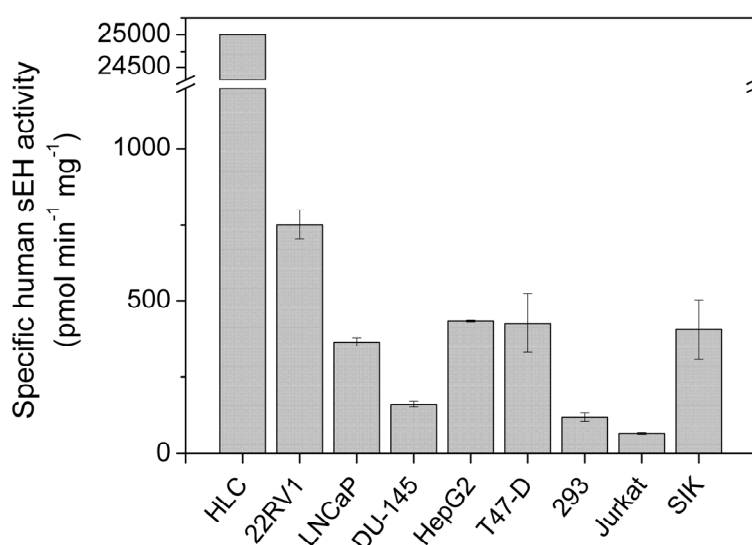


**Fig. 24** Specific activities of selected human cell lines. Displayed data represent means  $\pm$  standard deviation from determinations in triplicate.

It is evident that the examined prostate (22RV1, LNCaP, DU-145), hepatic (HepG2) and breast cancer (T47-D) cell lines express the enzyme of interest in fair amounts, with the highest specific activity level in 22RV1 cells. However, in comparison to these values, specific sEH activities *in vivo* are much higher. This is illustrated by the respective turnover of *t*DPPO by human liver cytosol (HLC) under similar assay conditions (Draper and Hammock, 1999; compare to Figure 24). The tested embryonic kidney cell line 293 as well as Jurkat, a T-cell leukemia cell line, show both detectable but still low specific sEH activities, and were thus not considered for further RNAi experiments. SIK was also able to turn over the sEH-specific substrate *t*DPPO at a relatively high speed, but was not considered for further RNAi experiments either due to its epidermal origin, which will be discussed later.

In addition, several cell lines were tested that showed no or very little ( $\leq 10 \text{ nmol min}^{-1} \text{ mg}^{-1}$ ) specific sEH activity. TCC-SUP, T24, 5637 and SCaBER, all derived from human urinary bladder carcinoma, were in this category as well as B35M, Ramos and Raji, generated from human Burkitt lymphoma cells, and SU-DHL4 along with SU-DHL6, which were attained from human B-cell lymphoma.

It should be noted that none of the mentioned cell lines displayed significant glutathione *S*-transferase (GST) activity, which would interfere with the performed sEH activity tests employing *t*DPPO. This can be assumed due to the results obtained from hexanol extractions of the *t*DPPO / cell lysate reactions, which did not differ from the performed negative controls. The extraction reagent hexanol – in contrast to isooctane – is able to selectively extract diols from the aqueous test reactions leaving GST conjugates in the lower hypophase (Borhan et al., 1995; Slim et al., 2001).

### 2.3.2 Optimization of electroporation conditions for 22RV1

After the selection of the prostate cancer cell line 22RV1 as model system for further RNAi experiments due to its high and thus easily detectable sEH expression level, electroporation conditions were optimized employing the Nucleofector technology. Therefore, 22RV1 cells were resuspended in three different electroporation solutions and electroporated with selected instrument-internal programs introducing a plasmid for GFP expression in mammalian systems. By examining the GFP-expressing

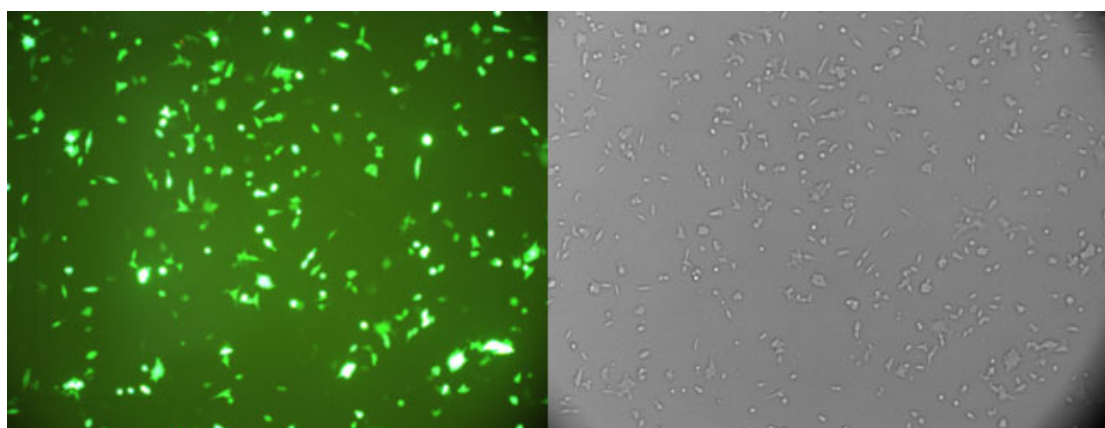


**Fig. 25** GFP expression of 22RV1 cells, which were electroporated employing the Nucleofector program T-27 to introduce a GFP-encoding mammalian expression vector. The picture was taken 24 h after electroporation by means of an inverted light / fluorescent microscope and an attached digital camera at 100x magnification. The right part of the figure displays the sight under light-microscopic conditions, whereas the left one shows the same cells when viewed utilizing the fluorescent mode of the microscope equipped with the dichroic mirror unit IMT2-DMB.

percentage of living cells after 24 hours, it was found that a combination of solution V and program T-27 was most successful concerning electroporation efficiency. Under these conditions, 75% of the cells displayed GFP expression (Figure 25).

### 2.3.3 RNAi experiments

Initial RNAi experiments, intended to test the possibility of silencing human sEH by this endogenous mechanism, were carried out by lipid-mediated introduction of 4 different siRNAs as well as a mixture of all of them into 22RV1 cells (Table 12). The test of various different siRNAs in order to reveal the most effective one is necessary, because despite some discovered rules for rational siRNA design (Khvorova et al.,

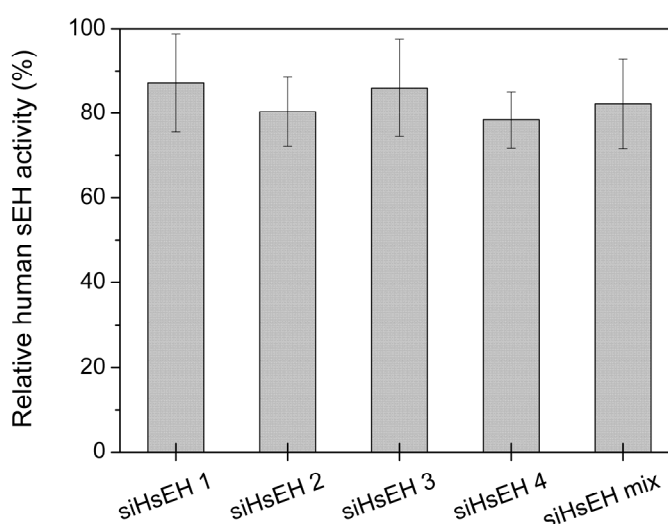


**Fig. 26** Effect of lipofection-mediated introduction of 4 different siRNAs as well as a mixture of them on human sEH activity in 22RV1 cells. Enzyme activities at 48 h past lipofection are displayed relative to treatment with a non-targeting siRNA. Data represent results of 3 independent experiments and are shown as means  $\pm$  standard deviation (refer to method part for calculation details).

2003; Schwarz et al., 2003; Hsieh et al., 2004; Reynolds et al., 2004) reliable prediction of their silencing potential is still impossible. Figure 26 illustrates that the down-regulation of human sEH while employing lipofection was not satisfactory: reduction in enzyme activity was 21% at the most. Nevertheless, visual analysis of cells, which were treated with lipid-complexed siRNAs possessing a fluorescent tag, gave the impression of efficient delivery into the cells (Figure 27 A).

In order to explore an alternative siRNA delivery method to 22RV1 cells and thus to improve the silencing effect of the employed siRNAs, electroporation of these potential effector molecules was tested. After optimization of the respective conditions, one experiment with fluorescently labeled siRNAs was performed. Examination by means of an inverted fluorescence microscope (Figure 27 B) revealed these duplex molecules to be present in basically all treated cells. In addition, they were evenly

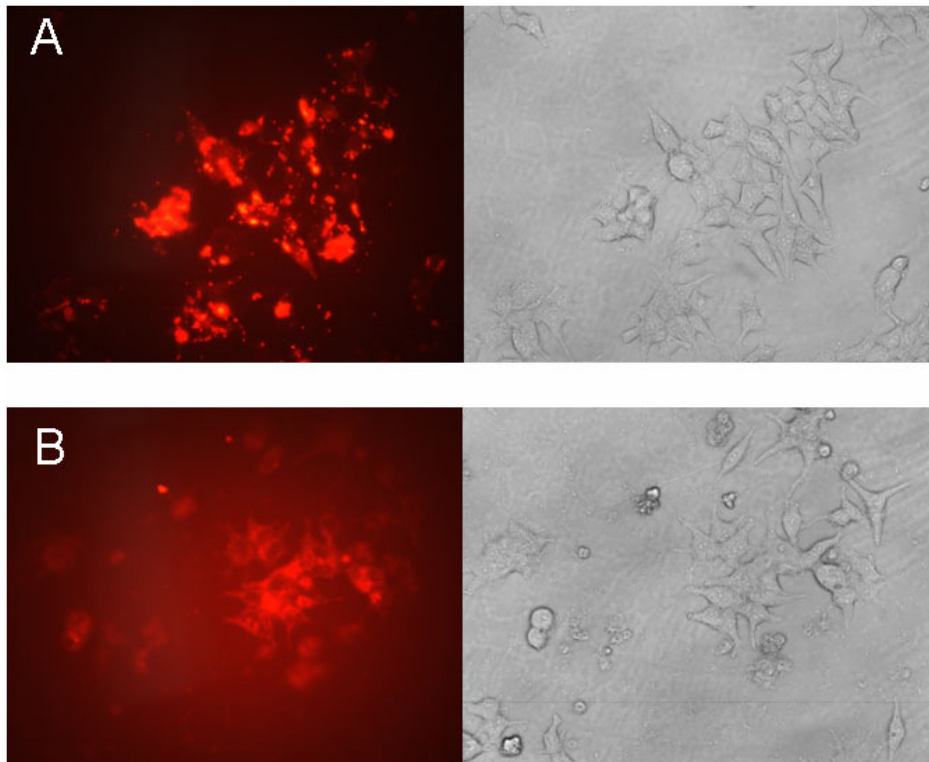


**Fig. 27** Representative photomicrographs of 22RV1 cells treated with fluorescently labeled siRNAs. All pictures were taken at 48 h after treatment by means of an inverted light / fluorescence microscope (Olympus IMT-2, Olympus Corp., Melville, NY, USA) and an attached digital camera (Olympus MicroFire, Olympus Corp., Melville, NY, USA) at 400x magnification. The right part of each picture documents the sight under light-microscopic conditions, whereas the left one displays the same cells when viewed by means of the fluorescent mode of the microscope equipped with the dichroic mirror unit IMT2-DMG. siRNA introduction was performed via lipofection (A) and electroporation (B).

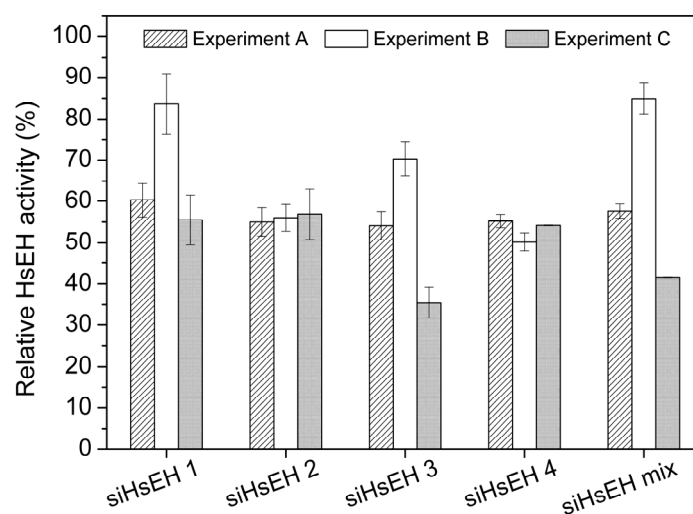


**Fig. 28** RNAi effect of several siRNAs on human sEH activity in 22RV1 cells following electroporation. Results of three individual experiments, represented by the different bar types, are displayed relative to treatments with a non-targeting siRNA. Data are shown as means  $\pm$  standard deviation of determination (see text for detailed information on calculation).

spread within the cells, whereas in case of lipid-mediated transfection, aggregates of siRNAs were observed. This finding was promising with regard to the down-regulation of human sEH. And indeed, subsequent RNAi experiments targeting this protein were found to prohibit human sEH activity up to 60% relative to cells treated with a non-targeting siRNA. However, as Figure 28 reveals, there was significant variation between the single repeats of this experiment. Especially results of experiment B were found to differ from the rest of the observations suggesting experimental difficulties in this particular case.

In an attempt to examine the impact of the RNAi effect on human sEH expression over time, the time-response of 22RV1 cells to the introduction of an sEH-targeting siRNA mixture was investigated in three independent experiments. Hereby, each time point of each experiment was determined relative to simultaneously performed cell treatment with non-targeting siRNAs. Overall, it seems that human sEH activity continuously decreased over the investigated time of 96 h due to the RNAi effect

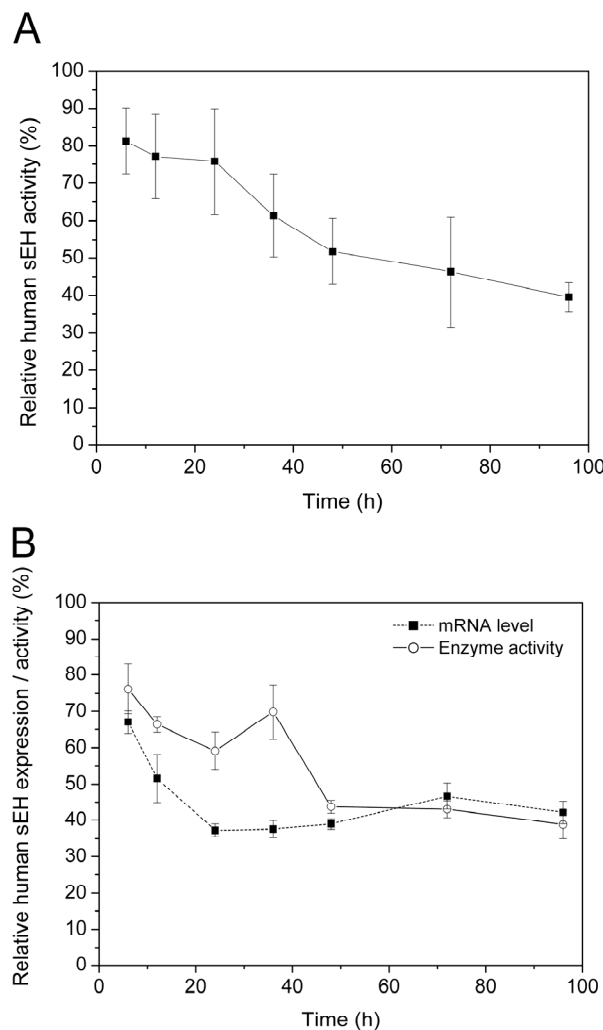


**Fig. 29** Time-response of 22RV1 cells to electroporation introducing a mixture of 4 human sEH-targeting siRNAs. Each datum point was set relative to simultaneously performed cell treatment with non-targeting siRNAs. **A** RNAi effect on enzyme activity. Data represent results from 3 independent experiments and are shown as means  $\pm$  standard deviation (refer to method part for calculation details). However, datum points at 36 h and 96 h only represent findings from 2 independent experiments. **B** Direct comparison of enzyme activity level and mRNA level during a single time-response experiment. Data are displayed as relative means of calculated values  $\pm$  standard deviation (for calculation of these values see methods part).

(Figure 29 A). Figure 29 B displays the analysis of a single time-response experiment. As expected, mRNA decrease occurs ahead of human sEH activity decay. However, the two parameters correlate fairly well with one exception at 36 h, which is possibly caused by an experimental error in the enzyme activity analysis of the sample, the negative control sample respectively.

The results of the initial RNAi experiments testing 4 different human sEH-targeting siRNAs could not establish one of the duplex molecules to be clearly more potent regarding RNAi initiation than the others. Therefore, siHsEH 3 was randomly selected and utilized along with a mixture of all 4 siRNAs in subsequent dose-response experiments. These tests were performed to replicate the results of the preceding RNAi experiments

as well as to establish and further characterize the employed cell model system regarding the *in vitro* silencing of human sEH. Figure 30 illustrates that siRNA amounts down to 0.2  $\mu\text{g}$  per electroporation reaction were able to evoke a similar silencing effect 48 h after electroporation as 10 or 20 times this quantity. On the other hand, siRNA amounts as low as 0.002  $\mu\text{g}$  per electroporation reaction basically displayed no RNAi effect. Interestingly, the mix of all 4 candidate siRNAs – even though employed at an identical total amount – generally displayed higher silencing effects than siHsEH 3. Although this observation is not statistically significant, it suggests another siRNA of the mixture to be more effective than siHsEH 3.

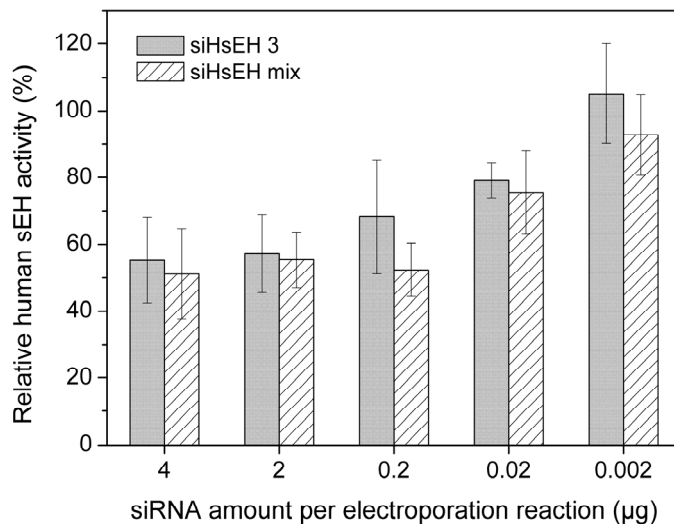


**Fig. 30** Dose-response of 22RV1 cells to electroporation with siHsEH 3 as well as a mixture of all 4 siRNAs. Human sEH activities indicating the RNAi effect are displayed relative to the respective variants, which were treated with the same amount of non-targeting siRNAs. Data represent results of 3 independent experiments and are shown as means  $\pm$  standard deviation.



## 2.4 Discussion

### 2.4.1 Selection of a suitable cell model system

While sEH is constitutively expressed in living vertebrates, this seems not to be the case for primary cell culture. From experience it can be stated that the cells examined continuously lose sEH activity right after isolation. For the intended RNAi study however, a steadily sEH-expressing, homogenous human cell line was the desired, yet unknown model system. There is certainly always the option of permanently or transiently transfecting cells, which will then express the gene of choice at high levels. However, these approaches are either time consuming or dependent on potentially varying transfection efficiencies. Therefore in an initial attempt, several human cell lines were screened for their natural sEH expression potency. Analysis of specific sEH activities by means of the sEH surrogate substrate *t*DPPO lead to the selection of 22RV1 as model system for the intended RNAi experiments. This prostate cancer cell line displays a specific sEH activity, which is at least 1.7 times higher than found in the other tested cell lines and which would be sufficient for further RNAi studies.

The observation that all tested prostate cancer cell lines possessed comparatively high specific human sEH activity levels is in accordance with earlier investigations suggesting androgen-induced sEH expression (Pinot et al., 1995b; Pang et al., 2002). Moreover, elevated sEH levels were found in cell lines derived from hepatic, kidney and breast tissues, which are all known to express sEH *in vivo* (reviewed in Newman et al., 2005). However, while sEH could be detected in human urinary bladder (Pacifici et al., 1988), the corresponding carcinoma cell lines TCC-SUP, T24, 5637 and SCaBER showed basically no such specific activity.

SIK, a cell line that was developed from human epidermal tissue and showed significant sEH activity, was not considered for further RNAi experiments. Such investigations greatly depend on the knowledge of the target gene sequence, which in case of human sEH is based on mRNA extractions from hepatic tissue. However, findings of Winder et al. (1993) suggest differences between liver and epidermal human sEH. This circumstance prohibited the employment of SIK as cellular model system in the intended RNAi experiments.

### 2.4.2 RNAi experiments

As it turned out, the selected cell model system is hard to transfect. This already became clear during unsuccessful attempts to introduce shRNA(short hairpin RNA)-expressing PCR products and plasmids, which were also intended to induce an RNAi effect targeting human sEH (data not shown). Moreover, this was also the case for HepG2, the second choice in terms of a suitable cell model system for subsequent RNAi experiments. Despite this difficulty, lipid-mediated siRNA transfection into 22RV1 cells was attempted but resulted in poor silencing of human sEH. It has to be noted that in this case transfection conditions were not optimized. However, the respective experiments were performed as recommended by the manufacturers of siRNAs and transfection reagent.

Consequently, the siRNA delivery method was changed to electroporation representing the state of the art method for the introduction of nucleic acids into cells. Reproducibility of the early experimental results employing this method, however, turned out to be suboptimal. Reasons for this are likely to be variations in electroporation efficiency and the corresponding cell survival rate due to minimal changes in cell condition before the electroporation treatment. Later on, a human sEH knockdown of ~ 50% could reproducibly be achieved in dose- and time-response experiments at 48 h after electroporation and was shown on the enzyme activity as well as the mRNA level. Moreover, this effect seems to be – according to the general tendency of the cellular time-response to siRNA electroporation – even stronger at a later time point. The observed relatively long-lasting RNAi effect is in accordance with recent reports in mammalian systems, which indicate that the duration of this endogenous silencing effect strongly depends on the respective cell division rate and thus on the intracellular siRNA dilution effect due to mitosis (Bartlett and Davis, 2006; Zimmermann et al., 2006). In case of the 22RV1 cells, relatively long doubling times between 40-60 h are common allowing a relatively long-lasting RNAi phenomenon.

Interestingly, an almost complete down-regulation of the target gene, as shown in similar studies (Reynolds et al., 2004), could not be achieved in the present investigation. Presuming a very efficient siRNA delivery method, this finding can have two causes: (a) all 4 tested siRNAs cannot evoke a stronger RNAi effect than observed or (b) the employed cell model system 22RV1 possesses an RNAi counter-regulatory mechanism ensuring a minimum sEH expression level in the cells. The latter option

is considered due to androgen-induced sEH gene expression in the prostate cancer cell line – an effect, which was observed before (Pinot et al., 1995b; Pang et al., 2002). However, more experiments are required to test this hypothesis. First, one investigation has to ultimately establish the functionality of the siRNA delivery method by means of a non-sEH-targeting, previously evaluated and highly functional siRNA serving as positive experimental control. Such investigations were already performed, but no effect on gene expression was seen – most likely due to fluorescence-labeling of the positive control siRNA. An additional experiment employing a non-prostate-derived cancer cell line (preferentially originating from kidney or liver such as HepG2 or 293) and testing the same siRNAs as employed in this study could finally reveal the reason(s) for the comparatively low silencing effect in this experimental series.

The present study illustrates that the RNAi effect is not as easy to evoke as one could get the impression from the multitude of recent publications employing RNAi to knock down certain target genes. However, this seems to be at least partially caused by the chosen cell model system 22RV1, which appears hard to penetrate and might influence sEH expression via an endogenous regulatory mechanism.

#### 2.4.3 RNAi as potential therapy approach to down-regulate human sEH activity

The investigations presented here and their respective outcome are regarded as a – even though still basic – successful attempt to abolish human sEH activity by RNAi offering an alternative to its chemical inhibition. This is particularly interesting with regard to the respective therapeutic applications of the option.

A therapeutic RNAi approach targeting sEH would have several benefits. First of all, the high specificity of the RNAi mechanism would enable to selectively and probably even allele-specifically knockdown sEH. For example, unfavorable sEH polymorphisms such as Arg287Gln, which was previously connected to coronary artery calcification in African-Americans (Fornage et al., 2004) could be eliminated in heterozygous individuals. In contrast, chemical sEH inhibitors might also interact with other cellular components and thus disturb relevant biological processes. Possible side effects of siRNAs such as off-target effects (Jackson et al., 2003; Saxena et al., 2003; Birmingham et al., 2006;

Fedorov et al., 2006) or unspecific effects resulting in the initiation of an interferon response (Kariko et al., 2004; Hornung et al., 2005; Judge et al., 2005; Reynolds et al., 2006) can possibly be excluded beforehand in *in vitro* investigations employing suitable cellular model systems. On the other hand, the biological impact of metabolic products from chemical inhibitors is disproportionately harder to discern. Furthermore, recent studies (Whelan, 2005; Zimmermann et al., 2006) promise a long-lasting *in vivo* knockdown after siRNA treatment, which would simplify a therapeutic treatment in comparison to taking single or even multiple daily doses of a chemical inhibitor.

Even though an sEH-targeting RNAi therapy approach possesses a number of advantages in comparison to chemical inhibition, there are still major obstacles to overcome before it can be employed. The two biggest hurdles for RNAi therapy in general, besides careful selection of an RNAi effector sequence, are specific siRNA delivery to targeted cells and the instability of siRNAs in blood, which is predominantly caused by kidney filtration or endogenous serum RNAses (reviewed in Dykxhoorn et al., 2006). The latter problem is particularly important for systemic delivery of siRNAs to vascular endothelium as it would be necessary for the treatment of hypertension by sEH-targeting siRNAs. However, this setback has already been addressed by several groups via linkage to or complexation with other molecules, as well as modifications of the siRNA sugar backbone (see Dykxhoorn et al., 2006; Leung and Whittaker, 2005 and references therein). A recent *in vivo* study by Santel et al. (2006) could even show successful systemic delivery of liposomally formulated siRNAs to murine vascular endothelium, which rises hope for an sEH-targeting RNAi therapy.

In addition, some successful site-directed *in vivo* siRNA delivery methods do exist that might be relevant for a potential therapeutic sEH knockdown: the local injection of siRNAs into eyes (Reich et al., 2003; Kim et al., 2004a) as well as their intranasal administration for pulmonary delivery (Bitko et al., 2005) seem both promising and relatively easy to achieve. In preliminary experiments with New Zealand White rabbits, topical treatment of the eye with AUDA (12-(3-adamantane-1-yl-ureido)-dodecanoic acid; an sEH inhibitor) and / or EETs was observed to cause a decrease in the intraocular pressure. This suggests a potential role for sEH inhibition in glaucoma treatment, which could – in analogy to the first clinically tested siRNA (Whelan, 2005) – likely be fulfilled by sEH-targeting siRNAs for an extended period of time. However, this option would be more attractive if further

improvements in siRNA stability and delivery made it possible to administer siRNAs, possibly in combination with EETs, in eye drops. Another study in rats proved that tobacco smoke-induced inflammation in the lung can successfully be treated by an sEH inhibitor, even more so in the presence of EETs (Smith et al., 2005). This finding is likely to be useful for the treatment of chronic obstructive pulmonary disease (COPD). Most possibly, the same but potentially longer lasting effect could be achieved by intra-nasally administered siRNAs.

As mentioned before, promising results have been achieved by chemical inhibition of sEH toward kidney protection against hypertensive-caused damage (Zhao et al., 2004; Imig et al., 2005). In this case however, local siRNA delivery can currently not be considered as alternative treatment. The present successful delivery method for siRNAs to kidneys *in vivo* consists of injection into the renal artery followed by electroporation (Takabatake et al., 2005). Thus, it is only justifiable for scientific approaches in animal models or if no other therapy option exists.

### 2.5 Conclusion

In the present study, RNAi-mediated silencing of human sEH was investigated in order to provide an alternative approach to chemical inhibition of this new drug target. After selection of a cell model system and optimization of the siRNA delivery technique, sEH enzyme activity and expression level could be reduced reproducibly by 50% in the prostate cancer cell line 22RV1. However, this result represents a significantly smaller RNAi effect than expected from literature. Therefore, it will be necessary to investigate the cause of this experimental result, once RNAi is considered for the therapeutic down-regulation of sEH. Nevertheless, extensive literature studies enable the conclusion that this is the first report of a successful knockdown of sEH by RNAi and might turn out to be useful in the treatment of glaucoma, COPD and perhaps even hypertension. Future developments in bioavailability of sEH inhibitors, as well as siRNA stability and target-specific delivery will reveal the applicability and relevance of both therapy options to abolish sEH activity.

## REFERENCES

- Adams, J. D., Jr., H. Yagi, W. Levin and D. M. Jerina (1995). "Stereo-selectivity and regio-selectivity in the metabolism of 7,8-dihydrobenzo[a]pyrene by cytochrome P450, epoxide hydrolase and hepatic microsomes from 3-methylcholanthrene-treated rats." Chem Biol Interact 95(1-2): 57-77.
- Aigner, A. (2006). "Gene silencing through RNA interference (RNAi) in vivo: Strategies based on the direct application of siRNAs." J Biotechnol 124(1): 12-25.
- Akashi, H., S. Matsumoto and K. Taira (2005). "Gene discovery by ribozyme and siRNA libraries." Nat Rev Mol Cell Biol 6(5): 413-22.
- Allen, R. H. and W. B. Jacoby (1969). "Tartaric acid metabolism. Synthesis with tartate epoxidase." Biol Chem 244: 2078-2084.
- Alvarez-Garcia, I. and E. A. Miska (2005). "MicroRNA functions in animal development and human disease." Development 132(21): 4653-62.
- Amar, L., M. Desclaux, N. Faucon-Biguot, J. Mallet and R. Vogel (2006). "Control of small inhibitory RNA levels and RNA interference by doxycycline induced activation of a minimal RNA polymerase III promoter." Nucleic Acids Res 34(5): e37.
- Aoki, M., T. Ishii, M. Kanaoka and T. Kimura (2006). "RNA interference in immune cells by use of osmotic delivery of siRNA." Biochem Biophys Res Commun 341(2): 326-33.
- Araki, Y., S. Takahashi, T. Kobayashi, H. Kajiho, S. Hoshino and T. Katada (2001). "Ski7p G protein interacts with the exosome and the Ski complex for 3'-to-5' mRNA decay in yeast." EMBO J 20(17): 4684-93.
- Aramayo, R. and R. L. Metzenberg (1996). "Meiotic transvection in fungi." Cell 86(1): 103-13.
- Arand, M., D. F. Grant, J. K. Beetham, T. Friedberg, F. Oesch and B. D. Hammock (1994). "Sequence similarity of mammalian epoxide hydrolases to the bacterial haloalkane dehalogenase and other related proteins. Implication for the potential catalytic mechanism of enzymatic epoxide hydrolysis." FEBS Letters 338(3): 251-6.
- Arand, M., A. Cronin, F. Oesch, S. L. Mowbray and T. A. Jones (2003). "The telltale structures of epoxide hydrolases." Drug Metab Rev 35(4): 365-83.
- Arand, M., A. Cronin, M. Adamska and F. Oesch (2005). "Epoxide hydrolases: structure, function, mechanism, and assay." Methods Enzymol 400: 569-88.
- Aravin, A. A., N. M. Naumova, A. V. Tulin, V. V. Vagin, Y. M. Rozovsky and V. A. Gvozdev (2001). "Double-stranded RNA-mediated silencing of genomic tandem repeats and transposable elements in the *D. melanogaster* germline." Curr Biol 11(13): 1017-27.
- Archelas, A. and R. Furstoss (2001). "Synthetic applications of epoxide hydrolases." Curr Opin Chem Biol 5(2): 112-9.
- Argiriadi, M. A., C. Morisseau, B. D. Hammock and D. W. Christianson (1999). "Detoxification of environmental mutagens and carcinogens: structure, mechanism, and evolution of liver epoxide hydrolase." Proc Natl Acad Sci U S A 96(19): 10637-42.

- Argiriadi, M. A., C. Morisseau, M. H. Goodrow, D. L. Dowdy, B. D. Hammock and D. W. Christianson (2000). "Binding of alkylurea inhibitors to epoxide hydrolase implicates active site tyrosines in substrate activation." *J Biol Chem* 275(20): 15265-70.
- Astrom, A., M. Eriksson, L. C. Eriksson, W. Birberg, A. Pilotti and J. W. DePierre (1986). "Subcellular and organ distribution of cholesterol epoxide hydrolase in the rat." *Biochim Biophys Acta* 882(3): 359-66.
- Aufsatz, W., M. F. Mette, A. J. Matzke and M. Matzke (2004). "The role of MET1 in RNA-directed de novo and maintenance methylation of CG dinucleotides." *Plant Mol Biol* 54(6): 793-804.
- Aza-Blanc, P., C. L. Cooper, K. Wagner, S. Batalov, Q. L. Deveraux and M. P. Cooke (2003). "Identification of modulators of TRAIL-induced apoptosis via RNAi-based phenotypic screening." *Mol Cell* 12(3): 627-37.
- Bannister, A. J., P. Zegerman, J. F. Partridge, E. A. Miska, J. O. Thomas, R. C. Allshire and T. Kouzarides (2001). "Selective recognition of methylated lysine 9 on histone H3 by the HP1 chromo domain." *Nature* 410(6824): 120-4.
- Bartlett, D. W. and M. E. Davis (2006). "Insights into the kinetics of siRNA-mediated gene silencing from live-cell and live-animal bioluminescent imaging." *Nucleic Acids Res* 34(1): 322-33.
- Beetham, J. K., T. Tian and B. D. Hammock (1993). "cDNA cloning and expression of a soluble epoxide hydrolase from human liver." *Arch Biochem Biophys* 305(1): 197-201.
- Beetham, J. K., D. Grant, M. Arand, J. Garbarino, T. Kiyosue, F. Pinot, F. Oesch, W. R. Belknap, K. Shinozaki and B. D. Hammock (1995). "Gene evolution of epoxide hydrolases and recommended nomenclature." *DNA Cell Biol* 14(1): 61-71.
- Bellevik, S., J. Zhang and J. Meijer (2002). "Brassica napus soluble epoxide hydrolase (BNSEH1)." *Eur J Biochem* 269: 5295-302.
- Berns, K., E. M. Hijmans, J. Mullenders, T. R. Brummelkamp, A. Velds, M. Heimerikx, R. M. Kerkhoven, M. Madiredjo, W. Nijkamp, B. Weigelt, R. Agami, W. Ge, G. Cavet, P. S. Linsley, R. L. Beijersbergen and R. Bernards (2004). "A large-scale RNAi screen in human cells identifies new components of the p53 pathway." *Nature* 428(6981): 431-7.
- Bernstein, E., A. A. Caudy, S. M. Hammond and G. J. Hannon (2001). "Role for a bidentate ribonuclease in the initiation step of RNA interference." *Nature* 409(6818): 363-6.
- Birmingham, A., E. M. Anderson, A. Reynolds, D. Ilsley-Tyree, D. Leake, Y. Fedorov, S. Baskerville, E. Maksimova, K. Robinson, J. Karpilow, W. S. Marshall and A. Khvorova (2006). "3' UTR seed matches, but not overall identity, are associated with RNAi off-targets." *Nat Methods* 3(3): 199-204.
- Bitko, V., A. Musiyenko, O. Shulyayeva and S. Barik (2005). "Inhibition of respiratory viruses by nasally administered siRNA." *Nat Med* 11(1): 50-5.
- Blaszczuk, J., J. E. Tropea, M. Bubunencko, K. M. Routzahn, D. S. Waugh, D. L. Court and X. Ji (2001). "Crystallographic and modeling studies of RNase III suggest a mechanism for double-stranded RNA cleavage." *Structure* 9(12): 1225-36.
- Blaszczuk, J., J. Gan, J. E. Tropea, D. L. Court, D. S. Waugh and X. Ji (2004). "Noncatalytic assembly of ribonuclease III with double-stranded RNA." *Structure* 12(3): 457-66.

- Blee, E. and F. Schuber (1992). "Occurrence of fatty acid epoxide hydrolases in soybean (*Glycine max*). Purification and characterization of the soluble form." Biochem J 282 ( Pt 3): 711-4.
- Bohnsack, M. T., K. Czaplinski and D. Gorlich (2004). "Exportin 5 is a RanGTP-dependent dsRNA-binding protein that mediates nuclear export of pre-miRNAs." RNA 10(2): 185-91.
- Borhan, B., T. Mebrahtu, S. Nazarian, M. J. Kurth and B. D. Hammock (1995). "Improved radiolabeled substrates for soluble epoxide hydrolase." Anal Biochem 231(1): 188-200.
- Boutros, M., A. A. Kiger, S. Armknecht, K. Kerr, M. Hild, B. Koch, S. A. Haas, H. F. Consortium, R. Paro and N. Perrimon (2004). "Genome-wide RNAi analysis of growth and viability in *Drosophila* cells." Science 303(5659): 832-5.
- Brennecke, J., D. R. Hipfner, A. Stark, R. B. Russell and S. M. Cohen (2003). "bantam encodes a developmentally regulated microRNA that controls cell proliferation and regulates the proapoptotic gene *hid* in *Drosophila*." Cell 113(1): 25-36.
- Brennecke, J., A. Stark, R. B. Russell and S. M. Cohen (2005). "Principles of microRNA-target recognition." PLoS Biol 3(3): e85.
- Bridge, A. J., S. Pebernard, A. Ducraux, A. L. Nicoulaz and R. Iggo (2003). "Induction of an interferon response by RNAi vectors in mammalian cells." Nat Genet 34(3): 263-4.
- Brummelkamp, T. R., R. Bernards and R. Agami (2002a). "A system for stable expression of short interfering RNAs in mammalian cells." Science 296(5567): 550-3.
- Brummelkamp, T. R., R. Bernards and R. Agami (2002b). "Stable suppression of tumorigenicity by virus-mediated RNA interference." Cancer Cell 2(3): 243-7.
- Cai, X., C. H. Hagedorn and B. R. Cullen (2004). "Human microRNAs are processed from capped, polyadenylated transcripts that can also function as mRNAs." RNA 10(12): 1957-66.
- Campbell, W. B., D. Gebremedhin, P. F. Pratt and D. R. Harder (1996). "Identification of epoxyeicosatrienoic acids as endothelium-derived hyperpolarizing factors." Circ Res 78(3): 415-23.
- Campbell, W. B. (2000). "New role for epoxyeicosatrienoic acids as anti-inflammatory mediators." Trends Pharmacol Sci 21(4): 125-7.
- Cao, X., W. Aufsatz, D. Zilberman, M. F. Mette, M. S. Huang, M. Matzke and S. E. Jacobsen (2003). "Role of the DRM and CMT3 methyltransferases in RNA-directed DNA methylation." Curr Biol 13(24): 2212-7.
- Capdevila, J. H., J. R. Falck and R. C. Harris (2000). "Cytochrome P450 and arachidonic acid bioactivation. Molecular and functional properties of the arachidonate monooxygenase." J Lipid Res 41(2): 163-81.
- Caplen, N. J., S. Parrish, F. Imani, A. Fire and R. A. Morgan (2001). "Specific inhibition of gene expression by small double-stranded RNAs in invertebrate and vertebrate systems." Proc Natl Acad Sci U S A 98(17): 9742-7.
- Carmell, M. A., Z. Xuan, M. Q. Zhang and G. J. Hannon (2002). "The Argonaute family: tentacles that reach into RNAi, developmental control, stem cell maintenance, and tumorigenesis." Genes Dev 16(21): 2733-42.



- Carmell, M. A. and G. J. Hannon (2004). "RNase III enzymes and the initiation of gene silencing." Nat Struct Mol Biol 11(3): 214-8.
- Carpenter, A. E. and D. M. Sabatini (2004). "Systematic genome-wide screens of gene function." Nat Rev Genet 5(1): 11-22.
- Carroll, M. A. and J. C. McGiff (2000). "A new class of lipid mediators: cytochrome P450 arachidonate metabolites." Thorax 55 Suppl 2: S13-6.
- Catalanotto, C., G. Azzalin, G. Macino and C. Cogoni (2000). "Gene silencing in worms and fungi." Nature 404(6775): 245.
- Catella, F., J. A. Lawson, D. J. Fitzgerald and G. A. FitzGerald (1990). "Endogenous biosynthesis of arachidonic acid epoxides in humans: increased formation in pregnancy-induced hypertension." Proc Natl Acad Sci U S A 87(15): 5893-7.
- Caudy, A. A., M. Myers, G. J. Hannon and S. M. Hammond (2002). "Fragile X-related protein and VIG associate with the RNA interference machinery." Genes Dev 16(19): 2491-6.
- Caudy, A. A., R. F. Ketting, S. M. Hammond, A. M. Denli, A. M. Bathoorn, B. B. Tops, J. M. Silva, M. M. Myers, G. J. Hannon and R. H. Plasterk (2003). "A micrococcal nuclease homologue in RNAi effector complexes." Nature 425(6956): 411-4.
- Cerutti, H. and J. A. Casas-Mollano (2006). "On the origin and functions of RNA-mediated silencing: from protists to man." Curr Genet 50(2): 81-99.
- Cerutti, L., N. Mian and A. Bateman (2000). "Domains in gene silencing and cell differentiation proteins: the novel PAZ domain and redefinition of the Piwi domain." Trends Biochem Sci 25(10): 481-2.
- Chacos, N., J. H. Capdevila, J. R. Falck, S. Manna, C. Martin-Wixtrom, S. S. Gill, B. D. Hammock and R. W. Estabrook (1983). "The reaction of arachidonic acid epoxides (epoxyeicosatrienoic acids) with a cytosolic epoxide hydrolase." Arch Biochem Biophys 223: 639-648.
- Chatterjee-Kishore, M. and C. P. Miller (2005). "Exploring the sounds of silence: RNAi-mediated gene silencing for target identification and validation." Drug Discov Today 10(22): 1559-65.
- Chen, J. K., D. W. Wang, J. R. Falck, J. Capdevila and R. C. Harris (1999). "Transfection of an active cytochrome P450 arachidonic acid epoxygenase indicates that 14,15-epoxyeicosatrienoic acid functions as an intracellular second messenger in response to epidermal growth factor." J Biol Chem 274(8): 4764-9.
- Chendrimada, T. P., R. I. Gregory, E. Kumaraswamy, J. Norman, N. Cooch, K. Nishikura and R. Shiekhattar (2005). "TRBP recruits the Dicer complex to Ago2 for microRNA processing and gene silencing." Nature 436(7051): 740-4.
- Chicas, A., C. Cogoni and G. Macino (2004). "RNAi-dependent and RNAi-independent mechanisms contribute to the silencing of RIPed sequences in *Neurospora crassa*." Nucleic Acids Res 32(14): 4237-43.
- Choung, S., Y. J. Kim, S. Kim, H. O. Park and Y. C. Choi (2006). "Chemical modification of siRNAs to improve serum stability without loss of efficacy." Biochem Biophys Res Commun 342(3): 919-27.
- Collins, R. E. and X. Cheng (2005). "Structural domains in RNAi." FEBS Lett 579(26): 5841-9.

- Cougot, N., S. Babajko and B. Seraphin (2004). "Cytoplasmic foci are sites of mRNA decay in human cells." J Cell Biol 165(1): 31-40.
- Couzin, J. (2002). "Breakthrough of the year. Small RNAs make big splash." Science 298(5602): 2296-7.
- Cronin, A., S. Mowbray, H. Durk, S. Homburg, I. Fleming, B. Fisslthaler, F. Oesch and M. Arand (2003). "The N-terminal domain of mammalian soluble epoxide hydrolase is a phosphatase." Proc Natl Acad Sci U S A 100(4): 1552-7.
- Dande, P., T. P. Prakash, N. Sioufi, H. Gaus, R. Jarres, A. Berdeja, E. E. Swayze, R. H. Griffey and B. Bhat (2006). "Improving RNA interference in mammalian cells by 4'-thio-modified small interfering RNA (siRNA): effect on siRNA activity and nuclease stability when used in combination with 2'-O-alkyl modifications." J Med Chem 49(5): 1624-34.
- Davis, B. B., D. A. Thompson, L. L. Howard, C. Morisseau, B. D. Hammock and R. H. Weiss (2002). "Inhibitors of soluble epoxide hydrolase attenuate vascular smooth muscle cell proliferation." Proc Natl Acad Sci U S A 99(4): 2222-7.
- Davydov, I. V., D. Woods, Y. J. Safiran, P. Oberoi, H. O. Fearnhead, S. Fang, J. P. Jensen, A. M. Weissman, J. H. Kenten and K. H. Vousden (2004). "Assay for ubiquitin ligase activity: high-throughput screen for inhibitors of HDM2." J Biomol Screen 9(8): 695-703.
- de Carvalho, F., G. Gheysen, S. Kushnir, M. Van Montagu, D. Inze and C. Castresana (1992). "Suppression of beta-1,3-glucanase transgene expression in homozygous plants." EMBO J 11(7): 2595-602.
- de Vries, E. J. and D. B. Janssen (2003). "Biocatalytic conversion of epoxides." Curr Opin Biotechnol 14(4): 414-20.
- Denli, A. M., B. B. Tops, R. H. Plasterk, R. F. Ketting and G. J. Hannon (2004). "Processing of primary microRNAs by the Microprocessor complex." Nature 432(7014): 231-5.
- Dietze, E. C., J. Magdalou and B. D. Hammock (1990). "Human and murine cytosolic epoxide hydrolase: physical and structural properties." Int J Biochem 22(5): 461-70.
- Dietze, E. C., E. Kuwano and B. D. Hammock (1994). "Spectrophotometric substrates for cytosolic epoxide hydrolase." Anal Biochem 216(1): 176-87.
- Ding, H., D. S. Schwarz, A. Keene, B. Affar el, L. Fenton, X. Xia, Y. Shi, P. D. Zamore and Z. Xu (2003). "Selective silencing by RNAi of a dominant allele that causes amyotrophic lateral sclerosis." Aging Cell 2(4): 209-17.
- Doi, N., S. Zenno, R. Ueda, H. Ohki-Hamazaki, K. Ui-Tei and K. Saigo (2003). "Short-interfering-RNA-mediated gene silencing in mammalian cells requires Dicer and eIF2C translation initiation factors." Curr Biol 13(1): 41-6.
- Dorrance, A. M., N. Rupp, D. M. Pollock, J. W. Newman, B. D. Hammock and J. D. Imig (2005). "An epoxide hydrolase inhibitor, 12-(3-adamantan-1-yl-ureido)dodecanoic acid (AUDA), reduces ischemic cerebral infarct size in stroke-prone spontaneously hypertensive rats." J Cardiovasc Pharmacol 46(6): 842-8.
- Dowler, T., D. Bergeron, A. L. Tedeschi, L. Paquet, N. Ferrari and M. J. Damha (2006). "Improvements in siRNA properties mediated by 2'-deoxy-2'-fluoro-beta-D-arabinonucleic acid (FANA)." Nucleic Acids Res 34(6): 1669-75.

- Draper, A. J. and B. D. Hammock (1999). "Inhibition of soluble and microsomal epoxide hydrolase by zinc and other metals." Toxicol Sci 52(1): 26-32.
- Du, T. and P. D. Zamore (2005). "microPrimer: the biogenesis and function of microRNA." Development 132(21): 4645-52.
- Dudda, A., G. Spiteller and F. Kobelt (1996). "Lipid oxidation products in ischemic porcine heart tissue." Chem Phys Lipids 82(1): 39-51.
- Dykxhoorn, D. M., D. Palliser and J. Lieberman (2006). "The silent treatment: siRNAs as small molecule drugs." Gene Ther 13(6): 541-52.
- Elbashir, S. M., J. Harborth, W. Lendeckel, A. Yalcin, K. Weber and T. Tuschl (2001a). "Duplexes of 21-nucleotide RNAs mediate RNA interference in cultured mammalian cells." Nature 411(6836): 494-8.
- Elbashir, S. M., W. Lendeckel and T. Tuschl (2001b). "RNA interference is mediated by 21- and 22-nucleotide RNAs." Genes Dev 15(2): 188-200.
- Enayetallah, A. E., R. A. French, M. Barber and D. F. Grant (2006). "Cell-specific subcellular localization of soluble epoxide hydrolase in human tissues." J Histochem Cytochem 54(3): 329-35.
- Enayetallah, A. E. and D. F. Grant (2006). "Effects of human soluble epoxide hydrolase polymorphisms on isoprenoid phosphate hydrolysis." Biochem Biophys Res Commun 341(1): 254-60.
- Fagard, M., S. Boutet, J. B. Morel, C. Bellini and H. Vaucheret (2000). "AGO1, QDE-2, and RDE-1 are related proteins required for post-transcriptional gene silencing in plants, quelling in fungi, and RNA interference in animals." Proc Natl Acad Sci U S A 97(21): 11650-4.
- Fang, X., M. VanRollins, T. L. Kaduce and A. A. Spector (1995). "Epoxyeicosatrienoic acid metabolism in arterial smooth muscle cells." J Lipid Res 36(6): 1236-46.
- Fang, X., S. A. Moore, L. L. Stoll, G. Rich, T. L. Kaduce, N. L. Weintraub and A. A. Spector (1998). "14,15-Epoxyeicosatrienoic acid inhibits prostaglandin E2 production in vascular smooth muscle cells." Am J Physiol 275(6 Pt 2): H2113-21.
- Fang, X., N. L. Weintraub, L. L. Stoll and A. A. Spector (1999). "Epoxyeicosatrienoic acids increase intracellular calcium concentration in vascular smooth muscle cells." Hypertension 34(6): 1242-6.
- Fedorov, Y., E. M. Anderson, A. Birmingham, A. Reynolds, J. Karpilow, K. Robinson, D. Leake, W. S. Marshall and A. Khvorova (2006). "Off-target effects by siRNA can induce toxic phenotype." RNA 12(7): 1188-96.
- Finley, B. L. and B. D. Hammock (1988). "Increased cholesterol epoxide hydrolase activity in clofibrate-fed animals." Biochem Pharmacol 37(16): 3169-75.
- Fire, A., S. Xu, M. K. Montgomery, S. A. Kostas, S. E. Driver and C. C. Mello (1998). "Potent and specific genetic interference by double-stranded RNA in *Caenorhabditis elegans*." Nature 391(6669): 806-11.
- Fisslthaler, B., R. Popp, L. Kiss, M. Potente, D. R. Harder, I. Fleming and R. Busse (1999). "Cytochrome P450 2C is an EDHF synthase in coronary arteries." Nature 401(6752): 493-7.

- Fitzpatrick, F. A., M. D. Ennis, M. E. Baze, M. A. Wynalda, J. E. McGee and W. F. Liggett (1986). "Inhibition of cyclooxygenase activity and platelet aggregation by epoxyeicosatrienoic acids. Influence of stereochemistry." J Biol Chem 261(32): 15334-8.
- Fleming, I. (2001). "Cytochrome p450 and vascular homeostasis." Circ Res 89(9): 753-62.
- Fornage, M., E. Boerwinkle, P. A. Doris, D. Jacobs, K. Liu and N. D. Wong (2004). "Polymorphism of the soluble epoxide hydrolase is associated with coronary artery calcification in African-American subjects: The Coronary Artery Risk Development in Young Adults (CARDIA) study." Circulation 109(3): 335-9.
- Fornage, M., C. R. Lee, P. A. Doris, M. S. Bray, G. Heiss, D. C. Zeldin and E. Boerwinkle (2005). "The soluble epoxide hydrolase gene harbors sequence variation associated with susceptibility to and protection from incident ischemic stroke." Hum Mol Genet 14(19): 2829-37.
- Freitag, M., D. W. Lee, G. O. Kothe, R. J. Pratt, R. Aramayo and E. U. Selker (2004). "DNA methylation is independent of RNA interference in *Neurospora*." Science 304(5679): 1939.
- Fretland, A. J. and C. J. Omiecinski (2000). "Epoxide hydrolases: biochemistry and molecular biology." Chem Biol Interact 129(1-2): 41-59.
- Fu, J. Y., J. Haeggstrom, P. Collins, J. Meijer and O. Radmark (1989). "Leukotriene A4 hydrolase: analysis of some human tissues by radioimmunoassay." Biochim Biophys Acta 1006(1): 121-6.
- Fukagawa, T., M. Nogami, M. Yoshikawa, M. Ikeno, T. Okazaki, Y. Takami, T. Nakayama and M. Oshimura (2004). "Dicer is essential for formation of the heterochromatin structure in vertebrate cells." Nat Cell Biol 6(8): 784-91.
- Fukushima, A., M. Hayakawa, S. Sugiyama, M. Ajioka, T. Ito, T. Satake and T. Ozawa (1988). "Cardiovascular effects of leukotoxin (9, 10-epoxy-12-octadecenoate) and free fatty acids in dogs." Cardiovasc Res 22(3): 213-8.
- Gaetke, L. M., C. J. McClain, R. T. Talwalkar and S. I. Shedlofsky (1997). "Effects of endotoxin on zinc metabolism in human volunteers." Am J Physiol 272(6 Pt 1): E952-6.
- Gill, S. S. (1983). "Purification of mouse liver cytosolic epoxide hydrolase." Biochem Biophys Res Commun 112(2): 763-9.
- Goll, M. G. and T. H. Bestor (2005). "Eukaryotic cytosine methyltransferases." Annu Rev Biochem 74: 481-514.
- Golzio, M., L. Mazzolini, P. Moller, M. P. Rols and J. Teissie (2005). "Inhibition of gene expression in mice muscle by in vivo electrically mediated siRNA delivery." Gene Ther 12(3): 246-51.
- Gomez, G. A., C. Morisseau, B. D. Hammock and D. W. Christianson (2004). "Structure of human epoxide hydrolase reveals mechanistic inferences on bifunctional catalysis in epoxide and phosphate ester hydrolysis." Biochemistry 43(16): 4716-23.
- Gomez, G. A., C. Morisseau, B. D. Hammock and D. W. Christianson (2006). "Human soluble epoxide hydrolase: structural basis of inhibition by 4-(3-cyclohexylureido)-carboxylic acids." Protein Sci 15(1): 58-64.
- Gonzalez-Alegre, P., V. M. Miller, B. L. Davidson and H. L. Paulson (2003). "Toward therapy for DYT1 dystonia: allele-specific silencing of mutant TorsinA." Ann Neurol 53(6): 781-7.

- Graier, W. F., S. Simecek and M. Sturek (1995). "Cytochrome P450 mono-oxygenase-regulated signalling of Ca<sup>2+</sup> entry in human and bovine endothelial cells." J Physiol 482 ( Pt 2): 259-74.
- Grant, D. F., D. H. Storms and B. D. Hammock (1993). "Molecular cloning and expression of murine liver soluble epoxide hydrolase." J Biol Chem 268(23): 17628-33.
- Grant, D. F., D. E. Moody, J. K. Beetham, D. H. Storms, M. Moghaddam, B. Borhan, F. Pinot, B. S. Winder and B. D. Hammock (1994). The response of soluble epoxide hydrolase and other hydrolytic enzymes to peroxisome proliferators. Peroxisome proliferators: unique inducers of drug-metabolizing enzymes. D. E. Moody. Boca Raton, FL, CRC Press, Inc.: 97-112.
- Gregory, R. I., K. P. Yan, G. Amuthan, T. Chendrimada, B. Doratotaj, N. Cooch and R. Shiekhattar (2004). "The Microprocessor complex mediates the genesis of microRNAs." Nature 432(7014): 235-40.
- Grishok, A., H. Tabara and C. C. Mello (2000). "Genetic requirements for inheritance of RNAi in *C. elegans*." Science 287(5462): 2494-7.
- Grishok, A., A. E. Pasquinelli, D. Conte, N. Li, S. Parrish, I. Ha, D. L. Baillie, A. Fire, G. Ruvkun and C. C. Mello (2001). "Genes and mechanisms related to RNA interference regulate expression of the small temporal RNAs that control *C. elegans* developmental timing." Cell 106(1): 23-34.
- Grishok, A. and C. C. Mello (2002). "RNAi (Nematodes: *Caenorhabditis elegans*)." Adv Genet 46: 339-60.
- Guengerich, F. P. (1982). "Epoxide hydrolase: properties and metabolic roles." Rev Biochem Toxicol 4: 5-30.
- Guo, A., J. Durner and D. F. Klessig (1998). "Characterization of a tobacco epoxide hydrolase gene induced during the resistance response of TMV." Plant J 15: 647-56.
- Haeggstrom, J. Z., A. Wetterholm, J. F. Medina and B. Samuelsson (1994). "Novel structural and functional properties of leukotriene A<sub>4</sub> hydrolase. Implications for the development of enzyme inhibitors." Adv Prostaglandin Thromboxane Leukot Res 22: 3-12.
- Hagerkvist, R., D. Mokhtari, J. W. Myers, A. Tengholm and N. Welsh (2005). "siRNA produced by recombinant dicer mediates efficient gene silencing in islet cells." Ann N Y Acad Sci 1040: 114-22.
- Hagstrom, J. E., J. Hegge, G. Zhang, M. Noble, V. Budker, D. L. Lewis, H. Herweijer and J. A. Wolff (2004). "A facile nonviral method for delivering genes and siRNAs to skeletal muscle of mammalian limbs." Mol Ther 10(2): 386-98.
- Halarnkar, P. P., R. N. Wixtrom, M. H. Silva and B. D. Hammock (1989). "Catabolism of epoxy fatty esters by the purified epoxide hydrolase from mouse and human liver." Arch Biochem Biophys 272(1): 226-36.
- Halarnkar, P. P. and D. A. Schooley (1990). "Reversed-phase liquid chromatographic separation of juvenile hormone and its metabolites, and its application for an in vivo juvenile hormone catabolism study in *Manduca sexta*." Anal Biochem 188(2): 394-7.
- Hall, A. H., J. Wan, A. Spesock, Z. Sergueeva, B. R. Shaw and K. A. Alexander (2006). "High potency silencing by single-stranded boranophosphate siRNA." Nucleic Acids Res 34(9): 2773-81.

- Hamar, P., E. Song, G. Kokeny, A. Chen, N. Ouyang and J. Lieberman (2004). "Small interfering RNA targeting Fas protects mice against renal ischemia-reperfusion injury." Proc Natl Acad Sci U S A 101(41): 14883-8.
- Hamilton, A. J. and D. C. Baulcombe (1999). "A species of small antisense RNA in posttranscriptional gene silencing in plants." Science 286(5441): 950-2.
- Hammock, B. D., D. E. Moody and A. Sevanian (1985). "Epoxide hydrolases in the catabolism of sterols and isoprenoids." Methods Enzymol 111: 303-11.
- Hammock, B. D., F. Pinot, J. K. Beetham, D. F. Grant, M. E. Arand and F. Oesch (1994). "Isolation of a putative hydroxyacyl enzyme intermediate of an epoxide hydrolase." Biochem Biophys Res Commun 198(3): 850-6.
- Hammock, B. D., D. H. Storms and D. F. Grant (1997). Epoxide hydrolases. Comprehensive toxicology. F. P. Guengerich. Oxford, Pergamon. 3 Biotransformation: 283-305.
- Hammond, S. M., E. Bernstein, D. Beach and G. J. Hannon (2000). "An RNA-directed nuclease mediates post-transcriptional gene silencing in Drosophila cells." Nature 404(6775): 293-6.
- Hammond, S. M., S. Boettcher, A. A. Caudy, R. Kobayashi and G. J. Hannon (2001). "Argonaute2, a link between genetic and biochemical analyses of RNAi." Science 293(5532): 1146-50.
- Hammond, S. M. (2005). "Dicing and slicing: the core machinery of the RNA interference pathway." FEBS Lett 579(26): 5822-9.
- Han, J., Y. Lee, K. H. Yeom, Y. K. Kim, H. Jin and V. N. Kim (2004). "The Drosha-DGCR8 complex in primary microRNA processing." Genes Dev 18(24): 3016-27.
- Harder, D. R., W. B. Campbell and R. J. Roman (1995). "Role of cytochrome P-450 enzymes and metabolites of arachidonic acid in the control of vascular tone." J Vasc Res 32(2): 79-92.
- He, L., J. M. Thomson, M. T. Hemann, E. Hernando-Monge, D. Mu, S. Goodson, S. Powers, C. Cordon-Cardo, S. W. Lowe, G. J. Hannon and S. M. Hammond (2005). "A microRNA polycistron as a potential human oncogene." Nature 435(7043): 828-33.
- Hemann, M. T., J. S. Fridman, J. T. Zilfou, E. Hernando, P. J. Paddison, C. Cordon-Cardo, G. J. Hannon and S. W. Lowe (2003). "An epi-allelic series of p53 hypomorphs created by stable RNAi produces distinct tumor phenotypes in vivo." Nat Genet 33(3): 396-400.
- Hennig, W. (1999). "Heterochromatin." Chromosoma 108(1): 1-9.
- Heymann, E. and W. Junge (1979). "Characterization of the isoenzymes of pig-liver esterase. 1. Chemical Studies." Eur J Biochem 95(3): 509-18.
- Hirt, D. L., J. Capdevila, J. R. Falck, M. D. Breyer and H. R. Jacobson (1989). "Cytochrome P450 metabolites of arachidonic acid are potent inhibitors of vasopressin action on rabbit cortical collecting duct." J Clin Invest 84(6): 1805-12.
- Hoelters, J., M. Ciccarella, M. Drechsel, C. Geissler, H. Gulkan, W. Bocker, M. Schieker, M. Jochum and P. Neth (2005). "Nonviral genetic modification mediates effective transgene expression and functional RNA interference in human mesenchymal stem cells." J Gene Med 7(6): 718-28.
- Holmquist, M. (2000). "Alpha/Beta-hydrolase fold enzymes: structures, functions and mechanisms." Curr Protein Pept Sci 1(2): 209-35.

- Hornung, V., M. Guenther-Biller, C. Bourquin, A. Ablasser, M. Schlee, S. Uematsu, A. Noronha, M. Manoharan, S. Akira, A. de Fougerolles, S. Endres and G. Hartmann (2005). "Sequence-specific potent induction of IFN- $\alpha$  by short interfering RNA in plasmacytoid dendritic cells through TLR7." Nat Med 11(3): 263-70.
- Hsieh, A. C., R. Bo, J. Manola, F. Vazquez, O. Bare, A. Khvorova, S. Scaringe and W. R. Sellers (2004). "A library of siRNA duplexes targeting the phosphoinositide 3-kinase pathway: determinants of gene silencing for use in cell-based screens." Nucleic Acids Res 32(3): 893-901.
- Huang, H., C. D. Fleming, K. Nishi, M. R. Redinbo and B. D. Hammock (2005a). "Stereoselective hydrolysis of pyrethroid-like fluorescent substrates by human and other mammalian liver carboxylesterases." Chem Res Toxicol 18(9): 1371-7.
- Huang, H., J. E. Stok, D. W. Stoutamire, S. J. Gee and B. D. Hammock (2005b). "Development of optically pure pyrethroid-like fluorescent substrates for carboxylesterases." Chem Res Toxicol 18(3): 516-27.
- Huang, H., K. Nishi, S. J. Gee and B. D. Hammock (2006). "Evaluation of chiral alpha-cyanoesters as general fluorescent substrates for screening enantioselective esterases." J Agric Food Chem 54(3): 694-9.
- Hunter, C., H. Sun and R. S. Poethig (2003). "The Arabidopsis heterochronic gene ZIPPY is an ARGONAUTE family member." Curr Biol 13(19): 1734-9.
- Hutvagner, G., J. McLachlan, A. E. Pasquinelli, E. Balint, T. Tuschl and P. D. Zamore (2001). "A cellular function for the RNA-interference enzyme Dicer in the maturation of the let-7 small temporal RNA." Science 293(5531): 834-8.
- Ikeda, R., K. Yoshida, S. Tsukahara, Y. Sakamoto, H. Tanaka, K. Furukawa and I. Inoue (2005). "The promyelotic leukemia zinc finger promotes osteoblastic differentiation of human mesenchymal stem cells as an upstream regulator of CBFA1." J Biol Chem 280(9): 8523-30.
- Imig, J. D., A. P. Zou, D. E. Stec, D. R. Harder, J. R. Falck and R. J. Roman (1996). "Formation and actions of 20-hydroxyeicosatetraenoic acid in rat renal arterioles." Am J Physiol 270(1 Pt 2): R217-27.
- Imig, J. D., X. Zhao, J. H. Capdevila, C. Morisseau and B. D. Hammock (2002). "Soluble epoxide hydrolase inhibition lowers arterial blood pressure in angiotensin II hypertension." Hypertension 39(2 Pt 2): 690-4.
- Imig, J. D., X. Zhao, C. Z. Zaharis, J. J. Olearczyk, D. M. Pollock, J. W. Newman, I. H. Kim, T. Watanabe and B. D. Hammock (2005). "An orally active epoxide hydrolase inhibitor lowers blood pressure and provides renal protection in salt-sensitive hypertension." Hypertension 46(4): 975-81.
- Ingelfinger, D., D. J. Arndt-Jovin, R. Luhrmann and T. Achsel (2002). "The human LSm1-7 proteins colocalize with the mRNA-degrading enzymes Dcp1/2 and Xrn1 in distinct cytoplasmic foci." RNA 8(12): 1489-501.
- Ishizaki, T., K. Shigemori, T. Nakai, S. Miyabo, M. Hayakawa, T. Ozawa, N. F. Voelkel and S. W. Chang (1995a). "Endothelin-1 potentiates leukotoxin-induced edematous lung injury." J Appl Physiol 79(4): 1106-11.

- Ishizaki, T., K. Shigemori, T. Nakai, S. Miyabo, T. Ozawa, S. W. Chang and N. F. Voelkel (1995b). "Leukotoxin, 9,10-epoxy-12-octadecenoate causes edematous lung injury via activation of vascular nitric oxide synthase." Am J Physiol 269(1 Pt 1): L65-70.
- Ishizuka, A., M. C. Siomi and H. Siomi (2002). "A Drosophila fragile X protein interacts with components of RNAi and ribosomal proteins." Genes Dev 16(19): 2497-508.
- Ito, M., K. Kawano, M. Miyagishi and K. Taira (2005). "Genome-wide application of RNAi to the discovery of potential drug targets." FEBS Lett 579(26): 5988-95.
- Jackson, A. L., S. R. Bartz, J. Schelter, S. V. Kobayashi, J. Burchard, M. Mao, B. Li, G. Cavet and P. S. Linsley (2003). "Expression profiling reveals off-target gene regulation by RNAi." Nat Biotechnol 21(6): 635-7.
- Jackson, A. L., J. Burchard, D. Leake, A. Reynolds, J. Schelter, J. Guo, J. M. Johnson, L. Lim, J. Karpilow, K. Nichols, W. Marshall, A. Khvorova and P. S. Linsley (2006). "Position-specific chemical modification of siRNAs reduces "off-target" transcript silencing." RNA 12(7): 1197-205.
- Jacobs, M. H., A. J. Van den Wijngaard, M. Pentenga and D. B. Janssen (1991). "Characterization of the epoxide hydrolase from an epichlorohydrin-degrading Pseudomonas sp." Eur J Biochem 202(3): 1217-22.
- Jensen, S., M. P. Gassama and T. Heidmann (1999). "Taming of transposable elements by homology-dependent gene silencing." Nat Genet 21(2): 209-12.
- Jia, S., K. Noma and S. I. Grewal (2004). "RNAi-independent heterochromatin nucleation by the stress-activated ATF/CREB family proteins." Science 304(5679): 1971-6.
- Jin, P., D. C. Zarnescu, S. Ceman, M. Nakamoto, J. Mowrey, T. A. Jongens, D. L. Nelson, K. Moses and S. T. Warren (2004). "Biochemical and genetic interaction between the fragile X mental retardation protein and the microRNA pathway." Nat Neurosci 7(2): 113-7.
- Johansson, C., A. Stark, M. Sandberg, B. Ek, L. Rask and J. Meijer (1995). "Tissue specific basal expression of soluble murine epoxide hydrolase and effects of clofibrate on the mRNA levels in extrahepatic tissues and liver." Arch Toxicol 70(1): 61-3.
- Jones, P. D., N. M. Wolf, C. Morisseau, P. Whetstone, B. Hock and B. D. Hammock (2005). "Fluorescent substrates for soluble epoxide hydrolase and application to inhibition studies." Anal Biochem 343(1): 66-75.
- Judge, A. D., V. Sood, J. R. Shaw, D. Fang, K. McClintock and I. MacLachlan (2005). "Sequence-dependent stimulation of the mammalian innate immune response by synthetic siRNA." Nat Biotechnol 23(4): 457-62.
- Kanellopoulou, C., S. A. Muljo, A. L. Kung, S. Ganesan, R. Drapkin, T. Jenuwein, D. M. Livingston and K. Rajewsky (2005). "Dicer-deficient mouse embryonic stem cells are defective in differentiation and centromeric silencing." Genes Dev 19(4): 489-501.
- Kang, K. D., P. D. Jones, H. Huang, R. Zhang, L. A. Mostovich, C. E. Wheelock, T. Watanabe, L. F. Gulyaeva and B. D. Hammock (2005). "Evaluation of alpha-cyano ethers as fluorescent substrates for assay of cytochrome P450 enzyme activity." Anal Biochem 344(2): 183-92.
- Kao, S. C., A. M. Krichevsky, K. S. Kosik and L. H. Tsai (2004). "BACE1 suppression by RNA interference in primary cortical neurons." J Biol Chem 279(3): 1942-9.



- Kariko, K., P. Bhuyan, J. Capodici and D. Weissman (2004). "Small interfering RNAs mediate sequence-independent gene suppression and induce immune activation by signaling through toll-like receptor 3." *J Immunol* 172(11): 6545-9.
- Kassis, J. A. (1994). "Unusual properties of regulatory DNA from the *Drosophila* engrailed gene: three "pairing-sensitive" sites within a 1.6-kb region." *Genetics* 136(3): 1025-38.
- Kawasaki, H. and K. Taira (2004). "Induction of DNA methylation and gene silencing by short interfering RNAs in human cells." *Nature* 431(7005): 211-7.
- Keck, J. L., E. R. Goedken and S. Marqusee (1998). "Activation/attenuation model for RNase H. A one-metal mechanism with second-metal inhibition." *J Biol Chem* 273(51): 34128-33.
- Kennerdell, J. R. and R. W. Carthew (1998). "Use of dsRNA-mediated genetic interference to demonstrate that frizzled and frizzled 2 act in the wingless pathway." *Cell* 95(7): 1017-26.
- Ketting, R. F., T. H. Haverkamp, H. G. van Luenen and R. H. Plasterk (1999). "Mut-7 of *C. elegans*, required for transposon silencing and RNA interference, is a homolog of Werner syndrome helicase and RNaseD." *Cell* 99(2): 133-41.
- Ketting, R. F. and R. H. Plasterk (2000). "A genetic link between co-suppression and RNA interference in *C. elegans*." *Nature* 404(6775): 296-8.
- Khvorovva, A., A. Reynolds and S. D. Jayasena (2003). "Functional siRNAs and miRNAs exhibit strand bias." *Cell* 115(2): 209-16.
- Kidner, C. A. and R. A. Martienssen (2005). "The developmental role of microRNA in plants." *Curr Opin Plant Biol* 8(1): 38-44.
- Kim, B., Q. Tang, P. S. Biswas, J. Xu, R. M. Schiffelers, F. Y. Xie, A. M. Ansari, P. V. Scaria, M. C. Woodle, P. Lu and B. T. Rouse (2004a). "Inhibition of ocular angiogenesis by siRNA targeting vascular endothelial growth factor pathway genes: therapeutic strategy for herpetic stromal keratitis." *Am J Pathol* 165(6): 2177-85.
- Kim, D. H., M. Longo, Y. Han, P. Lundberg, E. Cantin and J. J. Rossi (2004b). "Interferon induction by siRNAs and ssRNAs synthesized by phage polymerase." *Nat Biotechnol* 22(3): 321-5.
- Kim, D. H., M. A. Behlke, S. D. Rose, M. S. Chang, S. Choi and J. J. Rossi (2005a). "Synthetic dsRNA Dicer substrates enhance RNAi potency and efficacy." *Nat Biotechnol* 23(2): 222-6.
- Kim, I. H., C. Morisseau, T. Watanabe and B. D. Hammock (2004c). "Design, synthesis, and biological activity of 1,3-disubstituted ureas as potent inhibitors of the soluble epoxide hydrolase of increased water solubility." *J Med Chem* 47(8): 2110-22.
- Kim, I. H., F. R. Heitzler, C. Morisseau, K. Nishi, H. J. Tsai and B. D. Hammock (2005b). "Optimization of amide-based inhibitors of soluble epoxide hydrolase with improved water solubility." *J Med Chem* 48(10): 3621-9.
- Kishida, T., H. Asada, S. Gojo, S. Ohashi, M. Shin-Ya, K. Yasutomi, R. Terauchi, K. A. Takahashi, T. Kubo, J. Imanishi and O. Mazda (2004). "Sequence-specific gene silencing in murine muscle induced by electroporation-mediated transfer of short interfering RNA." *J Gene Med* 6(1): 105-10.
- Kiyosue, T., J. K. Beetham, F. Pinot, B. D. Hammock, K. Yamaguchi-Shinozaki and K. Shinozaki (1994). "Characterization of an *Arabidopsis* cDNA for a soluble epoxide hydrolase gene that is inducible by auxin and water stress." *Plant J* 6(2): 259-69.

- Knehr, M., H. Thomas, M. Arand, T. Gebel, H. D. Zeller and F. Oesch (1993). "Isolation and characterization of a cDNA encoding rat liver cytosolic epoxide hydrolase and its functional expression in *Escherichia coli*." J Biol Chem 268(23): 17623-7.
- Kolb, F. A., H. Zhang, K. Jaronczyk, N. Tahbaz, T. C. Hobman and W. Filipowicz (2005). "Human dicer: purification, properties, and interaction with PAZ PIWI domain proteins." Methods Enzymol 392: 316-36.
- Kraynack, B. A. and B. F. Baker (2006). "Small interfering RNAs containing full 2'-O-methylribonucleotide-modified sense strands display Argonaute2/eIF2C2-dependent activity." RNA 12(1): 163-76.
- Krick, S., B. G. Eul, J. Hanze, R. Savai, F. Grimminger, W. Seeger and F. Rose (2005). "Role of hypoxia-inducible factor-1alpha in hypoxia-induced apoptosis of primary alveolar epithelial type II cells." Am J Respir Cell Mol Biol 32(5): 395-403.
- Kroetz, D. L. and D. C. Zeldin (2002). "Cytochrome P450 pathways of arachidonic acid metabolism." Curr Opin Lipidol 13(3): 273-83.
- Lachner, M., D. O'Carroll, S. Rea, K. Mechtler and T. Jenuwein (2001). "Methylation of histone H3 lysine 9 creates a binding site for HP1 proteins." Nature 410(6824): 116-20.
- Lai, E. C., B. Tam and G. M. Rubin (2005). "Pervasive regulation of *Drosophila* Notch target genes by GY-box-, Brd-box-, and K-box-class microRNAs." Genes Dev 19(9): 1067-80.
- Landthaler, M., A. Yalcin and T. Tuschl (2004). "The human DiGeorge syndrome critical region gene 8 and Its D. melanogaster homolog are required for miRNA biogenesis." Curr Biol 14(23): 2162-7.
- Larsen, B. T., H. Miura, O. A. Hatoum, W. B. Campbell, B. D. Hammock, D. C. Zeldin, J. R. Falck and D. D. Gutterman (2006). "Epoxyeicosatrienoic and dihydroxyeicosatrienoic acids dilate human coronary arterioles via BK(Ca) channels: implications for soluble epoxide hydrolase inhibition." Am J Physiol Heart Circ Physiol 290(2): H491-9.
- Larsson, C., I. White, C. Johansson, A. Stark and J. Meijer (1995). "Localization of the human soluble epoxide hydrolase gene (EPHX2) to chromosomal region 8p21-p12." Hum Genet 95(3): 356-8.
- Lassus, P., X. Opitz-Araya and Y. Lazebnik (2002). "Requirement for caspase-2 in stress-induced apoptosis before mitochondrial permeabilization." Science 297(5585): 1352-4.
- Lee, C. R., K. E. North, M. S. Bray, M. Fornage, J. M. Seubert, J. W. Newman, B. D. Hammock, D. J. Couper, G. Heiss and D. C. Zeldin (2006a). "Genetic variation in soluble epoxide hydrolase (EPHX2) and risk of coronary heart disease: The Atherosclerosis Risk in Communities (ARIC) study." Hum Mol Genet 15(10): 1640-9.
- Lee, D. W., R. J. Pratt, M. McLaughlin and R. Aramayo (2003a). "An argonaute-like protein is required for meiotic silencing." Genetics 164(2): 821-8.
- Lee, H. C., T. Lu, N. L. Weintraub, M. VanRollins, A. A. Spector and E. F. Shibata (1999). "Effects of epoxyeicosatrienoic acids on the cardiac sodium channels in isolated rat ventricular myocytes." J Physiol 519 Pt 1: 153-68.
- Lee, Y., K. Jeon, J. T. Lee, S. Kim and V. N. Kim (2002). "MicroRNA maturation: stepwise processing and subcellular localization." Embo J 21(17): 4663-70.

- Lee, Y., C. Ahn, J. Han, H. Choi, J. Kim, J. Yim, J. Lee, P. Provost, O. Radmark, S. Kim and V. N. Kim (2003b). "The nuclear RNase III Drosha initiates microRNA processing." *Nature* 425(6956): 415-9.
- Lee, Y., M. Kim, J. Han, K. H. Yeom, S. Lee, S. H. Baek and V. N. Kim (2004a). "MicroRNA genes are transcribed by RNA polymerase II." *EMBO J* 23(20): 4051-60.
- Lee, Y., I. Hur, S. Y. Park, Y. K. Kim, M. R. Suh and V. N. Kim (2006b). "The role of PACT in the RNA silencing pathway." *EMBO J* 25(3): 522-32.
- Lee, Y. S., K. Nakahara, J. W. Pham, K. Kim, Z. He, E. J. Sontheimer and R. W. Carthew (2004b). "Distinct roles for Drosophila Dicer-1 and Dicer-2 in the siRNA/miRNA silencing pathways." *Cell* 117(1): 69-81.
- Lette, G., E. A. Kritikou, M. Jaeggi, A. Calixto, A. G. Fraser, R. S. Kamath, J. Ahringer and M. O. Hengartner (2004). "Genome-wide RNAi identifies p53-dependent and -independent regulators of germ cell apoptosis in *C. elegans*." *Cell Death Differ* 11(11): 1198-203.
- Leuschner, P. J., S. L. Ameres, S. Kueng and J. Martinez (2006). "Cleavage of the siRNA passenger strand during RISC assembly in human cells." *EMBO Rep* 7(3): 314-20.
- Lewis, B. P., I. H. Shih, M. W. Jones-Rhoades, D. P. Bartel and C. B. Burge (2003). "Prediction of mammalian microRNA targets." *Cell* 115(7): 787-98.
- Lewis, B. P., C. B. Burge and D. P. Bartel (2005). "Conserved seed pairing, often flanked by adenosines, indicates that thousands of human genes are microRNA targets." *Cell* 120(1): 15-20.
- Lewis, D. L., J. E. Hagstrom, A. G. Loomis, J. A. Wolff and H. Herweijer (2002). "Efficient delivery of siRNA for inhibition of gene expression in postnatal mice." *Nat Genet* 32(1): 107-8.
- Lingel, A., B. Simon, E. Izaurralde and M. Sattler (2003). "Structure and nucleic-acid binding of the Drosophila Argonaute 2 PAZ domain." *Nature* 426(6965): 465-9.
- Lingel, A., B. Simon, E. Izaurralde and M. Sattler (2004). "Nucleic acid 3'-end recognition by the Argonaute2 PAZ domain." *Nat Struct Mol Biol* 11(6): 576-7.
- Lipinski, C. A., F. Lombardo, B. W. Dominy and P. J. Feeney (2001). "Experimental and computational approaches to estimate solubility and permeability in drug discovery and development settings." *Adv Drug Deliv Rev* 46(1-3): 3-26.
- Lippman, Z., A. V. Gendrel, M. Black, M. W. Vaughn, N. Dedhia, W. R. McCombie, K. Lavine, V. Mittal, B. May, K. D. Kasschau, J. C. Carrington, R. W. Doerge, V. Colot and R. Martienssen (2004). "Role of transposable elements in heterochromatin and epigenetic control." *Nature* 430(6998): 471-6.
- Liu, J., M. A. Carmell, F. V. Rivas, C. G. Marsden, J. M. Thomson, J. J. Song, S. M. Hammond, L. Joshua-Tor and G. J. Hannon (2004). "Argonaute2 is the catalytic engine of mammalian RNAi." *Science* 305(5689): 1437-41.
- Liu, J., M. A. Valencia-Sanchez, G. J. Hannon and R. Parker (2005a). "MicroRNA-dependent localization of targeted mRNAs to mammalian P-bodies." *Nat Cell Biol* 7(7): 719-23.

- Liu, Y., Y. Zhang, K. Schmelzer, T. S. Lee, X. Fang, Y. Zhu, A. A. Spector, S. Gill, C. Morisseau, B. D. Hammock and J. Y. Shyy (2005b). "The antiinflammatory effect of laminar flow: the role of PPARgamma, epoxyeicosatrienoic acids, and soluble epoxide hydrolase." Proc Natl Acad Sci U S A 102(46): 16747-52.
- Lois, C., E. J. Hong, S. Pease, E. J. Brown and D. Baltimore (2002). "Germline transmission and tissue-specific expression of transgenes delivered by lentiviral vectors." Science 295(5556): 868-72.
- Lorenz, C., P. Hadwiger, M. John, H. P. Vornlocher and C. Unverzagt (2004). "Steroid and lipid conjugates of siRNAs to enhance cellular uptake and gene silencing in liver cells." Bioorg Med Chem Lett 14(19): 4975-7.
- Lu, A. Y. and G. T. Miwa (1980). "Molecular properties and biological functions of microsomal epoxide hydrase." Annu Rev Pharmacol Toxicol 20: 513-31.
- Lu, J., G. Getz, E. A. Miska, E. Alvarez-Saavedra, J. Lamb, D. Peck, A. Sweet-Cordero, B. L. Ebert, R. H. Mak, A. A. Ferrando, J. R. Downing, T. Jacks, H. R. Horvitz and T. R. Golub (2005). "MicroRNA expression profiles classify human cancers." Nature 435(7043): 834-8.
- Lu, T., T. Hoshi, N. L. Weintraub, A. A. Spector and H. C. Lee (2001a). "Activation of ATP-sensitive K(+) channels by epoxyeicosatrienoic acids in rat cardiac ventricular myocytes." J Physiol 537(Pt 3): 811-27.
- Lu, T., P. V. Katakam, M. VanRollins, N. L. Weintraub, A. A. Spector and H. C. Lee (2001b). "Dihydroxyeicosatrienoic acids are potent activators of Ca(2+)-activated K(+) channels in isolated rat coronary arterial myocytes." J Physiol 534(Pt 3): 651-67.
- Lund, E., S. Guttinger, A. Calado, J. E. Dahlberg and U. Kutay (2004). "Nuclear export of microRNA precursors." Science 303(5654): 95-8.
- Ma, J. B., K. Ye and D. J. Patel (2004). "Structural basis for overhang-specific small interfering RNA recognition by the PAZ domain." Nature 429(6989): 318-22.
- Ma, J. B., Y. R. Yuan, G. Meister, Y. Pei, T. Tuschl and D. J. Patel (2005a). "Structural basis for 5'-end-specific recognition of guide RNA by the A. fulgidus Piwi protein." Nature 434(7033): 666-70.
- Ma, Z., J. Li, F. He, A. Wilson, B. Pitt and S. Li (2005b). "Cationic lipids enhance siRNA-mediated interferon response in mice." Biochem Biophys Res Commun 330(3): 755-9.
- Macrae, I. J., K. Zhou, F. Li, A. Repic, A. N. Brooks, W. Z. Cande, P. D. Adams and J. A. Doudna (2006). "Structural basis for double-stranded RNA processing by Dicer." Science 311(5758): 195-8.
- Magdalou, J. and B. D. Hammock (1988). "1,2-Epoxycycloalkanes: substrates and inhibitors of microsomal and cytosolic epoxide hydrolases in mouse liver." Biochem Pharmacol 37(14): 2717-22.
- Mancini, J. A. and J. F. Evans (1995). "Cloning and characterization of the human leukotriene A4 hydrolase gene." Eur J Biochem 231(1): 65-71.
- Martinez, J., A. Patkaniowska, H. Urlaub, R. Luhrmann and T. Tuschl (2002a). "Single-stranded antisense siRNAs guide target RNA cleavage in RNAi." Cell 110(5): 563-74.
- Martinez, J. and T. Tuschl (2004). "RISC is a 5' phosphomonoester-producing RNA endonuclease." Genes Dev 18(9): 975-80.

- Martinez, L. A., I. Naguibneva, H. Lehrmann, A. Vervisch, T. Tchenio, G. Lozano and A. Harel-Bellan (2002b). "Synthetic small inhibiting RNAs: efficient tools to inactivate oncogenic mutations and restore p53 pathways." Proc Natl Acad Sci U S A 99(23): 14849-54.
- Matranga, C., Y. Tomari, C. Shin, D. P. Bartel and P. D. Zamore (2005). "Passenger-strand cleavage facilitates assembly of siRNA into Ago2-containing RNAi enzyme complexes." Cell 123(4): 607-20.
- Matsuda, T. and C. L. Cepko (2004). "Electroporation and RNA interference in the rodent retina in vivo and in vitro." Proc Natl Acad Sci U S A 101(1): 16-22.
- McCaffrey, A. P., K. Ohashi, L. Meuse, S. Shen, A. M. Lancaster, P. J. Lukavsky, P. Sarnow and M. A. Kay (2002). "Determinants of hepatitis C translational initiation in vitro, in cultured cells and mice." Mol Ther 5(6): 676-84.
- McElroy, N. R., P. C. Jurs, C. Morisseau and B. D. Hammock (2003). "QSAR and classification of murine and human soluble epoxide hydrolase inhibition by urea-like compounds." J Med Chem 46(6): 1066-80.
- McGee, J. and F. Fitzpatrick (1985). "Enzymatic hydration of leukotriene A4. Purification and characterization of a novel epoxide hydrolase from human erythrocytes." J Biol Chem 260(23): 12832-7.
- Meister, G., M. Landthaler, A. Patkaniowska, Y. Dorsett, G. Teng and T. Tuschl (2004). "Human Argonaute2 mediates RNA cleavage targeted by miRNAs and siRNAs." Mol Cell 15(2): 185-97.
- Meister, G. and T. Tuschl (2004). "Mechanisms of gene silencing by double-stranded RNA." Nature 431(7006): 343-9.
- Meister, G., M. Landthaler, L. Peters, P. Y. Chen, H. Urlaub, R. Luhrmann and T. Tuschl (2005). "Identification of novel argonaute-associated proteins." Curr Biol 15(23): 2149-55.
- Melquist, S. and J. Bender (2003). "Transcription from an upstream promoter controls methylation signaling from an inverted repeat of endogenous genes in Arabidopsis." Genes Dev 17(16): 2036-47.
- Mette, M. F., W. Aufsatz, J. van der Winden, M. A. Matzke and A. J. Matzke (2000). "Transcriptional silencing and promoter methylation triggered by double-stranded RNA." EMBO J 19(19): 5194-201.
- Miller, V. M., H. Xia, G. L. Marrs, C. M. Gouvion, G. Lee, B. L. Davidson and H. L. Paulson (2003). "Allele-specific silencing of dominant disease genes." Proc Natl Acad Sci U S A 100(12): 7195-200.
- Minakuchi, Y., F. Takeshita, N. Kosaka, H. Sasaki, Y. Yamamoto, M. Kouno, K. Honma, S. Nagahara, K. Hanai, A. Sano, T. Kato, M. Terada and T. Ochiya (2004). "Atelocollagen-mediated synthetic small interfering RNA delivery for effective gene silencing in vitro and in vivo." Nucleic Acids Res 32(13): e109.
- Misquitta, L. and B. M. Paterson (1999). "Targeted disruption of gene function in Drosophila by RNA interference (RNA-i): a role for nautilus in embryonic somatic muscle formation." Proc Natl Acad Sci U S A 96(4): 1451-6.
- Miyagishi, M., S. Matsumoto and K. Taira (2004). "Generation of an shRNAi expression library against the whole human transcripts." Virus Res 102(1): 117-24.

- Miyoshi, K., H. Tsukumo, T. Nagami, H. Siomi and M. C. Siomi (2005). "Slicer function of *Drosophila* Argonautes and its involvement in RISC formation." Genes Dev 19(23): 2837-48.
- Mochizuki, K. and M. A. Gorovsky (2004). "Small RNAs in genome rearrangement in *Tetrahymena*." Curr Opin Genet Dev 14(2): 181-7.
- Moghaddam, M. F., D. F. Grant, J. M. Cheek, J. F. Greene, K. C. Williamson and B. D. Hammock (1997). "Bioactivation of leukotoxins to their toxic diols by epoxide hydrolase." Nature Medicine 3(5): 562-6.
- Mombouli, J. V., S. Holzmann, G. M. Kostner and W. F. Graier (1999). "Potentiation of Ca<sup>2+</sup> signaling in endothelial cells by 11,12-epoxyeicosatrienoic acid." J Cardiovasc Pharmacol 33(5): 779-84.
- Montgomery, M. K., S. Xu and A. Fire (1998). "RNA as a target of double-stranded RNA-mediated genetic interference in *Caenorhabditis elegans*." Proc Natl Acad Sci U S A 95(26): 15502-7.
- Moody, D. E., D. N. Loury, B. D. Hammock, B. H. Ruebner, J. M. Cullen, J. H. Hillman, D. W. Hillman, M. S. Rao, W. T. London, H. W. Hann and et al. (1992). "Serum epoxide hydrolase (preneoplastic antigen) in human and experimental liver injury." Cancer Epidemiol Biomarkers Prev 1(5): 395-403.
- Morisseau, C., G. Du, J. W. Newman and B. D. Hammock (1998). "Mechanism of mammalian soluble epoxide hydrolase inhibition by chalcone oxide derivatives." Arch Biochem Biophys 356(2): 214-28.
- Morisseau, C., M. H. Goodrow, D. Dowdy, J. Zheng, J. F. Greene, J. R. Sanborn and B. D. Hammock (1999). "Potent urea and carbamate inhibitors of soluble epoxide hydrolases." Proc Natl Acad Sci U S A 96(16): 8849-54.
- Morisseau, C., J. K. Beetham, F. Pinot, S. Debernard, J. W. Newman and B. D. Hammock (2000). "Cress and potato soluble epoxide hydrolases: purification, biochemical characterization, and comparison to mammalian enzymes." Arch Biochem Biophys 378(2): 321-32.
- Morisseau, C., M. H. Goodrow, J. W. Newman, C. E. Wheelock, D. L. Dowdy and B. D. Hammock (2002). "Structural refinement of inhibitors of urea-based soluble epoxide hydrolases." Biochem Pharmacol 63(9): 1599-608.
- Morisseau, C. and B. D. Hammock (2002). Epoxide hydrolases. Wiley encyclopedia of molecular medicine. T. E. Creighton. New York, NY, John Wiley & Sons, Inc.: 1194-97.
- Morisseau, C. and B. D. Hammock (2005). "Epoxide hydrolases: mechanisms, inhibitor designs, and biological roles." Ann Rev Pharmacol Toxicol 45: 311-333.
- Morris, K. V., S. W. Chan, S. E. Jacobsen and D. J. Looney (2004). "Small interfering RNA-induced transcriptional gene silencing in human cells." Science 305(5688): 1289-92.
- Mourelatos, Z., J. Dostie, S. Paushkin, A. Sharma, B. Charroux, L. Abel, J. Rappsilber, M. Mann and G. Dreyfuss (2002). "miRNPs: a novel class of ribonucleoproteins containing numerous microRNAs." Genes Dev 16(6): 720-8.
- Mourrain, P., C. Beclin, T. Elmayan, F. Feuerbach, C. Godon, J. B. Morel, D. Jouette, A. M. Lacombe, S. Nikic, N. Picault, K. Remoue, M. Sanial, T. A. Vo and H. Vaucheret (2000). "Arabidopsis SGS2 and SGS3 genes are required for posttranscriptional gene silencing and natural virus resistance." Cell 101(5): 533-42.

- Muchardt, C., M. Guilleme, J. S. Seeler, D. Trouche, A. Dejean and M. Yaniv (2002). "Coordinated methyl and RNA binding is required for heterochromatin localization of mammalian HP1alpha." EMBO Rep 3(10): 975-81.
- Mullen, R. T., R. N. Trelease, H. Duerk, M. Arand, B. D. Hammock, F. Oesch and D. F. Grant (1999). "Differential subcellular localization of endogenous and transfected soluble epoxide hydrolase in mammalian cells: evidence for isozyme variants." FEBS Lett 445(2-3): 301-5.
- Mullin, C. A. and C. F. Wilkinson (1980). "Purification of an epoxide hydrolase from the midgut of the southern army worm (*Spodoptera eridania*)." Insect Biochem. 10: 681-91.
- Munzenmaier, D. H. and D. R. Harder (2000). "Cerebral microvascular endothelial cell tube formation: role of astrocytic epoxyeicosatrienoic acid release." Am J Physiol Heart Circ Physiol 278(4): H1163-7.
- Myers, J. W., J. T. Jones, T. Meyer and J. E. Ferrell, Jr. (2003). "Recombinant Dicer efficiently converts large dsRNAs into siRNAs suitable for gene silencing." Nat Biotechnol 21(3): 324-8.
- Nakagawa, Y., C. E. Wheelock, C. Morisseau, M. H. Goodrow, B. G. Hammock and B. D. Hammock (2000). "3-D QSAR analysis of inhibition of murine soluble epoxide hydrolase (MsEH) by benzoylureas, arylureas, and their analogues." Bioorg Med Chem Lett 8(11): 2663-73.
- Napoli, C., C. Lemieux and R. Jorgensen (1990). "Introduction of a Chimeric Chalcone Synthase Gene into Petunia Results in Reversible Co-Suppression of Homologous Genes in trans." Plant Cell 2(4): 279-289.
- Nashed, N. T., D. P. Michaud, W. Levin and D. M. Jerina (1985). "Properties of liver microsomal cholesterol 5,6-oxide hydrolase." Arch Biochem Biophys 241(1): 149-62.
- Newman, J. W., C. Morisseau, T. R. Harris and B. D. Hammock (2003). "The soluble epoxide hydrolase encoded by EPXH2 is a bifunctional enzyme with novel lipid phosphate phosphatase activity." Proc Natl Acad Sci U S A 100(4): 1558-63.
- Newman, J. W., J. E. Stok, J. D. Vidal, C. J. Corbin, Q. Huang, B. D. Hammock and A. J. Conley (2004). "Cytochrome p450-dependent lipid metabolism in preovulatory follicles." Endocrinology 145(11): 5097-105.
- Newman, J. W., C. Morisseau and B. D. Hammock (2005). "Epoxide hydrolases: their roles and interactions with lipid metabolism." Prog Lipid Res 44(1): 1-51.
- Node, K., Y. Huo, X. Ruan, B. Yang, M. Spiecker, K. Ley, D. C. Zeldin and J. K. Liao (1999). "Anti-inflammatory properties of cytochrome P450 epoxygenase-derived eicosanoids." Science 285(5431): 1276-9.
- Node, K., X. L. Ruan, J. Dai, S. X. Yang, L. Graham, D. C. Zeldin and J. K. Liao (2001). "Activation of Galpha s mediates induction of tissue-type plasminogen activator gene transcription by epoxyeicosatrienoic acids." J Biol Chem 276(19): 15983-9.
- Nykänen, A., B. Haley and P. D. Zamore (2001). "ATP requirements and small interfering RNA structure in the RNA interference pathway." Cell 107(3): 309-21.
- Oesch, F. (1973). "Mammalian epoxide hydrolases: inducible enzymes catalysing the inactivation of carcinogenic and cytotoxic metabolites derived from aromatic and olefinic compounds." Xenobiotica 3(5): 305-40.

- Ohrt, T., D. Merkle, K. Birkenfeld, C. J. Echeverri and P. Schwillle (2006). "In situ fluorescence analysis demonstrates active siRNA exclusion from the nucleus by Exportin 5." Nucleic Acids Res 34(5): 1369-80.
- Okamura, K., A. Ishizuka, H. Siomi and M. C. Siomi (2004). "Distinct roles for Argonaute proteins in small RNA-directed RNA cleavage pathways." Genes Dev 18(14): 1655-66.
- Ollis, D. L., E. Cheah, M. Cygler, B. Dijkstra, F. Frolow, S. M. Franken, M. Harel, S. J. Remington, I. Silman, J. Schrag and et al. (1992). "The alpha/beta hydrolase fold." Protein Eng 5(3): 197-211.
- Orban, T. I. and E. Izaurralde (2005). "Decay of mRNAs targeted by RISC requires XRN1, the Ski complex, and the exosome." RNA 11(4): 459-69.
- Ozawa, T., M. Hayakawa, T. Takamura, S. Sugiyama, K. Suzuki, M. Iwata, F. Taki and T. Tomita (1986). "Biosynthesis of leukotoxin, 9,10-epoxy-12 octadecenoate, by leukocytes in lung lavages of rat after exposure to hyperoxia." Biochem Biophys Res Commun 134(3): 1071-8.
- Ozawa, T., M. Hayakawa, K. Kosaka, S. Sugiyama, T. Ogawa, K. Yokoo, H. Aoyama and Y. Izawa (1991). "Leukotoxin, 9,10-epoxy-12-octadecenoate, as a burn toxin causing adult respiratory distress syndrome." Adv Prostaglandin Thromboxane Leukot Res 21B: 569-72.
- Pace-Asciak, C. R. and W. S. Lee (1989). "Purification of hepoxilin epoxide hydrolase from rat liver." J Biol Chem 264(16): 9310-3.
- Pacifici, G. M., A. Temellini, L. Giuliani, A. Rane, H. Thomas and F. Oesch (1988). "Cytosolic epoxide hydrolase in humans: development and tissue distribution." Arch Toxicol 62(4): 254-7.
- Paddison, P. J., A. A. Caudy, E. Bernstein, G. J. Hannon and D. S. Conklin (2002). "Short hairpin RNAs (shRNAs) induce sequence-specific silencing in mammalian cells." Genes Dev 16(8): 948-58.
- Pal-Bhadra, M., U. Bhadra and J. A. Birchler (1997). "Cosuppression in Drosophila: gene silencing of Alcohol dehydrogenase by white-Adh transgenes is Polycomb dependent." Cell 90(3): 479-90.
- Pal-Bhadra, M., U. Bhadra and J. A. Birchler (2002). "RNAi related mechanisms affect both transcriptional and posttranscriptional transgene silencing in Drosophila." Mol Cell 9(2): 315-27.
- Pal-Bhadra, M., U. Bhadra and J. A. Birchler (2004a). "Interrelationship of RNA interference and transcriptional gene silencing in Drosophila." Cold Spring Harb Symp Quant Biol 69: 433-8.
- Pal-Bhadra, M., B. A. Leibovitch, S. G. Gandhi, M. Rao, U. Bhadra, J. A. Birchler and S. C. Elgin (2004b). "Heterochromatic silencing and HP1 localization in Drosophila are dependent on the RNAi machinery." Science 303(5658): 669-72.
- Palliser, D., D. Chowdhury, Q. Y. Wang, S. J. Lee, R. T. Bronson, D. M. Knipe and J. Lieberman (2006). "An siRNA-based microbicide protects mice from lethal herpes simplex virus 2 infection." Nature 439(7072): 89-94.
- Pang, S. T., K. Dillner, X. Wu, A. Pousette, G. Norstedt and A. Flores-Morales (2002). "Gene expression profiling of androgen deficiency predicts a pathway of prostate apoptosis that involves genes related to oxidative stress." Endocrinology 143(12): 4897-906.
- Parizotto, E. A., P. Dunoyer, N. Rahm, C. Himber and O. Voinnet (2004). "In vivo investigation of the transcription, processing, endonucleolytic activity, and functional relevance of the spatial distribution of a plant miRNA." Genes Dev 18(18): 2237-42.



- Parker, J. S., S. M. Roe and D. Barford (2004). "Crystal structure of a PIWI protein suggests mechanisms for siRNA recognition and slicer activity." EMBO J 23(24): 4727-37.
- Parker, J. S., S. M. Roe and D. Barford (2005). "Structural insights into mRNA recognition from a PIWI domain-siRNA guide complex." Nature 434(7033): 663-6.
- Parker, R. and H. Song (2004). "The enzymes and control of eukaryotic mRNA turnover." Nat Struct Mol Biol 11(2): 121-7.
- Paul, C. P., P. D. Good, I. Winer and D. R. Engelke (2002). "Effective expression of small interfering RNA in human cells." Nat Biotechnol 20(5): 505-8.
- Pelissier, T., S. Thalmeir, D. Kempe, H. L. Sanger and M. Wassenegger (1999). "Heavy de novo methylation at symmetrical and non-symmetrical sites is a hallmark of RNA-directed DNA methylation." Nucleic Acids Res 27(7): 1625-34.
- Peri, K. G., G. Almazan, D. R. Varma and S. Chemtob (1998). "A role for protein kinase C alpha in stimulation of prostaglandin G/H synthase-2 transcription by 14,15-epoxyeicosatrienoic acid." Biochem Biophys Res Commun 244(1): 96-101.
- Pillai, R. S. (2005). "MicroRNA function: multiple mechanisms for a tiny RNA?" RNA 11(12): 1753-61.
- Pillai, R. S., S. N. Bhattacharyya, C. G. Artus, T. Zoller, N. Cougot, E. Basyuk, E. Bertrand and W. Filipowicz (2005). "Inhibition of translational initiation by Let-7 MicroRNA in human cells." Science 309(5740): 1573-6.
- Pinot, F., D. F. Grant, J. K. Beetham, A. G. Parker, B. Borhan, S. Landt, A. D. Jones and B. D. Hammock (1995a). "Molecular and biochemical evidence for the involvement of the Asp-333-His-523 pair in the catalytic mechanism of soluble epoxide hydrolase." J Biol Chem 270(14): 7968-74.
- Pinot, F., D. F. Grant, J. L. Spearow, A. G. Parker and B. D. Hammock (1995b). "Differential regulation of soluble epoxide hydrolase by clofibrate and sexual hormones in the liver and kidneys of mice." Biochem Pharmacol 50(4): 501-8.
- Pirollo, K. F., G. Zon, A. Rait, Q. Zhou, W. Yu, R. Hogrefe and E. H. Chang (2006). "Tumor-targeting nanoimmunoliposome complex for short interfering RNA delivery." Hum Gene Ther 17(1): 117-24.
- Powers, J., O. Bossinger, D. Rose, S. Strome and W. Saxton (1998). "A nematode kinesin required for cleavage furrow advancement." Curr Biol 8(20): 1133-6.
- Prakash, T. P., B. Kraynaek, B. F. Baker, E. E. Swayze and B. Bhat (2006). "RNA interference by 2',5'-linked nucleic acid duplexes in mammalian cells." Bioorg Med Chem Lett 16(12): 3238-40.
- Przybyla-Zawislak, B. D., P. K. Srivastava, J. Vazquez-Matias, H. W. Mohrenweiser, J. E. Maxwell, B. D. Hammock, J. A. Bradbury, A. E. Enayetallah, D. C. Zeldin and D. F. Grant (2003). "Polymorphisms in human soluble epoxide hydrolase." Mol Pharmacol 64(2): 482-90.
- Rand, T. A., K. Ginalski, N. V. Grishin and X. Wang (2004). "Biochemical identification of Argonaute 2 as the sole protein required for RNA-induced silencing complex activity." Proc Natl Acad Sci U S A 101(40): 14385-9.
- Rand, T. A., S. Petersen, F. Du and X. Wang (2005). "Argonaute2 cleaves the anti-guide strand of siRNA during RISC activation." Cell 123(4): 621-9.

- Rao, M. S. and J. K. Reddy (1991). "An overview of peroxisome proliferator-induced hepatocarcinogenesis." Environ Health Perspect 93: 205-9.
- Reich, S. J., J. Fosnot, A. Kuroki, W. Tang, X. Yang, A. M. Maguire, J. Bennett and M. J. Tolentino (2003). "Small interfering RNA (siRNA) targeting VEGF effectively inhibits ocular neovascularization in a mouse model." Mol Vis 9: 210-6.
- Reinhart, B. J., F. J. Slack, M. Basson, A. E. Pasquinelli, J. C. Bettinger, A. E. Rougvie, H. R. Horvitz and G. Ruvkun (2000). "The 21-nucleotide let-7 RNA regulates developmental timing in *Caenorhabditis elegans*." Nature 403(6772): 901-6.
- Reynolds, A., D. Leake, Q. Boese, S. Scaringe, W. S. Marshall and A. Khvorova (2004). "Rational siRNA design for RNA interference." Nat Biotechnol 22(3): 326-30.
- Reynolds, A., E. M. Anderson, A. Vermeulen, Y. Fedorov, K. Robinson, D. Leake, J. Karpilow, W. S. Marshall and A. Khvorova (2006). "Induction of the interferon response by siRNA is cell type- and duplex length-dependent." RNA 12(6): 988-93.
- Rhoades, M. W., B. J. Reinhart, L. P. Lim, C. B. Burge, B. Bartel and D. P. Bartel (2002). "Prediction of plant microRNA targets." Cell 110(4): 513-20.
- Rivas, F. V., N. H. Tolia, J. J. Song, J. P. Aragon, J. Liu, G. J. Hannon and L. Joshua-Tor (2005). "Purified Argonaute2 and an siRNA form recombinant human RISC." Nat Struct Mol Biol 12(4): 340-9.
- Robbins, M. A. and J. J. Rossi (2005). "Sensing the danger in RNA." Nat Med 11(3): 250-1.
- Rodriguez, A., S. Griffiths-Jones, J. L. Ashurst and A. Bradley (2004). "Identification of mammalian microRNA host genes and transcription units." Genome Res 14(10A): 1902-10.
- Roignant, J. Y., C. Carre, B. Mugat, D. Szymczak, J. A. Lepesant and C. Antoniewski (2003). "Absence of transitive and systemic pathways allows cell-specific and isoform-specific RNAi in *Drosophila*." RNA 9(3): 299-308.
- Roman, R. J. (2002). "P-450 metabolites of arachidonic acid in the control of cardiovascular function." Physiol Rev 82(1): 131-85.
- Romano, N. and G. Macino (1992). "Quelling: transient inactivation of gene expression in *Neurospora crassa* by transformation with homologous sequences." Mol Microbiol 6(22): 3343-53.
- Rubinson, D. A., C. P. Dillon, A. V. Kwiakowski, C. Sievers, L. Yang, J. Kopinja, D. L. Rooney, M. M. Ihrig, M. T. McManus, F. B. Gertler, M. L. Scott and L. Van Parijs (2003). "A lentivirus-based system to functionally silence genes in primary mammalian cells, stem cells and transgenic mice by RNA interference." Nat Genet 33(3): 401-6.
- Rybina, I. V., H. Liu, Y. Gor and S. J. Feinmark (1997). "Regulation of leukotriene A4 hydrolase activity in endothelial cells by phosphorylation." J Biol Chem 272(50): 31865-71.
- Saffery, R., H. Sumer, S. Hassan, L. H. Wong, J. M. Craig, K. Todokoro, M. Anderson, A. Stafford and K. H. Choo (2003). "Transcription within a functional human centromere." Mol Cell 12(2): 509-16.
- Samuelsson, B. (1983). "Leukotrienes: mediators of immediate hypersensitivity reactions and inflammation." Science 220(4597): 568-75.

- Sandberg, M. and J. Meijer (1996). "Structural characterization of the human soluble epoxide hydrolase gene (EPHX2)." Biochem Biophys Res Commun 221(2): 333-9.
- Sandberg, M., C. Hassett, E. T. Adman, J. Meijer and C. J. Omiecinski (2000). "Identification and functional characterization of human soluble epoxide hydrolase genetic polymorphisms." J Biol Chem 275(37): 28873-81.
- Santel, A., M. Aleku, O. Keil, J. Endruschat, V. Esche, G. Fisch, S. Dames, K. Löffler, M. Fechtner, W. Arnold, K. Giese, A. Klippel and J. Kaufmann (2006). "A novel siRNA-lipoplex technology for RNA interference in the mouse vascular endothelium." Gene Ther 13(16): 1222-34.
- Sarkar, S. N., K. L. Peters, C. P. Elco, S. Sakamoto, S. Pal and G. C. Sen (2004). "Novel roles of TLR3 tyrosine phosphorylation and PI3 kinase in double-stranded RNA signaling." Nat Struct Mol Biol 11(11): 1060-7.
- Sasaki, T., A. Shiohama, S. Minoshima and N. Shimizu (2003). "Identification of eight members of the Argonaute family in the human genome small star, filled." Genomics 82(3): 323-30.
- Sato, K., M. Emi, Y. Ezura, Y. Fujita, D. Takada, T. Ishigami, S. Umemura, Y. Xin, L. L. Wu, S. Larrinaga-Shum, S. H. Stephenson, S. C. Hunt and P. N. Hopkins (2004). "Soluble epoxide hydrolase variant (Glu287Arg) modifies plasma total cholesterol and triglyceride phenotype in familial hypercholesterolemia: intrafamilial association study in an eight-generation hyperlipidemic kindred." J Hum Genet 49(1): 29-34.
- Saxena, S., Z. O. Jonsson and A. Dutta (2003). "Small RNAs with imperfect match to endogenous mRNA repress translation. Implications for off-target activity of small inhibitory RNA in mammalian cells." J Biol Chem 278(45): 44312-9.
- Sayer, J. M., H. Yagi, P. J. van Bladeren, W. Levin and D. M. Jerina (1985). "Stereoselectivity of microsomal epoxide hydrolase toward diol epoxides and tetrahydroepoxides derived from benz[a]anthracene." J Biol Chem 260(3): 1630-40.
- Scherr, M., K. Battmer, A. Ganser and M. Eder (2003). "Modulation of gene expression by lentiviral-mediated delivery of small interfering RNA." Cell Cycle 2(3): 251-7.
- Schiøtt, B. and T. C. Bruice (2002). "Reaction mechanism of soluble epoxide hydrolase: insights from molecular dynamics simulations." J Am Chem Soc 124(49): 14558-70.
- Schmelzer, K. R., L. Kubala, J. W. Newman, I. H. Kim, J. P. Eiserich and B. D. Hammock (2005). "Soluble epoxide hydrolase is a therapeutic target for acute inflammation." Proc Natl Acad Sci U S A 102(28): 9772-7.
- Schmidt, A., G. Palumbo, M. P. Bozzetti, P. Tritto, S. Pimpinelli and U. Schafer (1999). "Genetic and molecular characterization of sting, a gene involved in crystal formation and meiotic drive in the male germ line of *Drosophila melanogaster*." Genetics 151(2): 749-60.
- Schramke, V. and R. Allshire (2003). "Hairpin RNAs and retrotransposon LTRs effect RNAi and chromatin-based gene silencing." Science 301(5636): 1069-74.
- Schwarz, D. S., G. Hutvagner, B. Haley and P. D. Zamore (2002). "Evidence that siRNAs function as guides, not primers, in the *Drosophila* and human RNAi pathways." Mol Cell 10(3): 537-48.
- Schwarz, D. S., G. Hutvagner, T. Du, Z. Xu, N. Aronin and P. D. Zamore (2003). "Asymmetry in the assembly of the RNAi enzyme complex." Cell 115(2): 199-208.

- Schwarz, D. S., Y. Tomari and P. D. Zamore (2004). "The RNA-induced silencing complex is a Mg<sup>2+</sup>-dependent endonuclease." Curr Biol 14(9): 787-91.
- Seki, K., A. Hirai, M. Noda, Y. Tamura, I. Kato and S. Yoshida (1992). "Epoxyeicosatrienoic acid stimulates ADP-ribosylation of a 52 kDa protein in rat liver cytosol." Biochem J 281 ( Pt 1): 185-90.
- Sellers, K. W., C. Sun, C. Diez-Freire, H. Waki, C. Morisseau, J. R. Falck, B. D. Hammock, J. F. Paton and M. K. Raizada (2005). "Novel mechanism of brain soluble epoxide hydrolase-mediated blood pressure regulation in the spontaneously hypertensive rat." Faseb J 19(6): 626-8.
- Sen, G. L. and H. M. Blau (2005). "Argonaute 2/RISC resides in sites of mammalian mRNA decay known as cytoplasmic bodies." Nat Cell Biol 7(6): 633-6.
- Shan, G. and B. D. Hammock (2001). "Development of sensitive esterase assays based on  $\alpha$ -cyano-containing esters." Anal Biochem 299: 54-62.
- Sheth, U. and R. Parker (2003). "Decapping and decay of messenger RNA occur in cytoplasmic processing bodies." Science 300(5620): 805-8.
- Shiu, P. K., N. B. Raju, D. Zickler and R. L. Metzenberg (2001). "Meiotic silencing by unpaired DNA." Cell 107(7): 905-16.
- Shiu, P. K. and R. L. Metzenberg (2002). "Meiotic silencing by unpaired DNA: properties, regulation and suppression." Genetics 161(4): 1483-95.
- Simeoni, F., M. C. Morris, F. Heitz and G. Divita (2003). "Insight into the mechanism of the peptide-based gene delivery system MPG: implications for delivery of siRNA into mammalian cells." Nucleic Acids Res 31(11): 2717-24.
- Sinal, C. J., M. Miyata, M. Tohkin, K. Nagata, J. R. Bend and F. J. Gonzalez (2000). "Targeted disruption of soluble epoxide hydrolase reveals a role in blood pressure regulation." J Biol Chem 275(51): 40504-10.
- Siolas, D., C. Lerner, J. Burchard, W. Ge, P. S. Linsley, P. J. Paddison, G. J. Hannon and M. A. Cleary (2005). "Synthetic shRNAs as potent RNAi triggers." Nat Biotechnol 23(2): 227-31.
- Sioud, M. (2005). "Induction of inflammatory cytokines and interferon responses by double-stranded and single-stranded siRNAs is sequence-dependent and requires endosomal localization." J Mol Biol 348(5): 1079-90.
- Sledz, C. A., M. Holko, M. J. de Veer, R. H. Silverman and B. R. Williams (2003). "Activation of the interferon system by short-interfering RNAs." Nat Cell Biol 5(9): 834-9.
- Slim, R., B. D. Hammock, M. Toborek, L. W. Robertson, J. W. Newman, C. H. Morisseau, B. A. Watkins, V. Saraswathi and B. Hennig (2001). "The role of methyl-linoleic acid epoxide and diol metabolites in the amplified toxicity of linoleic acid and polychlorinated biphenyls to vascular endothelial cells." Toxicol Appl Pharmacol 171(3): 184-93.
- Smith, K. R., K. E. Pinkerton, T. Watanabe, T. L. Pedersen, S. J. Ma and B. D. Hammock (2005). "Attenuation of tobacco smoke-induced lung inflammation by treatment with a soluble epoxide hydrolase inhibitor." Proc Natl Acad Sci U S A 102(6): 2186-91.
- Snyder, G. D., U. M. Krishna, J. R. Falck and A. A. Spector (2002). "Evidence for a membrane site of action for 14,15-EET on expression of aromatase in vascular smooth muscle." Am J Physiol Heart Circ Physiol 283(5): H1936-42.

- Song, E., S. K. Lee, J. Wang, N. Ince, N. Ouyang, J. Min, J. Chen, P. Shankar and J. Lieberman (2003a). "RNA interference targeting Fas protects mice from fulminant hepatitis." Nat Med 9(3): 347-51.
- Song, E., P. Zhu, S. K. Lee, D. Chowdhury, S. Kussman, D. M. Dykxhoorn, Y. Feng, D. Palliser, D. B. Weiner, P. Shankar, W. A. Marasco and J. Lieberman (2005). "Antibody mediated in vivo delivery of small interfering RNAs via cell-surface receptors." Nat Biotechnol 23(6): 709-17.
- Song, J. J., J. Liu, N. H. Tolia, J. Schneiderman, S. K. Smith, R. A. Martienssen, G. J. Hannon and L. Joshua-Tor (2003b). "The crystal structure of the Argonaute2 PAZ domain reveals an RNA binding motif in RNAi effector complexes." Nat Struct Biol 10(12): 1026-32.
- Song, J. J., S. K. Smith, G. J. Hannon and L. Joshua-Tor (2004). "Crystal structure of Argonaute and its implications for RISC slicer activity." Science 305(5689): 1434-7.
- Soriano, A., A. D. Radice, A. H. Herbitter, E. F. Langsdorf, J. M. Stafford, S. Chan, S. Wang, Y. H. Liu and T. A. Black (2006). "Escherichia coli acetyl-coenzyme A carboxylase: characterization and development of a high-throughput assay." Anal Biochem 349(2): 268-76.
- Spector, A. A., X. Fang, G. D. Snyder and N. L. Weintraub (2004). "Epoxyeicosatrienoic acids (EETs): metabolism and biochemical function." Prog Lipid Res 43(1): 55-90.
- Srivastava, P. K., V. K. Sharma, D. S. Kalonia and D. F. Grant (2004). "Polymorphisms in human soluble epoxide hydrolase: effects on enzyme activity, enzyme stability, and quaternary structure." Arch Biochem Biophys 427(2): 164-9.
- Stapleton, A., J. K. Beetham, F. Pinot, J. E. Garbarino, D. R. Rockhold, M. Friedman, B. D. Hammock and W. R. Belknap (1994). "Cloning and expression of soluble epoxide hydrolase from potato." Plant J 6(2): 251-8.
- Stein, P., P. Svoboda, M. Anger and R. M. Schultz (2003). "RNAi: mammalian oocytes do it without RNA-dependent RNA polymerase." RNA 9(2): 187-92.
- Stewart, S. A., D. M. Dykxhoorn, D. Palliser, H. Mizuno, E. Y. Yu, D. S. An, D. M. Sabatini, I. S. Chen, W. C. Hahn, P. A. Sharp, R. A. Weinberg and C. D. Novina (2003). "Lentivirus-delivered stable gene silencing by RNAi in primary cells." RNA 9(4): 493-501.
- Sun, J., X. Sui, J. A. Bradbury, D. C. Zeldin, M. S. Conte and J. K. Liao (2002). "Inhibition of vascular smooth muscle cell migration by cytochrome p450 epoxygenase-derived eicosanoids." Circ Res 90(9): 1020-7.
- Sun, W., G. Li and A. W. Nicholson (2004). "Mutational analysis of the nuclease domain of Escherichia coli ribonuclease III. Identification of conserved acidic residues that are important for catalytic function in vitro." Biochemistry 43(41): 13054-62.
- Svoboda, P., P. Stein, W. Filipowicz and R. M. Schultz (2004). "Lack of homologous sequence-specific DNA methylation in response to stable dsRNA expression in mouse oocytes." Nucleic Acids Res 32(12): 3601-6.
- Tabara, H., A. Grishok and C. C. Mello (1998). "RNAi in C. elegans: soaking in the genome sequence." Science 282(5388): 430-1.
- Tabara, H., M. Sarkissian, W. G. Kelly, J. Fleenor, A. Grishok, L. Timmons, A. Fire and C. C. Mello (1999). "The rde-1 gene, RNA interference, and transposon silencing in C. elegans." Cell 99(2): 123-32.

- Takabatake, Y., Y. Isaka, M. Mizui, H. Kawachi, F. Shimizu, T. Ito, M. Hori and E. Imai (2005). "Exploring RNA interference as a therapeutic strategy for renal disease." Gene Ther 12(12): 965-73.
- Takeda, K. and S. Akira (2005). "Toll-like receptors in innate immunity." Int Immunol 17(1): 1-14.
- Takei, Y., K. Kadomatsu, Y. Yuzawa, S. Matsuo and T. Muramatsu (2004). "A small interfering RNA targeting vascular endothelial growth factor as cancer therapeutics." Cancer Res 64(10): 3365-70.
- Tamaru, H. and E. U. Selker (2003). "Synthesis of signals for de novo DNA methylation in *Neurospora crassa*." Mol Cell Biol 23(7): 2379-94.
- Timmons, L. and A. Fire (1998). "Specific interference by ingested dsRNA." Nature 395(6705): 854.
- Tiscornia, G., O. Singer, M. Ikawa and I. M. Verma (2003). "A general method for gene knockdown in mice by using lentiviral vectors expressing small interfering RNA." Proc Natl Acad Sci U S A 100(4): 1844-8.
- Tolentino, M. J., A. J. Brucker, J. Fosnot, G. S. Ying, I. H. Wu, G. Malik, S. Wan and S. J. Reich (2004). "Intravitreal injection of vascular endothelial growth factor small interfering RNA inhibits growth and leakage in a nonhuman primate, laser-induced model of choroidal neovascularization." Retina 24(1): 132-8.
- Tomanin, R. and M. Scarpa (2004). "Why do we need new gene therapy viral vectors? Characteristics, limitations and future perspectives of viral vector transduction." Curr Gene Ther 4(4): 357-72.
- Tomari, Y., C. Matranga, B. Haley, N. Martinez and P. D. Zamore (2004). "A protein sensor for siRNA asymmetry." Science 306(5700): 1377-80.
- Tuschl, T., P. D. Zamore, R. Lehmann, D. P. Bartel and P. A. Sharp (1999). "Targeted mRNA degradation by double-stranded RNA in vitro." Genes Dev 13(24): 3191-7.
- Uprichard, S. L. (2005). "The therapeutic potential of RNA interference." FEBS Lett 579(26): 5996-6007.
- Urban-Klein, B., S. Werth, S. Abuharbeid, F. Czubayko and A. Aigner (2005). "RNAi-mediated gene-targeting through systemic application of polyethylenimine (PEI)-complexed siRNA in vivo." Gene Ther 12(5): 461-6.
- van der Krol, A. R., L. A. Mur, M. Beld, J. N. Mol and A. R. Stuitje (1990). "Flavonoid genes in petunia: addition of a limited number of gene copies may lead to a suppression of gene expression." Plant Cell 2(4): 291-9.
- van der Werf, M. J., H. J. Swarts and J. A. de Bont (1999). "Rhodococcus erythropolis DCL14 contains a novel degradation pathway for limonene." Appl Environ Microbiol 65(5): 2092-102.
- van Hoof, A., R. R. Staples, R. E. Baker and R. Parker (2000). "Function of the ski4p (Csl4p) and Ski7p proteins in 3'-to-5' degradation of mRNA." Mol Cell Biol 20(21): 8230-43.
- van Hoof, A., P. A. Frischmeyer, H. C. Dietz and R. Parker (2002). "Exosome-mediated recognition and degradation of mRNAs lacking a termination codon." Science 295(5563): 2262-4.
- Vanhecke, D. and M. Janitz (2005). "Functional genomics using high-throughput RNA interference." Drug Discov Today 10(3): 205-12.

- VanRollins, M., T. L. Kaduce, H. R. Knapp and A. A. Spector (1993). "14,15-Epoxyeicosatrienoic acid metabolism in endothelial cells." J Lipid Res 34(11): 1931-42.
- Vermeulen, A., L. Behlen, A. Reynolds, A. Wolfson, W. S. Marshall, J. Karpilow and A. Khvorova (2005). "The contributions of dsRNA structure to Dicer specificity and efficiency." RNA 11(5): 674-82.
- Verschueren, K. H., F. Seljee, H. J. Rozeboom, K. H. Kalk and B. W. Dijkstra (1993). "Crystallographic analysis of the catalytic mechanism of haloalkane dehalogenase." Nature 363(6431): 693-8.
- Voinnet, O., Y. M. Pinto and D. C. Baulcombe (1999). "Suppression of gene silencing: a general strategy used by diverse DNA and RNA viruses of plants." Proc Natl Acad Sci U S A 96(24): 14147-52.
- Volpe, T. A., C. Kidner, I. M. Hall, G. Teng, S. I. Grewal and R. A. Martienssen (2002). "Regulation of heterochromatic silencing and histone H3 lysine-9 methylation by RNAi." Science 297(5588): 1833-7.
- Wang, F., N. Koyama, H. Nishida, T. Haraguchi, W. Reith and T. Tsukamoto (2006). "The assembly and maintenance of heterochromatin initiated by transgene repeats are independent of the RNA interference pathway in Mammalian cells." Mol Cell Biol 26(11): 4028-40.
- Wang, Q. and G. G. Carmichael (2004). "Effects of length and location on the cellular response to double-stranded RNA." Microbiol Mol Biol Rev 68(3): 432-52.
- Wassenegger, M., S. Heimes, L. Riedel and H. L. Sanger (1994). "RNA-directed de novo methylation of genomic sequences in plants." Cell 76(3): 567-76.
- Watanabe, T., D. Schulz, C. Morisseau and B. D. Hammock (2006). "High-throughput pharmacokinetic method: Cassette dosing in mice associated with minuscule serial bleedings and LC/MS/MS analysis." Anal Chim Acta 559(1): 37-44.
- Westerhout, E. M., M. Vink, P. C. Joost Haasnoot, A. T. Das and B. Berkhout (2006). "A conditionally replicating HIV-based vector that stably expresses an antiviral shRNA against HIV-1 replication." Mol Ther 14(2): 268-75.
- Wheeler, D. B., A. E. Carpenter and D. M. Sabatini (2005). "Cell microarrays and RNA interference chip away at gene function." Nat Genet 37 Suppl: S25-30.
- Wheelock, C. E., A. M. Wheelock, R. Zhang, J. E. Stok, C. Morisseau, S. E. Le Valley, C. E. Green and B. D. Hammock (2003). "Evaluation of  $\alpha$ -cyanoesters as fluorescent substrates for examining interindividual variation in general and pyrethroid-selective esterases in human liver microsomes." Anal Biochem(315): 208-222.
- Whelan, J. (2005). "First clinical data on RNAi." Drug Discov Today 10(15): 1014-5.
- Widstrom, R. L., A. W. Norris and A. A. Spector (2001). "Binding of cytochrome P450 monooxygenase and lipoxygenase pathway products by heart fatty acid-binding protein." Biochemistry 40(4): 1070-6.
- Williams, R. W. and G. M. Rubin (2002). "ARGONAUTE1 is required for efficient RNA interference in *Drosophila* embryos." Proc Natl Acad Sci U S A 99(10): 6889-94.

- Winder, B. S., J. Nourooz-Zadeh, R. R. Isseroff, M. F. Moghaddam and B. D. Hammock (1993). "Properties of enzymes hydrating epoxides in human epidermis and liver." *Int J Biochem* 25(9): 1291-301.
- Wixtrom, R. N. and B. D. Hammock (1985). Membrane-bound and soluble-fraction epoxide hydrolases: Methodological aspects. *Pharmacology and toxicology*. D. Zakim and D. A. Vessey. New York, John Wiley & Sons, Inc. 1 Methodological Aspects of Drug Metabolizing Enzymes: 1-93.
- Wixtrom, R. N., M. H. Silva and B. D. Hammock (1988). "Affinity purification of cytosolic epoxide hydrolase using derivatized epoxy-activated Sepharose gels." *Anal Biochem* 169(1): 71-80.
- Wong, P. Y., K. T. Lin, Y. T. Yan, D. Ahern, J. Iles, S. Y. Shen, R. K. Bhatt and J. R. Falck (1993). "14(R),15(S)-epoxyeicosatrienoic acid (14(R),15(S)-EET) receptor in guinea pig mononuclear cell membranes." *J Lipid Mediat* 6(1-3): 199-208.
- Wu-Scharf, D., B. Jeong, C. Zhang and H. Cerutti (2000). "Transgene and transposon silencing in *Chlamydomonas reinhardtii* by a DEAH-box RNA helicase." *Science* 290(5494): 1159-62.
- Xiang, S., J. Fruehauf and C. J. Li (2006). "Short hairpin RNA-expressing bacteria elicit RNA interference in mammals." *Nat Biotechnol* 24(6): 697-702.
- Xie, X., J. Lu, E. J. Kulbokas, T. R. Golub, V. Mootha, K. Lindblad-Toh, E. S. Lander and M. Kellis (2005). "Systematic discovery of regulatory motifs in human promoters and 3' UTRs by comparison of several mammals." *Nature* 434(7031): 338-45.
- Xie, Z., L. K. Johansen, A. M. Gustafson, K. D. Kasschau, A. D. Lellis, D. Zilberman, S. E. Jacobsen and J. C. Carrington (2004). "Genetic and functional diversification of small RNA pathways in plants." *PLoS Biol* 2(5): E104.
- Yamada, T., C. Morisseau, J. E. Maxwell, M. A. Argiriadi, D. W. Christianson and B. D. Hammock (2000). "Biochemical evidence for the involvement of tyrosine in epoxide activation during the catalytic cycle of epoxide hydrolase." *J Biol Chem* 275(30): 23082-8.
- Yan, K. S., S. Yan, A. Farooq, A. Han, L. Zeng and M. M. Zhou (2003). "Structure and conserved RNA binding of the PAZ domain." *Nature* 426(6965): 468-74.
- Yano, J., K. Hirabayashi, S. Nakagawa, T. Yamaguchi, M. Nogawa, I. Kashimori, H. Naito, H. Kitagawa, K. Ishiyama, T. Ohgi and T. Irimura (2004). "Antitumor activity of small interfering RNA/cationic liposome complex in mouse models of cancer." *Clin Cancer Res* 10(22): 7721-6.
- Yekta, S., I. H. Shih and D. P. Bartel (2004). "MicroRNA-directed cleavage of HOXB8 mRNA." *Science* 304(5670): 594-6.
- Yi, R., Y. Qin, I. G. Macara and B. R. Cullen (2003). "Exportin-5 mediates the nuclear export of pre-microRNAs and short hairpin RNAs." *Genes Dev* 17(24): 3011-6.
- Yoneyama, M., M. Kikuchi, T. Natsukawa, N. Shinobu, T. Imaizumi, M. Miyagishi, K. Taira, S. Akira and T. Fujita (2004). "The RNA helicase RIG-I has an essential function in double-stranded RNA-induced innate antiviral responses." *Nat Immunol* 5(7): 730-7.
- Yu, J. and A. P. McMahon (2006). "Reproducible and inducible knockdown of gene expression in mice." *Genesis* 44(5): 252-61.



- Yu, Z., F. Xu, L. M. Huse, C. Morisseau, A. J. Draper, J. W. Newman, C. Parker, L. Graham, M. M. Engler, B. D. Hammock, D. C. Zeldin and D. L. Kroetz (2000). "Soluble epoxide hydrolase regulates hydrolysis of vasoactive epoxyeicosatrienoic acids." Circulatory Research 87(11): 992-8.
- Zamore, P. D. (2001). "Thirty-three years later, a glimpse at the ribonuclease III active site." Mol Cell 8(6): 1158-60.
- Zeldin, D. C., J. Kobayashi, J. R. Falck, B. S. Winder, B. D. Hammock, J. R. Snapper and J. H. Capdevila (1993). "Regio- and enantiofacial selectivity of epoxyeicosatrienoic acid hydration by cytosolic epoxide hydrolase." J Biol Chem 268(9): 6402-7.
- Zeldin, D. C., S. Wei, J. R. Falck, B. D. Hammock, J. R. Snapper and J. H. Capdevila (1995). "Metabolism of epoxyeicosatrienoic acids by cytosolic epoxide hydrolase: substrate structural determinants of asymmetric catalysis." Arch Biochem Biophys 316(1): 443-51.
- Zeldin, D. C. (2001). "Epoxygenase pathways of arachidonic acid metabolism." J Biol Chem 276(39): 36059-62.
- Zeng, Y. and B. R. Cullen (2002). "RNA interference in human cells is restricted to the cytoplasm." RNA 8(7): 855-60.
- Zeng, Y., R. Yi and B. R. Cullen (2003). "MicroRNAs and small interfering RNAs can inhibit mRNA expression by similar mechanisms." Proc Natl Acad Sci U S A 100(17): 9779-84.
- Zeng, Y. and B. R. Cullen (2004). "Structural requirements for pre-microRNA binding and nuclear export by Exportin 5." Nucleic Acids Res 32(16): 4776-85.
- Zeng, Y. and B. R. Cullen (2005). "Efficient processing of primary microRNA hairpins by Drosha requires flanking nonstructured RNA sequences." J Biol Chem 280(30): 27595-603.
- Zeng, Y., R. Yi and B. R. Cullen (2005). "Recognition and cleavage of primary microRNA precursors by the nuclear processing enzyme Drosha." EMBO J 24(1): 138-48.
- Zhang, H., F. A. Kolb, V. Brondani, E. Billy and W. Filipowicz (2002). "Human Dicer preferentially cleaves dsRNAs at their termini without a requirement for ATP." EMBO J 21(21): 5875-85.
- Zhang, H., F. A. Kolb, L. Jaskiewicz, E. Westhof and W. Filipowicz (2004a). "Single processing center models for human Dicer and bacterial RNase III." Cell 118(1): 57-68.
- Zhang, J. H., T. D. Chung and K. R. Oldenburg (1999). "A Simple Statistical Parameter for Use in Evaluation and Validation of High Throughput Screening Assays." J Biomol Screen 4(2): 67-73.
- Zhang, R., K. D. Kang, G. Shan and B. D. Hammock (2003). "Design, synthesis and evaluation of novel P450 fluorescent probes bearing  $\sigma$ -cyanoether." Tetrahedron Lett.(44): 4331-4334.
- Zhang, X., P. Shan, D. Jiang, P. W. Noble, N. G. Abraham, A. Kappas and P. J. Lee (2004b). "Small interfering RNA targeting heme oxygenase-1 enhances ischemia-reperfusion-induced lung apoptosis." J Biol Chem 279(11): 10677-84.
- Zhao, X., T. Yamamoto, J. W. Newman, I. H. Kim, T. Watanabe, B. D. Hammock, J. Stewart, J. S. Pollock, D. M. Pollock and J. D. Imig (2004). "Soluble epoxide hydrolase inhibition protects the kidney from hypertension-induced damage." Journal of the American Society Nephrology 15(5): 1244-53.

- Zheng, L., J. Liu, S. Batalov, D. Zhou, A. Orth, S. Ding and P. G. Schultz (2004). "An approach to genomewide screens of expressed small interfering RNAs in mammalian cells." Proc Natl Acad Sci U S A 101(1): 135-40.
- Zilberman, D., X. Cao and S. E. Jacobsen (2003). "ARGONAUTE4 control of locus-specific siRNA accumulation and DNA and histone methylation." Science 299(5607): 716-9.
- Zimmermann, T. S., A. C. Lee, A. Akinc, B. Bramlage, D. Bumcrot, M. N. Fedoruk, J. Harborth, J. A. Heyes, L. B. Jeffs, M. John, A. D. Judge, K. Lam, K. McClintock, L. V. Nechev, L. R. Palmer, T. Racie, I. Rohl, S. Seiffert, S. Shanmugam, V. Sood, J. Soutschek, I. Toudjarska, A. J. Wheat, E. Yaworski, W. Zedalis, V. Koteliansky, M. Manoharan, H. P. Vornlocher and I. MacLachlan (2006). "RNAi-mediated gene silencing in non-human primates." Nature 441(7089): 111-4.

## PUBLICATIONS

The following two publications are based on experimental results of the present dissertation and were released during the ongoing doctorate.

Jones, P. D., N. M. Wolf, C. Morisseau, P. Whetstone, B. Hock and B. D. Hammock (2005).

"Fluorescent substrates for soluble epoxide hydrolase and application to inhibition studies." Anal Biochem 343(1): 66-75.

Wolf, N. M., C. Morisseau, P. D. Jones, B. Hock and B. D. Hammock (2006). "Development of a high-throughput screen for soluble epoxide hydrolase inhibition." Anal Biochem 355(1):71-80.

## CURRICULUM VITAE

### Persönliche Daten

Nicola Maria Wolf  
geboren am 13. November 1975 in Wertingen  
ledig

### Schulbildung

Sept. 82 – Juli 88 Grund- und Hauptschule, Thierhaupten  
Sept. 88 – Juli 92 Dr.-Max-Josef-Metzger-Schule (Staatliche Realschule), Meitingen  
Sept. 92 – Juli 96 Übergangsklasse und Oberstufe am Holbein-Gymnasium, Augsburg

### Studium

Nov. 96 – Sept. 02 Gartenbauwissenschaften, Technische Universität München – Weihenstephan

### Praktika

März 97 – Mai 97 Gärtnerei Hartmann, Augsburg  
Nov. 98 – Dez. 98 Unternehmensberatung Rudolf Dirr, Asbach-Bäumenheim  
Feb. 99 – Apr. 99 Marie-Selby-Botanical-Gardens, Sarasota, Florida, USA  
Mai 99 – Juli 99 Baumschule Dirr & Schneider, Asbach-Bäumenheim  
Aug. 99 – Okt. 99 Agrolab, Oberhummel (Labor für agro-chemische Untersuchungen)

### Promotion

Seit Nov. 02 Technische Universität München, Fakultät Wissenschaftszentrum  
Weihenstephan für Ernährung, Landnutzung und Umwelt und  
University of California Davis, Department of Entomology  
  
Finanzierung durch ein Promotionsstipendium der Bayerischen  
Forschungstiftung